Tectono-depositional characterization and sedimentary provenance of the
Mesoproterozoic Fury and Hecla Basin, Nunavut, Canada

by

Mollie Claire McKenna Patzke

A thesis submitted in partial fulfillment of the requirements
for the degree of Doctor of Philosophy (PhD)
in Mineral Deposits and Precambrian Geology

The Office of Graduate Studies
Laurentian University
Sudbury, Ontario, Canada

THESIS DEFENCE COMMITTEE/COMITÉ DE SOUTENANCE DE THÈSE
Laurentian Université/Université Laurentienne
Office of Graduate Studies/Bureau des études supérieures

Title of Thesis
Titre de la thèse   Tectono-depositional characterization and sedimentary provenance of the Mesoproterozoic Fury and Hecla Basin, Nunavut, Canada

Name of Candidate
Nom du candidat   Patzke, Mollie

Degree
Diplôme   Doctor of Philosophy

Department/Program Département/Programme	Date of Defence
Mineral Deposits and Precambrian Geology	Date de la soutenance September 20, 2022

APPROVED/APPROUVÉ

Thesis Examiners/Examinateurs de thèse:

Dr. Alessandro Ielpi
(Supervisor/Directeur(trice) de thèse)

Dr. Galen Halverson
(Committee member/Membre du comité)

Approved for the Office of Graduate Studies
Approuvé pour le Bureau des études supérieures
Tammy Eger, PhD
Vice-President Research (Office of Graduate Studies)
Vice-rectrice à la recherche (Bureau des études supérieures)
Laurentian University / Université Laurentienne

Dr. Paul Durkin
(External Examiner/Examinateur externe)

Dr. Shawna White
(Internal Examiner/Examinateur(trice) interne)

ACCESSIBILITY CLAUSE AND PERMISSION TO USE

Abstract

Understanding the original depositional environments, architecture, and sediment sources of intracratonic basins is integral to terrane analysis in Precambrian cratons. Proterozoic intracratonic basins are widespread throughout Arctic North America, yet their inception and evolution are poorly understood. The late Mesoproterozoic amalgamation of the supercontinent Rodinia represents, specifically, an exemplary time to investigate intracratonic basin development due to many basins being formed. Four basins in eastern arctic Canada and Greenland, known as the Bylot basins, are thought to be genetically linked due to broadly similar lithologies, age, and geographic proximity. Southernmost in this basin system is the Fury and Hecla Basin, which straddles the homonymous strait and is exposed on Baffin Island and Melville Peninsula. Establishing a correlative framework between the Fury and Hecla Basin and the better characterized Borden Basin is key to a refined understanding of the broader Bylot basins.

The late Mesoproterozoic strata filling the Fury and Hecla basin, cumulatively known as the Fury and Hecla Group, comprise six formations: Nyeboe, Sikosak Bay, Hansen, Agu Bay, Whyte Inlet, and Autridge; of these, three (the Nyeboe, Sikosak Bay, and Whyte Inlet formations) are sandstone-dominated. Facies analysis indicates that the lowermost Nyeboe Formation records a range of depositional environments including terrestrial, backshore eolian, marine intertidal, wave-dominated marine shelf, and marine-offshore transitional. The Sikosak Bay and Whyte Inlet formations were largely deposited in a wave-dominated marine-shelf realm and show evidence of large sandwave buildup due to prolonged longshore drift. Seven sandstone samples were analyzed for detrital zircon U-Pb geochronology from the Fury and Hecla Group, and yielded grains with ages ranging from ~3350 to ~1695 Ma. Altogether, detrital zircon grains show a bimodal age

distribution with peaks at ~2.7 Ga and ~1.9 Ga. Notably, the Archean age peak is more prominent in the lower stratigraphy, whereas the Paleoproterozoic peak is more significant in the upper stratigraphy.

Facies and provenance analyses suggest that the Fury and Hecla Basin opened in a half-graben setting, with its master fault located on the present-day northern side of the basin. Initially, sediment was likely derived from erosion of local basement rocks. Facies mapping suggests that the basin expanded its catchment area with time. This trend was accompanied by increasing recycling of older siliciclastic successions from nearby basins – a provenance pattern that dominated over local sediment sourcing in the upper strata. As such, despite broadly similar lithologies and age, the Fury and Hecla Basin shows different depositional environments and a unique evolution, when compared to the known data, from the other Bylot basins.

Keywords: facies analysis; detrital zircon; geochronology; basin analysis; depositional environments; clastic sedimentology; Fury and Hecla Basin, Bylot Basins; intracratonic basin.

Co-Authorship statement and research funding

This thesis consists of a collection of three independent but related manuscripts, plus an introductory and a final chapter. Chapter 2 contains an edited version of a manuscript published in the *Canada-Nunavut Geoscience Office Summary of Activities* in the year 2018, with additional content that will be published in the 2022 issue of the same publication. Chapter 3 was published in the *Journal of Sedimentary Research* in November 2021. Chapter 4 will be submitted to *Precambrian Research* in winter 2023.

The thesis was conceptualized by Drs. Alessandro Ielpi, Galen Halverson, and Ross Stevenson, and was primarily sponsored by the Natural Sciences and Engineering Research Council of Canada, the Canada-Nunavut Geoscience Office, and the Polar Continental Shelf Program. All fieldwork was completed by the candidate under the guidance of Dr. Alessandro Ielpi (Laurentian University), Dr. Galen Halverson (McGill University), and Holly Steenkamp and Lorraine Lebeau (Canada-Nunavut Geoscience Office). Petrographic sample processing was conducted by the candidate under the guidance of Willard Desjardins and Christopher Beckett-Brown (Laurentian University). Geochronological sample preparation and processing was conducted at the Geological Survey of Canada′s Sensitive High-Resolution Ion Microprobe laboratory under the guidance of Nicole Rayner and Tom Pestaj. Additional collaboration, support and review were provided by co-authors herein.

The first and second manuscript are co-authored by Drs. Alessandro Ielpi, Galen Halverson and J. Wilder Greenman. The third manuscript is co-authored by J. Wilder Greenman, Dr. Rob Rainbird, Nicole Rayner, Dr. Galen Halverson, and Dr. Alessandro Ielpi. All manuscript and accompanying figures and tables were originally drafted by the candidate, with revisions and edits

provided by all co-authors.

Acknowledgments

I acknowledge that work for this project was primarily conducted at Laurentian University in Sudbury, Ontario, which is located on the traditional lands of the Atikameksheng Anishnawbek and Wahnapitae First Nations, and on grounds of the Robinson-Huron Treaty of 1850. Research for this project took place in Nunavut, meaning ″our land″ in Inuktitut, and I gratefully acknowledge the Inuk people for their permission and support. Allyship to Indigenous peoples is an ongoing process and I recognize that land acknowledgements are only a small step towards truth and reconciliation.

The utmost thanks go to my primary supervisor Alessandro Ielpi. Thank you for giving me many opportunities, and being a great mentor, supporter, and motivator. I also want to express gratitude to my co-supervisor Galen Halverson for your advice in and out of the field and your continued positivity. I also want to thank my colleague, Wilder Greenman, for your help throughout this project. Thank you also to Rob Rainbird for all your guidance and providing a home away from home for my time spent in Ottawa. Thanks to Tom Pestaj and Nicole Rayner for help with geochronology data. I want to thank all the people of the CNGO, especially Holly Steenkamp and Lorraine Lebeau who were mentors to me in the field. I would like to express my appreciation to the many people who were part of making the 2018 and 2019 field seasons a success, particularly, Celine Gilbert and Carol-Anne Généreux, and pilots Jason Lagimodier, Paula Vera, and Jacob Kalturnyk. Thank you also to Roxane Mehes and the other HES people that were extremely helpful along the way.

I want to give special thanks to the SWAG lab members during my time at Laurentian: Lorraine, Natasha, Robbie, Sophie, Jade, Jenna, Mia, and Melissa. I also would like to thank my

Table of Contents

List of Tables

List of Figures

List of Appendices

Preface

Fury and Hecla Strait and Igloolik

The Fury and Hecla Basin and Fury and Hecla Group are named after the Fury and Hecla Strait separating the northern tip of the Melville Peninsula from northwestern Baffin Island. The strait is significant for history, navigation, wildlife, and culture. It was named after the HMS Fury and the HMS Hecla, two ships from the British navy commanded by Sir Edward Parry during his second attempt to explore for the Northwest Passage in the 1820s[1]. Sir Parry himself documented sedimentary rocks outcropping along the strait[1]. The strait proved difficult to cross due to its ice coverage. During the voyage, the HMS Fury and HMS Hecla wintered in the local Inuit community of Igloolik, representing the first known contact between Igloolik and European explorers[2].

Archaeological artifacts and Inuit oral history suggest humans inhabited the Igloolik area continuously for nearly 4000 years[2]. Igloolik Inuit people refer to the Fury and Hecla strait as *Ikiq*, meaning strait in Inuktitut[2]. Proximity to the strait makes Igloolik a knowledge hub for sea ice, as well as wildlife as it is a migratory route for bowhead whales, beluga whales, walrus, narwhals, seals and polar bears[2]. Changing climate has been noticed by local Igloolik residents and threatens traditional hunting grounds and cultural identity. Curbing climate change and protecting the waters and land around the Fury and Hecla Strait is necessary to preserve the beautiful landscape and way of life for the ancestors of its ancient inhabitants.

[1]Chandler, F.W. 1988. Geology of the Late Precambrian Fury and Hecla Group, Northwest Baffin Island, District of Franklin. Geological Survey Canada Bulletin 370. pp. 26−32.

[2]Ljubicic, G. (2014). Igloolik. Inuit Siku Atlas. Retrieved June 27, 2022, from *https://sikuatlas.ca/index.html?module=module.sikuatlas.igloolik*

Chapter 1

1   Introduction to thesis

1.1   Geological background and statement of scope

The ancestral core of North America, known as Laurentia, is a collage of Precambrian crustal fragments (cratons) that amalgamated during times of enhanced orogenesis (Hoffman, 1988). Laurentia preserves variably deformed Archean to Paleoproterozoic basement crustal rocks overlain by an array of Proterozoic sedimentary basins that formed in diverse geodynamic settings. The sedimentary rocks preserved in these basins can be investigated to reveal many aspects of ancient Earth, including its surface environments and pathways of sediment transport. The Fury and Hecla Basin is one such Precambrian basin and consists of weakly deformed sedimentary rocks that are exposed in outcrops that straddle the Fury and Hecla Strait – a narrow seaway that separates northern Baffin Island from the mainland's Melville Peninsula (Nunavut, Canada).

Overlying Archean to Paleoproterozoic basement rocks of the Rae craton (Jackson and Berman, 2000), the Mesoproterozoic Fury and Hecla Group fills the Fury and Hecla Basin and is split into six lithostratigraphic formations (from the base): the Nyeboe, Sikosak Bay, Hansen, Agu Bay, Whyte Inlet and Autridge formations (Chandler et al., 1980; Chandler, 1988). Blackadar (1958) was the first geologist to map the distribution of rock types in the region. Later, the area received attention due to its perceived potential for uranium deposits (Ferguson and Goleby, 1980; Chandler et al., 1980; Chandler, 1988; Long and Tuner, 2012). Resulting work led to the first detailed sedimentological studies of the Fury and Hecla Basin, which suggested marine deposition with thin exposures and outliers of fluvial sediments (Chandler, 1988; Long and Turner, 2012;

Long, 2017).

The Fury and Hecla Basin is thought to be part of the larger Bylot basin systems, which include the Aston-Hunting, Thule, and Borden basins. These basins are exposed on northeastern Nunavut, Canada, and northwestern Greenland, and have been considered coeval since early studies (e.g., Blackadar and Fraser, 1960) based on broad lithologic similarities, age, and geographical location. To date, the Borden Basin has received the most attention owing to its spectacular exposures, known metallogeny, and proximity to the communities of Arctic Bay and Pond Inlet.

The maximum age constraint on the Bylot basins is inferred from fine-grained extrusive mafic rocks found at the base of the stratigraphic successions of each of the basins, which are postulated to be part of the widespread Mackenzie igneous event at ~1.27 Ga based on magnetic paleopoles (Jackson and Iannelli, 1981; Fahrig et al., 1981; LeCheminant and Heaman, 1989). Mafic dykes associated with the Franklin igneous event crosscut the strata of the Bylot basins, providing an upper age bracket of ca. 720 Ma (Heaman et al., 1992; Pehrsson and Buchan, 1999), though the youngest strata are generally regarded as being older due to speculated lithostratigraphic relationships with Mackenzie igneous event mafic flows, and younger geochronologic controls in the middle stratigraphy (Turner et al., 2016). More recent work, including what is contained in this thesis, has focused on attaining both depositional and detrital ages on the Bylot basins. Organic-rich shales in the Agu Bay Formation in the middle Fury and Hecla group recently yielded a Re-Os depositional age of 1087.1 ± 5.9 Ma (Greenman et al., 2021). This age is comparable to Re-Os ages of 1048 Ma and 1046 Ma obtained on the Arctic Bay and Victor Bay formations, respectively, in middle Bylot Supergroup of the Borden Basin (Gibson

et al., 2018). These ages corroborate a U-Th-Pb black shale age obtained on the Arctic Bay Formation (Turner and Kamber, 2012) and firmly establish that most of the Bylot basin strata were deposited some 200 Myr after the Mackenzie igneous event. Therefore, the Bylot basins might have experienced at least two separate phases of subsidence, the latter of which was broadly coeval with that of the Grenville orogeny (Greenman et al., 2021), a major and prolonged mountain-building event that is related to the amalgamation and tenure of one of Earth′s supercontinents – Rodinia (Li et al., 2008).

This thesis provides the first detailed, comprehensive sedimentological, architectural, and detrital-zircon geochronological study of the Fury and Hecla Basin, with a specific focus on its sandstone-dominated units (the Nyeboe, Sikosak Bay and Whyte Inlet formations). In doing so, the thesis contributes towards a refined understanding of the timing and fill of the Bylot basins – aspects that are critical to the geodynamic and paleogeographic reconstruction of the Rodinia supercontinent. More broadly, this thesis provides new information on the mechanisms of basin formation during supercontinent amalgamation, a topic that requires further investigation, especially during Precambrian time (e.g., Rainbird et al., 2010). Together, with other researchers studying the mafic, carbonate and shale dominated units, this thesis contributes to the broader Fury and Hecla project which aims to fully characterize the Fury and Hecla basin in its spatial and chronological context (Steenkamp et al., 2018).

1.2   Thesis Objectives

Specific objectives for this thesis are presented as follows:

- To determine the depositional environments in the sandstone-dominated units of the Fury and Hecla Group.

The basal Nyeboe Formation contains sandstone, dolostone, and mafic volcanic rocks, and has thus far been attributed to deposition in a dominantly marine and, to a much lesser extent, fluvial settings (Chandler, 1988; Long and Turner, 2012). The Sikosak Bay Formation has been described as a marine sandstone (Chandler, 1988, Long and Turner, 2012). The Whyte Inlet Formation has been inferred to contain mainly shallow marine sandstone and only minor amounts of fluvial sandstone (Chandler, 1988; Long and Turner, 2012; Long, 2017). While previous studies provided broad or site-specific descriptions of inferred depositional environments, this study presents the first detailed and basin-comprehensive characterization, which is also combined with structural observations. Understanding original depositional environments for a sedimentary basin is key to resolving its geodynamic evolution.

- To identify the sources of clastic sediment in the Fury and Hecla Group.

The identification of sediment pathways – that is, the reconstruction of source areas that provided detritus through erosion of bedrock or previous supracrustal panels, and how such detritus was transported to its eventual sink – is an important tool in basin analysis to understand the coeval evolution of orogens and nearby sedimentary basins. Provenance analysis is often achieved through detrital geochronology of minerals resilient to surface weathering, most commonly zircon. This method is based on the comparison of detrital-age spectra with potential protoliths and is often complemented by analysis of paleocurrent indicators in the sedimentary rocks. To date, no detrital zircon geochronology has been conducted on the Fury and Hecla Group, such that its provenance is not resolved. Mature quartzarenite is the dominant lithology throughout the basin, which makes it an ideal

candidate for a detrital zircon provenance study owing to its chemical maturity and abundance of weathering-resilient heavy minerals. Evaluating the provenance of the Fury and Hecla Basin can shed light on how the basin evolved with respect to the other Bylot basins for which provenance data are already available (namely the Borden Basin). As such, combining the results of detrital zircon geochronology and paleocurrent analyses from multiple basins in the region can provide a refined understanding of the paleogeography for the entire basin system during its evolution.

- To understand how the Fury and Hecla Basin correlates with the other Bylot basins, including the well-studied Borden Basin.

Broad correlations between the Fury and Hecla, Borden, Aston-Hunting and Thule Basins have been discussed in Blackadar and Fraser (1960), Lemon and Blackadar (1963), Blackadar (1970), Kerr (1979), Fahrig et al. (1981), Jackson and Iannelli (1981), and Long and Turner (2012). Their similarities include: (1) their nonconformable stratigraphic position atop gneissic basement rocks of the Rae Craton, (2) occurrence of basal basaltic sills and/or flows inferred to be part of the Mackenzie igneous event (~1.27 Ga; Fahrig et al., 1981; LeCheminant and Heaman, 1989), and (3) similar patterns of basin faulting. A detrital zircon provenance study is to date only available for the Borden Basin, which notably includes a signature from Grenvillian-aged detritus (~1.1 Ga) in its upper stratigraphy (Turner et al., 2016). This thesis aims to use facies analysis and detrital zircon geochronology to draw comparisons – and point out differences – between the geological history of the Fury and Hecla and the other Bylot basins. The Borden Basin is the most thoroughly studied Bylot basin and offers the best opportunity for a meaningful

comparison.

- To suggest partial model analogues to illustrate the tectono-depositional setting of the Fury and Hecla Basin and make inferences on how the tectonic setting of the Fury and Hecla Basin is related to the assembly of supercontinent Rodina.

The Bylot basins have remained enigmatic for decades, and several different interpretations have been proposed for their origin. Based on observations that were largely drawn from the Borden Basin, Olson (1977), and then Jackson and Iannelli (1981) suggested that the Bylot basins were the product of an aulacogen – that is, a failed rift of continental crust, with accommodation space generated first by extension then thermal subsidence. Sherman (2002) alternatively proposed that the upper strata of the Borden Basin recorded a basin polarity shift that, in their view, was related to far-field convergence, therefore inferring that both mechanisms of crustal relaxation and flexure could have been responsible for the evolution of the Bylot basins. Long and Turner (2012) suggested that the inception of the Borden Basin was driven by thermal lithospheric sagging, and subsequently Turner et al. (2016) hypothesized that the Bylot basins are impactogens, that is, basins formed by the onset of far-field stress related to the collision of Amazonia, Baltica, or Siberia into Laurentia during the amalgamation of Rodinia. Gibson et al. (2019) proposed that the Bylot basin strata could be interpreted as a series of extensional events, with intervening thermally generated subsidence. Greenman et al. (2021) suggested that contemporaneous extension and black-shale deposition throughout Laurentia during the amalgamation of Rodinia are correlated events that can be linked to magmatism further to the present-day south, in the region currently occupied by the Mid-

Continent Rift (Swanson-Hysell et al., 2019). Combining broad structural observations, facies mapping and analysis, provenance, and paleoflow data from the Fury and Hecla and other Bylot basins may enable the production of a refined basin evolution model. Original data from this thesis may be used to reach new conclusions about their tectono-depositional setting and, in turn, to suggest new models for how basins could form during the amalgamation of supercontinents.

1.3   Structure of the thesis

This thesis is organized into five chapters. Chapter 1 serves as a general introduction. Chapters 2‒4 are intended to be stand-alone journal papers, and therefore contain some repetition in the introduction and geological background sections of the papers. While these chapters are independent in their structure, they are nonetheless related in that they present detailed aspects of sedimentology, depositional architecture, and detrital zircon geochronology from the Fury and Hecla Basin. Chapter 5 contains concluding remarks and thoughts about future work. Specific information on the format of the core science chapters of the thesis are provided as follows.

Chapter two is titled: ″**Sedimentology and depositional architecture of the sandstone-dominated units in the Fury and Hecla Basin**″ and is modified and augmented from article published in the *Canada-Nunavut Geoscience Office Summary of Activities, 2018*, entitled ″Sedimentology of the sandstone-dominated units in the Fury and Hecla Basin, northern Baffin Island, Nunavut.″ The sedimentology and a brief overview of the depositional environments from the Nyeboe, Sikosak Bay and Whyte Inlet formations are discussed therein. In this chapter, the original article is supplemented by additional material that is intended for publication in an upcoming Canada-Nunavut Geoscience Office Summary of Activities (2022). The additional

material concerns with a detailed photogrammetric, paleoflow, depositional-architecture, and stratigraphic analysis of a multi-km-scale exposure of the Whyte Inlet Formation where shelf-scale depositional elements such as clinoforms and sandwaves can be observed in their entirety.

Chapter three is titled: **"The initiation of the Mesoproterozoic Bylot basins (Nunavut, Arctic Canada) as recorded in the Nyeboe Formation, Fury and Hecla Group),"** and was published in the *Journal of Sedimentary Research* in November 2021 (volume 91, pages 1166−1187). This article uses facies analysis of the lowermost formation of the Fury and Hecla Group, the Nyeboe Formation, and large-scale structural observations across the basin to determine that the Fury and Hecla Basin may have opened in a half-graben setting with the master fault bounding the basin on the north side. This chapter provides a first sedimentological and basin analysis framework to explain the inception of the Fury and Hecla Basin.

Chapter four is titled: **"Detrital zircon provenance of the Fury and Hecla Group: Refining the tectono-depositional framework of the Mesoproterozoic Bylot basins (Arctic Laurentia),"** and is intended for submission to *Precambrian Research* in winter 2023. The article uses detrital zircon provenance analysis of the Fury and Hecla Basin to understand what sources the basin records and how the basin evolved through time. The data show a significant asynchrony between the detrital ages recorded in the Fury and Hecla Basin and its depositional age. Such discrepancy is symptomatic of a prolonged lag between the original crystallization ages of the detrital minerals and their eventual deposition − a feature that is typical (if not diagnostic) of multi-cycle sandstones in cratonic settings. The chapter presents original detrital geochronology data and, through the comparison of cumulative density distributions and both original and compiled paleoflow data, discusses possible scenarios of sedimentary recycling that depict a refined

paleogeographic picture for the Proterozoic of eastern Arctic Canada.

1.4   Statement of original contributions

The following is a synthesis of the original contributions presented by the candidate:

- Presents a first detailed study of the depositional environments represented in the sandstone-dominated units of the Fury and Hecla Basin.

- Proves that facies mapping combined with large-scale structural observations can be successfully applied in the context of Precambrian basin analysis.

- Uses interdisciplinary methods to depict for the first time the depositional architecture of shelf-scale depositional elements formed by marine sandwaves in Precambrian time.

- Interprets the mechanism and basin setting during the initial phase of deposition within the Fury and Hecla Group.

- Presents the first provenance study of the Fury and Hecla Group, and details how its sediment sourcing resulted from the interplay of local derivation from basement rocks and recycling of sediment from older sedimentary basins nearby.

- Synthesizes paleocurrent data to suggest that most paleoflow indicators point to a western paleoflow except for the Whyte Inlet Formation which shows stacked marine clinoforms that point to an eastward paleoflow.

- Compares the Borden and Fury and Hecla Basin using facies analysis and detrital zircon geochronology to evaluate the similarities and differences between the two basins.

1.5   References

Blackadar, R.G. 1970. Precambrian Geology Northwestern Baffin Island, District of Franklin. Geological Survey Canada Bulletin 191. pp. 1‑89.

Blackadar, R.G., Fraser, J.A. 1960. Precambrian geology of arctic Canada, a summary account. Geological Survey Canada Paper 60-8. pp. 1‑24.

Chandler, F.W., Charbonneau, B.W., Ciesielski, A., Maurice, Y.T., White, S. 1980. Geological studies of the Late Precambrian supracrustal rocks and underlying granitic basement, Fury and Hecla Strait area, Baffin Island, District of Franklin. Current research. Geological Survey of Canada Paper 80-1A. pp. 125‑132.

Chandler, F.W. 1988. Geology of the Late Precambrian Fury and Hecla Group, Northwest Baffin Island, District of Franklin. Geological Survey Canada Bulletin 370. pp. 26‑32.

Fahrig, W.F., Christie, K.W., Jones, D.L. 1981. Proterozoic Basins of Canada. Geological Survey of Canada 81‑10. pp. 303‑312.

Ferguson, J., Goleby, A.B. 1980. Uranium in the Pine Creek Geosyncline. International Atomic Energy Agency, Vienna. 783 p.

Gibson, T.M., Shih, P.M., Cumming, V.M., Fischer, W.W., Crockford, P.W., Hodgskiss, M.S. W., Halverson, G.P. 2018. Precise age of Bangiomorpha pubescens dates the origin of eukaryotic photosynthesis. Geology. v. 46‑2. pp. 135‑138.

Greenman, J.W., Patzke, M., Halverson, G.P., Ielpi, A. 2018. Refinement of the stratigraphy of the late Mesoproterozoic Fury and Hecla Basin, Baffin Island, Nunavut, with a specific focus on the Agu Bay and Autridge formations. Summary of Activities 2018, Canada-Nunavut

Geoscience Office. pp. 85‒96.

Greenman, J.W., Rooney, A.D., Patzke, M., Ielpi, A., and Halverson, G.P., 2021: Re-Os geochronology highlights widespread latest Mesoproterozoic (ca. 1090‒1050) cratonic basin development on northern Laurentia; Geology, v. 49, p. 779‒783.

Heaman, L.M., LeCheminant, A.N., Rainbird, R.H. 1992. Nature and timing of Franklin igneous events, Canada: Implications for a Late Proterozoic mantle plume and the break-up of Laurentia. Earth and Planetary Science Letters. v. 96 (1‒2). pp. 38‒48.

Hoffman, P.F., 1988. United Plates of America, the birth of a craton-Early Proterozoic assembly and growth of Laurentia. Annual Review of Earth and Planetary Sciences, 16, pp.543-603.

Jackson, G.D., Iannelli, T.R. 1981. Rift-related cyclic sedimentation in the Neohelikian Borden Basin, Northern Baffin Island. Proterozoic Basins of Canada. v. 81‒10. pp. 269‒302.

Jackson, G.D. and Berman, R.G. 2000: Precambrian metamorphic and tectonic evolution of northern Baffin Island, Nunavut, Canada; The Canadian Mineralogist, v. 38, p. 399‒421.

Kerr, J.W. 1979. Evolution of the Canadian Arctic Islands- a transition between the Atlantic and arctic oceans. Geological Survey Canada Open File Report No. 618. 130 p.

LeCheminant, A.N., Heaman, L.M. 1989. Mackenzie igneous events, Canada: Middle Proterozoic hotspot magmatism associated with ocean opening. Earth and Planetary Science Letters. v. 96 (1‒2). pp. 38‒48.

Lemon, R.R.H., Blackadar, R.G. 1963. Admiralty Inlet Area, Baffin Island, District of Franklin. Geological Survey Canada Memoir 328. pp. 1‒84.

Li, Z. X., Bogdanova, S. V., Collins, A. S., Davidson, A., De Waele, B., Ernst, R. E., Fitzsimons, I.C.W., Fuck, R.A., Gladkochub, D.P., Jacobs, J. Karlstrom, K.E., Lu, S., Natapov, L.M., Pease, V., Pisarevsky, S.A., Thrane, K., Vernikovsky, V., 2008: Assembly, configuration, and break-up history of Rodinia: A synthesis; Precambrian Research, 160(1-2), 179‒210.

Long, D.G.F. 2017. Evidence of flash floods in Precambrian gravel dominated ephemeral river deposits. Sedimentary Geology. v. 347. pp. 53‒66.

Long, D.G.F., Turner, E.C. 2012. Tectonic, sedimentary and metallogenic re-evaluation of basal strata in the Mesoproterozoic Bylot basins, Nunavut, Canada: Are unconformity-type uranium concentrations a realistic expectation? Precambrian Research. v. 214‒215. pp. 192‒209.

Olson, R.A. 1977. Geology and genesis of zinc-lead deposits within a late Proterozoic dolomite, northern Baffin Island, N.W.T. Thesis: PhD, University of British Colombia. 387 p.

Pehrsson, S.J., Buchan, K.L. 1999. Borden dykes of Baffin Island, northwest territories: A Franklin U-Pb baddeleyite age and a paleomagnetic reinterpretation. Canadian Journal of Earth Sciences. v. 36‒1. pp. 65‒73.

Rainbird, R.H., Davis, W.J., Pehrsson, S.J., Wodicka, N., Rayner, N., Skulski, T. 2010. Early Paleoproterozoic supracrustal assemblages of the Rae domain, Nunavut, Canada: Intracratonic basin development during supercontinent break-up and assembly. Precambrian Research. v. 181 (1‒4). pp. 167‒186.

Sherman, A.G., James, N.P., Narbonne, G.M. 2002. Evidence for reversal of basin polarity during carbonate ramp development in the Mesoproterozoic Borden Basin, Baffin Island.

Canadian Journal of Earth Sciences. v. 39‑4. pp. 519‑538.

Steenkamp, H.M., Bovingdon, P.J., Dufour, F., Généreux, A., Greenman, J.W., Halverson, G.P., Ielpi, A., Patzke, M. and Tinkham, D.K. 2018: New regional bedrock mapping of Precambrian rocks north of Fury and Hecla Strait, northwestern Baffin Island, Nunavut; in Summary of Activities 2018, Canada-Nunavut Geoscience Office, p. 47‑62.

Swanson-Hysell, N.L., Ramezani, J., Fairchild, L.M. and Rose, I.R., 2019. Failed rifting and fast drifting: Midcontinent Rift development, Laurentia's rapid motion and the driver of Grenvillian orogenesis. GSA Bulletin, 131(5-6), pp.913-940.

Turner, E.C., Kamber, B.S. 2012. Arctic Bay Formation, Borden Basin, Nunavut (Canada): Basin evolution, black shale, and dissolved metal systematics in the Mesoproterozoic ocean. Precambrian Research. v. 208‑211. pp. 1‑18.

Turner, E.C., Long, D.G.F., Rainbird, R.H., Petrus, J.A., Rayner, N.M. 2016. Late Mesoproterozoic rifting in Arctic Canada during Rodinia assembly: Impactogens, trans-continental far-field stress and zinc mineralisation. Terra Nova. v. 28‑3. pp. 188‑194.

Chapter 2

2 Sedimentology and depositional architecture of the sandstone-dominated units in the Fury and Hecla Basin

Mollie Patzke,[1] J. Wilder Greenman,[2] Galen P. Halverson,[2] and Alessandro Ielpi[1]

[1]Harquail School of Earth Sciences, Laurentian University, Sudbury, Ontario P3E 2C6, Canada

[2]Department of Earth and Planetary Sciences/Geotop, McGill University, Montréal, Quebec H3A 0E8, Canada

2.1   Abstract

Mesoproterozoic basins are abundant in the Canadian Arctic and contain valuable records of sedimentation in the interiors and margins of ancient supercontinents. The Fury and Hecla Basin, exposed on Baffin Island and Melville Peninsula in Nunavut, provides great exposure of clastic strata to conduct sedimentary analyses with high-resolution. Fieldwork-based methods were applied to understanding the depositional history of the sandstone-dominated units of the Fury and Hecla Group. The basal Nyeboe Formation contains mudstone, sandstone and dolostone units representing alluvial to fluvial terrestrial, clastic shelf and clastic and carbonate nearshore marine environments. This unit also contains several isolated sub-marine volcanic flows. The Sikosak Bay Formation is a monotonous quartzarenite that records deposition in the shoreface zone. The Whyte Inlet Formation, in the upper stratigraphy of the Fury and Hecla Group, contains local exposure of fluvial strata, but was primarily deposited in the shoreface to offshore-transition zones of a clastic shelf. The northeast cape of Melville Peninsula offers great exposure for in-depth

architectural and morphodynamic analyses of shelf clinoforms based on satellite imagery and ground-based field work. Large clinoforms verge to the east in stacked succession indicating open-ocean deposition strongly influenced by wave-reworking, possibly sustained by low latitude trade winds, and are comparable to large sandbars seen in modern ocean settings. These wave-induced sandbars are seldom recognized in Precambrian strata and provide a case study for future comparisons. These results are also significant due to clastic shelf sand bars being an important hydrocarbon reservoir in younger rocks.

2.2   Introduction

The Mesoproterozoic basin system collectively known as the Bylot basins is composed of relatively unmetamorphosed and undeformed supracrustal rocks− mostly sedimentary− exposed in the Canadian Arctic Archipelago and northwestern Greenland (Figures 2-1, 2a; Jackson and Iannelli, 1981; Long and Turner, 2012). This basin system comprises the Hunting-Aston Basin, exposed on Prince of Wales Island and on northernmost Somerset Island (Tuke et al., 1966; Mayr et al., 2004); the Borden Basin on Baffin Island and Bylot Island (Jackson and Iannelli, 1981); the Fury and Hecla Basin, exposed on Baffin Island and northern Melville Peninsula (Fig. 2-2a; Chandler, 1988); and the Thule Basin of northwestern Greenland and eastern Ellesmere Island (Jackson, 1986; Dawes, 1997). The maximum depositional age for the basins is ca. 1270 Ma, based on the affinity of basal volcanic units to the Mackenzie dyke swarm (LeCheminant and Heaman, 1989). In the Borden Basin, depositional ages from U-Pb-Th whole rock black shale dated the Arctic Bay Formation at ~ 1092 ± 59 Ma (Turner and Kamber, 2012), and Re-Os analyses on black shale dated the Arctic Bay Formation 1048 ± 12 Ma and the Victor Bay

Formation 1046 ± 16 Ma (Fig. 1 in Gibson et al., 2018). Similar to the Arctic Bay Formation, black

shale from the Agu Bay Formation located in the middle to lower strata (Figure 2-3) of the Fury

and Hecla Basin yielded a Re-Os age of 1087.1 ± 5.9 Ma (Greenman et al., 2021).

The Bylot basins are thought to record the final stages of convergence and amalgamation of

the supercontinent Rodinia (Cawood et al., 2007; Pehrsson et al., 2016). Due to their interpretation

as rift basins located in proximity to one another, this basin system was originally interpreted as a

set of fault-bounded aulacogens (Olson, 1977; Jackson and Iannelli, 1981). A greater

understanding of the geochronologic constraints and sedimentary architecture led Turner et al.

(2016) to abandon the aulacogen interpretation. More recently, the Bylot basins are interpreted as

having a complex depositional history, with basin generation attributed to impactogen

development from far-field stresses due to the assembly of the supercontinent Rodinia (Turner et

al., 2016). Most of the sedimentological work in the area has focused on the well-exposed and

minerally endowed Borden Basin (Turner, 2009; 2011; Long and Turner, 2012; Turner and

Kamber, 2012; Hahn et al., 2015), whereas associated regions such as the Fury and Hecla Basin

have received less attention. Greenman et al. (2021) proposed widespread sedimentation was

linked to extension and associated with the mid-continent rift.

Early work by Blackadar (1958, 1963, 1970) and Blackadar and Lemon (1963) in the Fury

and Hecla Basin area provided a foundation of geological mapping and stratigraphic subdivision.

Additional fieldwork in the 1980s (Chandler et al., 1980; Chandler and Stevens, 1981; Jackson and

Iannelli, 1981; Chandler, 1988) built on the early geological mapping work and provided a more

thorough stratigraphy that was the basis for this study (Figure 2-2b). Jackson and Iannelli (1981),

LeCheminant and Heaman (1989) and Heaman et al. (1992) proposed correlations between the

mafic rocks exposed in the basal units of the Fury and Hecla Basin to the south and west in the Canadian Arctic Archipelago and on the mainland, broadly constraining the age of the Fury and Hecla Basin between the 1.27 Ga Mackenzie igneous event and the dykes of the 723 Ma Franklin igneous event that cross-cut the entire Fury and Hecla Group (Heaman et al., 1992). More recent fieldwork focused on selected exposures in the eastern and southern Fury and Hecla Basin (Long and Turner, 2012; Long, 2017).

The Fury and Hecla Geoscience Project of the Canada-Nunavut Geoscience Office has employed geologists with diverse skills and backgrounds to improve the mapping, geological understanding, and economic potential of the area from 2018 to 2020 (Figure 2-1; Steenkamp et al., 2018). A significant component of the project is dedicated to: the stratigraphic and sedimentological refinement of the sedimentary succession known as the Fury and Hecla Group, which is exposed in the area; the establishment of solid geochronological constraints on basin initiation and evolution; and the characterization of sedimentary provenance in the Fury and Hecla Group based on detrital zircon geochronology. In this paper, the author presents the preliminary results of stratigraphic and sedimentological fieldwork conducted on the Baffin Island side of the Fury and Hecla Basin and focuses on the sedimentary facies recognized in three sandstone-dominated units exposed therein. We also provide additional attention to the northeast cape of Melville Peninsula, which contains excellent exposure of the Whyte Inlet Formation.

2.2.1 Relevance to the study of nearshore-marine clastic shelves

The Fury and Hecla Basin's fill is dominated by shallow-marine sandstone, with exceptional coastal outcrops where sedimentological and depositional-architectural features can

be observed over a range of scales, from centimeters to kilometers. This setting makes the sandstone-dominated formations of the Fury and Hecla particularly suitable for the architectural analysis of nearshore-marine clastic shelves. Depositional elements from nearshore marine clastic shelves, such as large-scale sandbars, are well understood and described from modern shelves but have been historically hard to recognize in ancient settings due to subtle differences in their stratigraphic signature (Fleming, 1980; Suter, 2006). Barrier islands and sandbars in modern clastic shelf environments are known to nucleate in both tidal and wave-dominated environments (Suter, 2006). In tidal depositional environments, these compound bedforms are created by laterally moving currents onto and off the shelf in response to seasonal sea level fluxes (Flemming, 1980). Their foresets generally dip obliquely to the axis of the tidal ridge as seen, for example, in the modern coast of South Africa affected by the Agulhas current (Flemming, 1980) and Middlekerke Bank in Belgium (Berne et al., 1994). Unidirectional cross bed sets often coarsen upward and are topped with bidirectional ripples and mud drapes (Suter, 2006). Tidal sandbars have seldom been inferred to have been deposited in Precambrian tidal environments (e.g., Walker and Plint, 1992). Tidal sandbars have a distinct ichnofacies signature that is not possible or recognized in the Precambrian. In contrast, wave-dominated sand bars are often attributed to storm activity. They can occur on the shoreface, oblique to the shoreline, or in the offshore where they are subparallel to the shoreline (Snedden and Dalrymple, 1999). They can be recognized through graded storm depositional features, and lack of tidal indicators, in and around the strata in question (Suter, 2006). A noticeable difference between sandbars formed in tidal and wave-dominated environments is the lack of mud drapes or silt layers in direct contact with the sand strata in storm deposits (Snedden and Dalrymple, 1999). Storm-induced sand ridges are also characterized by an

erosional lower boundary overlain by storm beds (Snedden and Dalrymple, 1999). Storm beds are granule beds from when sand-grained fractions are entrained and bypassed further downslope, such that granules are concentrated as floor lags during storm activity. Tidal sand ridges can form in epeiric seas whereas storm wave-dominated sand ridges are less likely to form in non-ocean type water bodies due to the necessity of a large fetch (Suter, 2006). Overall, storm sand ridges are rarely well-documented in Precambrian deposits (e.g., Johnson, 1977). Understanding stratigraphic record of these features will better constrain the depositional setting and therefore, the evolution of the basin.

2.2.2 Regional geology

The Fury and Hecla Basin is an area of sedimentary and interlayered minor mafic volcanic rocks exposed along the seaboard and inland of Fury and Hecla Strait, which separates Baffin Island to the north from Melville Peninsula to the south (Figure 2-2b). The minimum extent of the basin, based on currently mapped outcrops, is at least 140 km east-west by 75 km north-south. Although the Fury and Hecla Basin is geographically centred on 69°52′N, 84°10′W, most exposures are located north of Fury and Hecla Strait (Figure 2-2b).

The Fury and Hecla Group succession consists predominantly of sandstone with subordinate conglomerate, red to black shale, and dolostone (Chandler, 1988; Long and Turner, 2012). The Fury and Hecla Group reaches a maximum estimated thickness of 6 km (Figure 2-3; Chandler, 1988), although many of its formations display lateral thickness variations and true thicknesses are difficult to ascertain. The Fury and Hecla Group nonconformably overlies an Archean to late Paleoproterozoic basement composed of granitoid gneisses, mafic intrusions, and

minor metasedimentary outcrops (Bovingdon et al., 2018). Basement rocks are likely part of the Committee belt of the Rae craton (Jackson and Berman, 2000). The Rae craton preserves a complex history of Archean terrane assembly, early Paleoproterozoic orogenesis (Berman et al., 2013), and middle Paleoproterozoic extension and basin development (Ernst and Buchan, 2001; Rainbird et al., 2010). On Baffin Island, overlying deposits of the Fury and Hecla Group form a gently deformed monocline that dips 15−20º to the south, which is crosscut by multiple arrays of faults with east to south-southeast strikes.

2.3   Methods

Fieldwork was conducted out of a camp located on the Gifford River (Figure 2-1) in July to August 2018, and out of the hamlet of Igloolik (Figure 2-1) in July 2019. Daily traverses were supported by helicopter drop off and pick up. In the field, grain size, sorting, colour, and compositional and textural maturity were recorded for transects across selected units at specific locations. At outcrop scale, the geometry, stratigraphic position, and thickness of strata were recorded. Thickness was ascertained using basic trigonometry from the measured outcrop thickness and the dip. General depositional environmental analysis was interpreted following Collinson et al. (2006).

Additional observations aimed at reconstructing depositional architecture of a select exposure immediately south the narrowest point on the Fury and Hecla Strait (northeast cape of Melville Peninsula; Figure 2b) took place in the 2019 field season. Regional lineaments, tens to hundreds meters in thickness, were first identified and interpreted on freely distributed satellite imagery by Maxar Technology© and digitized as polyline features using Sas. Planet™ and

ArcMap™ software. The line-drawings obtained from this process were ground-checked in the field while on a traverse to verify lineaments and interpretations. Sedimentologic, bed-by-bed logging, and paleocurrent data were also collected on traverse during both field seasons. Paleocurrent data were measured on three-dimensional exposures of flow-regime bedforms such as trough cross-beds. Paleocurrent data were corrected for the dip and are visualized using rose diagrams that were developed in the opensource visible geology online stereonet program.

2.4   Results

2.4.1 Stratigraphic descriptions

Results of field mapping agree with the subdivision of formations based on lithology of the Fury and Hecla Group defined by Chandler (1988), that is, the Nyeboe, Hansen, Sikosak Bay, Agu Bay, Whyte Inlet and Autridge formations (Figure 2-3; Steenkamp et al., 2018). The Nyeboe Formation is bound at the base by a covered unconformity and is up to 500 m thick and consists of basal immature conglomerate and breccia passing upward into red, medium-grained arkose and subarkose, displaying an overall fining-upward trend (Figure 2-3a). Red siltstone and fine-grained sandstone with recessive weathering are present at stratigraphic intervals of approximately 50−100 m. The formation also contains basalt flows exposed in the western part of the basin (each up to 10 m thick, with well-developed amygdules, columnar jointing and local pillow forms; Figure 3b), minor bedsets of quartzarenite and a 40-m-thick succession of mixed clastic-carbonate deposits that pinches out eastward. Sedimentary facies recognized in the Nyeboe Formation are described below and have been presented in Patzke et al. (2021).

The Hansen Formation forms sharp contacts and consists of an eastward-thinning mafic volcanic unit with well-developed columnar jointing (Figure 2-3c). This unit is classified based on lithology, displays variable unconformable stratigraphic relationships. The Hansen Formation is a competent unit that crosscuts the lowest sedimentary formations, the Nyeboe and Sikosak Bay formations: in the western part of the study area, it separates the Nyeboe and Sikosak Bay formations, whereas in the centre of the study area it is between the Sikosak Bay and Agu Bay formations; it is absent in the east (Figure 2-2b). The Hansen Formation pinches out to the east. Although Chandler (1988) suggested that the formation represents a subaerial flow (based on a high Fe(III)/Fe(II) ratio), the heterogeneous stratigraphic relationships documented suggest a post depositional origin (i.e., a dyke or shallow sill). Therefore, it is now regarded as a shallowly emplaced sill (Steenkamp et al. 2018; Dufour et al. 2020).

The Sikosak Bay Formation has gradational contacts with its bounding sedimentary formation units. The formation is up to 150 m thick and consists entirely of white quartzarenite (Figure 2-3d). Sedimentary facies in the Sikosak Bay Formation are detailed below. The Agu Bay Formation comprises basal local metre-scale stromatolitic bioherms (dolomite member), black shale (~75 m thick; black shale member) and up to 500 m of red siltstone with interbedded sandstone (redbed member; Figure 2-3e). A detailed description of the Agu Bay Formation is found in Greenman et al. (2018), and this unit yielded a whole rock black shale Re-Os age of 1087.1 ± 5.9 Ma (Greenman et al., 2021). The Whyte Inlet Formation is a white to pink quartzarenite-dominated succession up to 3 km thick (Figure 2-3f) that thins westward (Figure 2-2b). Thin granule- to pebble-grade lags recurs in the stratigraphy every 5−10 m, and conglomerates and intraformational breccia are also present. The latter are common in the easternmost study area,

where the Whyte Inlet Formation overlies basement rocks (Figure 2-2; Long, 2017). As it′s the focus of the architectural investigation, sedimentary facies recognized in the Whyte Inlet Formation are detailed below. The Autridge Formation is composed of two members: the lower Mikkelsen member consists of a 1.5 km thick succession of quartzarenite with minor shale; the upper Cape Appel member consists of a 500 m thick succession of dark shale with minor quartzarenite (Figure 2-3g). The Autridge Formation is exposed only in the western study area and is inferred to pinch out in the centre of the basin (Chandler, 1988). A detailed description of the Autridge Formation is presented in Greenman et al. (2018).

2.4.2 Facies of the Nyeboe, Sikosak Bay and Whyte Inlet on Baffin Island

The Nyeboe Formation contains eight lithofacies defined by this study: conglomerate and breccia, planar-stratified sandstone, cross-stratified sandstone, hummocky cross-stratified sandstone, planar-stratified heterolithic beds, pin-stripe−laminated sandstone, planar-bedded dolostone and sandstone, and basalt flows. Conglomerate and breccia (Figure 2-4a) have either a monomictic quartz-pebble framework with a fine-grained sandy matrix (at the formation′s base), or polymictic associations of sandstone and quartz pebble to boulder conglomerate with a medium -grained sandstone matrix (in the middle of the formation). Polymictic breccia locally overlies the basal nonconformity and is composed of granitoid, iron-formation and aphanitic-mafic clasts in a siltstone matrix. Planar-stratified (Figure 2-4b), cross-stratified (Figure 2-4c) and hummocky cross -stratified sandstones (Figure 2-4d) form the bulk of the Nyeboe Formation and consist of quartzarenite that is locally micaceous. Strata are commonly bounded by wave ripples and are locally organized into large foresets. Stratigraphically, these facies overlie basal conglomerates and breccia in the east and lay directly above the basal nonconformity in the west-central study

area. Planar-stratified heterolithic beds are composed of mudstone and fine-grained sandstone at various intervals in the succession. Desiccation cracks, mottling and blocky weathering are present in some exposures (Figure 2-4e). Pin-stripe‑laminated sandstone occupies the lower to middle stratigraphic level of the formation in the central study area. This facies is organized into <2 m thick cross beds sets with lamination defined by millimetre-scale grainsize segregation. Sandstone lamination displays tangential bottom sets and is characterized by a higher compositional and textural maturity than other sandstone facies (Figure 2-4f). Small evaporite pseudomorphs are also present along the bottomsets of this facies. Planar-bedded dolostone and sandstone is defined by decimetre thick alternation of dolomite-cemented siliciclastic beds and microbially laminated dolostone. Siliciclastic beds exhibit planar lamination or herringbone cross laminated sets. Columnar stromatolites with decimetre-scale synoptic relief are locally preserved (Figure 2-4g). This facies is best developed in the central basin area and pinches out to the east. The Nyeboe Formation also contains rare basalt flows that appear to pinch out eastward. The basalt flows contain amygdules and pillow structures (Figure 2-4h). A comprehensive depositional model for the Nyeboe Formation is presented in Patzke et al. (2021) and Chapter 3.

The Sikosak Bay Formation is monotonously characterized by planar-stratified sandstone. This facies consists of medium- to coarse-grained, texturally mature quartzarenite (Figure 2-5a) organized in beds bounded by wave ripples. Bedsets of planar-stratified sandstone are generally horizontal, although a large foreset is present in the centre of the basin exposed area.

The Whyte Inlet Formation contains five lithofacies: intraformational breccia, wave-rippled sandstone, cross-stratified sandstone, planar-stratified sandstone and planar-stratified granules conglomerate. Intraformational breccia was observed and documented at only one

location, where the Whyte Inlet Formation nonconformably overlies basement rocks in the east (Figure 2-2). These coarse-grained facies have been described in greater detail by Long and Turner (2012) and Long (2017). Wave-rippled sandstone (Figure 2-5b), cross-stratified sandstone (Figure 5c) and planar-stratified sandstone (Figure 2-5d) form the bulk of the formation's thickness and consist of tan, medium-grained, well-sorted quartzarenite. All the sandstone facies are repeated at approximately 10 m intervals by a pavement (<2 cm thick) of rounded granule conglomerate composed of well-rounded quartz and lithic clasts (Figure 2-6).

2.4.3 Depositional architecture of the Whyte Inlet Formation

2.4.3.1 Field observations

The northeast cape of Melville Peninsula offers spectacular exposure of the Whyte Inlet Formation (red box on Fig. 2-2B), which has a thickness greater than 1 km (Figure 2-6). This exposure represents the easternmost expression of the Whyte Inlet Formation (Figure 2-2b). Observations from a range of scales reveal sedimentary and architectural features (Figure 2-7a–f). The strata have a structural dip that increases from ~15 degrees at the base (south) to ~30 degrees at the top (north), and generally have a strike of ~110 degrees from north (see figure 2 in Greenman et al., 2019). This section of the Whyte Inlet Formation overlies Archean granodiorite with syenite pegmatite basement rocks (Figure 2-7a). The contact is covered. Outcroppings of the Whyte Inlet Formation extend from the Melville Peninsula forming a cape, jutting out into the Fury and Hecla Strait (Figures 2-2b; 2-7b, c and f). The outcrop generally forms a stepwise topography (Figure 7d–f). The section comprises lithologies that range from fine-grained sandstone to cobble-grade conglomerate (Figure 2-6). Lower strata contain coarse-grained sandstone with floating quartz

cobbles in the first five meters (Figures 2-6, and 2-8a). Pebble- to cobble-sized clasts are common in the lower (first 225 m) and upper stratigraphy (870 m to the top of the stratigraphy). Floating clasts occur sometimes in the sandstone matrix or as part of organized beds (Figure 2-8a and b). Trough crossbedding and ripple cross-lamination is ubiquitous (Figures 2-8c−d). The formation′s stratigraphy at this location comprises planar and undulated bedding surfaces, with bound metre-scale beds and bedsets that reach maximum thickness of ~35 m (Figure 2-6). In the upper stratigraphy, roughly ~1100 m up-section, a well-preserved sedimentary slump feature is also observed (Figure 2-8f). This slump feature is 75 cm wide and about 2 m in height. Exposure is nearly continuous and is not blocked by vegetation or surficial deposits. Large scale-architectural elements are readily visible in satellite imagery (Figures 2-7 and 2-9). Well-preserved large-scale foresets are visible throughout the stratigraphy, where they are often composed of cross-beds (Figure 2-8e). Foresets are the bounding surfaces of cross beds and cross bed sets. The overall structure is referred to as a clinoform.

2.4.3.2 Paleoflow patterns

Paleoflow measurements were collected from trough cross-beds (n=223) from 30 different locations (Figures 2-10 and 2-11). Sets consisting of about ten measurements each were collected at 30 different locations spanning the stratigraphy for a total of 223 measurements (Figure 2-10). Paleocurrent measurements were merged into nine groups based on the apparent directional changes in the clinoformal architectural elements to which they belong on the ground (Figures 2-10, 11 and 2-Table 1). The paleocurrents are numbered from 1 to 9 following the younging direction of the strata from south to north (Fig. 2-10). On the northeast cape, the Whyte Inlet Formation records a dominant eastern flow direction. The paleoflow shifts slightly up-section,

from southeastward to eastward, bimodal with southwestern and northeastern components, and eventually northeastward (Figures 2-10 and 2-11). On the northeast cape, the strata young to the north. The first 200 m of stratigraphy are characterized by a southeast paleocurrent direction. Around 400 m in the stratigraphy, the paleoflow indicators become bimodal, with main components of flow to the east-northeast and south-southwest (PC 4, Fig. 2-10). At 800 m, the paleocurrents show a unimodal direction towards the east with a slight northern component (Figure 2-10). A group of foresets ground-checked to the west of the main traverse line shows a wider spread in their paleoflow distribution, although still with a dominant eastward component (Figure 2-11).

2.4.3.3 Clinoform architecture

Five large-scale clinoforms are identified, four along the stratigraphic section traverse and one on the western side of the peninsula: PC (paleocurrent) 3; PC 4; PC 5; and PCs, 7, 8, 10; and PC 11 (Figure 2-11). PCs 10 and 11 are not part of the main traverse and were investigated separately. The section youngs south to north. The clinoforms are stacked with little stratigraphic thickness between them. Clinoforms predominantly dip to the east. All clinoform-forming structures have a component of eastward paleocurrent, therefore the vergence of the clinoforms and paleocurrent structures are approximately consistent. Clinoforms, corrected by tectonic dip, range in thickness between 210-280 m, averaging ~230 m. Their apparent width (since a correction with respect to slope-normal conditions could not be performed) is ~700 m.

2.5   Discussion

2.5.1 Depositional setting

Three main depositional environments are recorded in the Nyeboe Formation: terrestrial, clastic-dominated near-shore marine, and clastic-carbonate near-shore marine. Episodes of subaqueous volcanism, recorded by pillow-structured basalt, also took place during sedimentation (Busby-Spera and White, 1987). Basal gravel-dominated units, and possibly part of the micaceous cross bedded sandstone, represent a scree-slope (breccia) to alluvial-fluvial (conglomerate and sandstone) depositional setting, which existed in the early depositional phases of the Nyeboe Formation (Went, 2005). Directly above the basal nonconformity, these deposits may represent the infill of small, incised valleys; this inference is supported by the poor sorting and limited along-strike extent of these deposits, although no significant basement topography was documented (Takashimizu and Masuda, 2000). Most of the Nyeboe Formation is composed of lithofacies that point to constant wave agitation (wave ripples, hummocky forms) and prolonged sediment reworking that, in part, accounts for the textural and mineralogical maturity of quartzarenite facies (planar-stratified sandstone, cross-stratified sandstone, and hummocky cross-stratified sandstone). These features are consistent with a wave-dominated clastic shelf and more specifically, an upper to intermediate shoreface setting (Allen, 1968). Minor finer-grained units (planar stratified heterolithic beds) may indicate either temporary flooding and deposition below the storm-wave base or emergence and incipient pedogenesis in backshore to lagoon settings (based on mottling and desiccation cracks) (Marconato et al., 2014). In backshore settings, pin-stripe−laminated sandstone can indicate the growth and migration of small eolian dunes that are protected from storm activity (Mountney, 2006). Finally, the establishment of a mixed clastic-carbonate, intertidal and wave-influenced marine setting is recorded by the planar-stratified sandstone and dolostone,

which contains small stromatolites and herringbone cross-stratified sets. This facies indicates that, at times, the basin was subject to sea-level rise (Kah et al. 2009). The stratigraphic and geographic proximity to eolian deposits floored by evaporite pseudomorph layers may indicate a protected sub -environment that allowed for the local establishment of carbonate facies (e.g., Herbers et al., 2016). A detailed tectono-depositional model describing the vertical and lateral facies variations in the Nyeboe Formation in relation to the early stages of basin development is presented in Patzke et al. (2021) and Chapter 3.

The Sikosak Bay Formation is compositionally and texturally very mature, and its monotonous sedimentology─ defined by planar quartzarenite beds with ubiquitous wave ripples ─ points to a long-lived marine shoreface setting (Covey, 1986).

2.5.2 Whyte Inlet depositional architecture and morphodynamics

A terrestrial, probably proximal fluvial, depositional setting is recorded by the intraformational breccia draping the basement nonconformity in the easternmost exposures of the Whyte Inlet Formation, consistent with fluvial interpretation reported by Long and Turner (2012) and Long (2017). The bulk of the Whyte Inlet Formation, however, consists of interbedded facies of wave-rippled sandstone, cross-stratified sandstone, and planar-stratified sandstone that indicate deposition in a shallow clastic shelf (most likely in the shoreface to upper offshore-transition zone of a storm wave-dominated clastic shelf. Structures such as crossbedding and ripples are diagnostic of the shoreface, and hummocky cross-stratification is diagnostic of the offshore transition zone (Walker and Plint, 1992; Clifton, 2006). Graded storm deposits (i.e., tempestites) are recognized based on their erosional boundaries (flat or undulated), and by pebble or cobble

lags overlain by hummocky cross-stratification and ripples (Harms et al., 1975). Repeated planar-stratified granule conglomerate is interpreted to represent storm events, in which sand-grained fractions are entrained and bypassed further downslope, such that granules are concentrated as floor lags.

Clinoforms preserved in the Whyte Inlet Formation are interpreted to represent large sand ridges, parallel to the coastline, created by storm wave deposition, based on (1) the lack of tidal indicators (i.e., bimodal flow sedimentary structures, mud drapes, etc.), and (2) the presence of storm deposits such as tempestites and individual hummocky cross-stratification sets (Figure 2-8). The monotonous stratigraphic development of the Whyte Inlet Formation implies a long-term balance between sediment supply and basin-floor subsidence (Covey, 1986), likely in a regime of slow-paced, continued aggradation where storm-related sand ridges could be best preserved (Suter, 2006).

The predominantly eastern paleoflow preserved in the structures likely records wave deflection upon impacting the shoreline at an oblique angle, although some horizons through the stratigraphy could have also been influenced by geostrophic effect. The apparent clinoform orientation is mostly consistent to the eastern quadrant while the paleocurrent distribution changes up-section. The paleocurrent data indicate a change in sediment dispersal pattern, with sourcing mainly from the west. The hypothesis of possible geostrophic effects on sedimentation can be given credibility considering that storm-wave-induced sand bars often form from storm activity characteristic of middle latitudes (hurricanes and typhoons; Suter, 2006). These strata were deposited at ~1.1 Ga (Greenman et al., 2021), a time where Laurentia was likely situated in the Northern Hemisphere side of the Mesoproterozoic intertropical convergence zone (Li et al., 2008),

and rotated about 135 degrees clockwise with respect to its current orientation. In this scenario, the Fury and Hecla Basin would have faced north-easterly trade winds that would have resulted in now -preserved east-facing paleoflow indicators and clinoforms oriented along-axis with a seaway located between Laurentia and Siberia (Fig. 9 in Li et al., 2008). These geometric relationships are best expressed in PC 3, PC 5, PCs, 7, 8, 10 and PC 11. PC 4 also points to the east, but the clinoform angles are shallower, and therefore its orientation remains ambiguous. Local changes, seen in the dip direction of the structures, were probably influenced by longshore currents that responded to local irregularities in the shoreline at the time.

While our data is limited to a relatively small area in the southeastern portion of the basin, it does not appear to be an outlier (Patzke et al., 2018; Greenman et al., 2019). The bulk of the Whyte Inlet Formation implies that the clastic shelf belonged to a water body that was likely openly prone to receive wave agitation from a large body of water (that is, not a scenario of an epeiric sea). These geometric features are comparable in size to modern sand ridges found on the southern North American Atlantic Ocean margin (Stubblefield et al., 1984; Goff et al., 1999), i.e., at a scale (hundreds of meters) that implies vigorous wave agitation that is common of open oceanic systems with virtually unlimited fetch. The Autridge Formation may be evidence for basin deepening to the west as it records marine offshore transition and offshore facies (Chandler, 1988; Greenman et al. 2018). Therefore, the northeast cape exposure of the Whyte Inlet Formation may record a sand ridge build up on a marine shoreface environment in a system that deepens to the west over time.

2.6   Conclusions

The Fury and Hecla Basin contains six formations composed of several facies that reflect terrestrial to offshore-marine deposition. The Nyeboe, Sikosak Bay and Whyte Inlet formations are sand-dominated units and were the focus of this contribution. The Nyeboe Formation, located at the base of the Fury and Hecla Group, can be subdivided in three different depositional environments: terrestrial alluvial to fluvial, clastic shelf and carbonate-clastic nearshore marine. Volcanic flows, indicative of a sub-marine origin, also contribute to the Nyeboe Formation strata. The Sikosak Bay Formation records monotonous shoreface deposition. In the ~1 km thick Whyte Inlet Formation, deposition predominantly occurred on a clastic shelf environment that ranged from foreshore to offshore transition, with localised fluvial deposition in the northeastern part of the basin. More broadly, thick, and monotonous tracts of nearshore-marine sandstones in the Whyte Inlet Formation suggests a context of slow, continuous subsidence paced by accumulation of strata during its deposition.

Architecture and morphodynamic features of sandstone clinoforms in the Whyte Inlet Formation are interpreted to represent large-scale sand ridges. The Whyte Inlet Formation was likely deposited in an open oceanic system, and we hypothesize that its paleocurrent distribution likely records wave action. This wave action may record original geostrophic currents running sub-parallel to the depositional coastline at the time. This interpretation is consistent with the current understanding of landmasses distribution at ~1.1 Ga, with a possible open-water continental seaway found between Laurentia and Siberia. The storm-induced sand ridges documented in the stratigraphic record of the Whyte Inlet Formation serve as a key case study to address the dearth of well-documented Precambrian examples of this type of bedform.

2.7   Acknowledgements

2.8   Figures

Figure 2-1: Study area map

Overview map of the Fury and Hecla Geoscience Project; see Steenkamp et al. (2018) for more details.
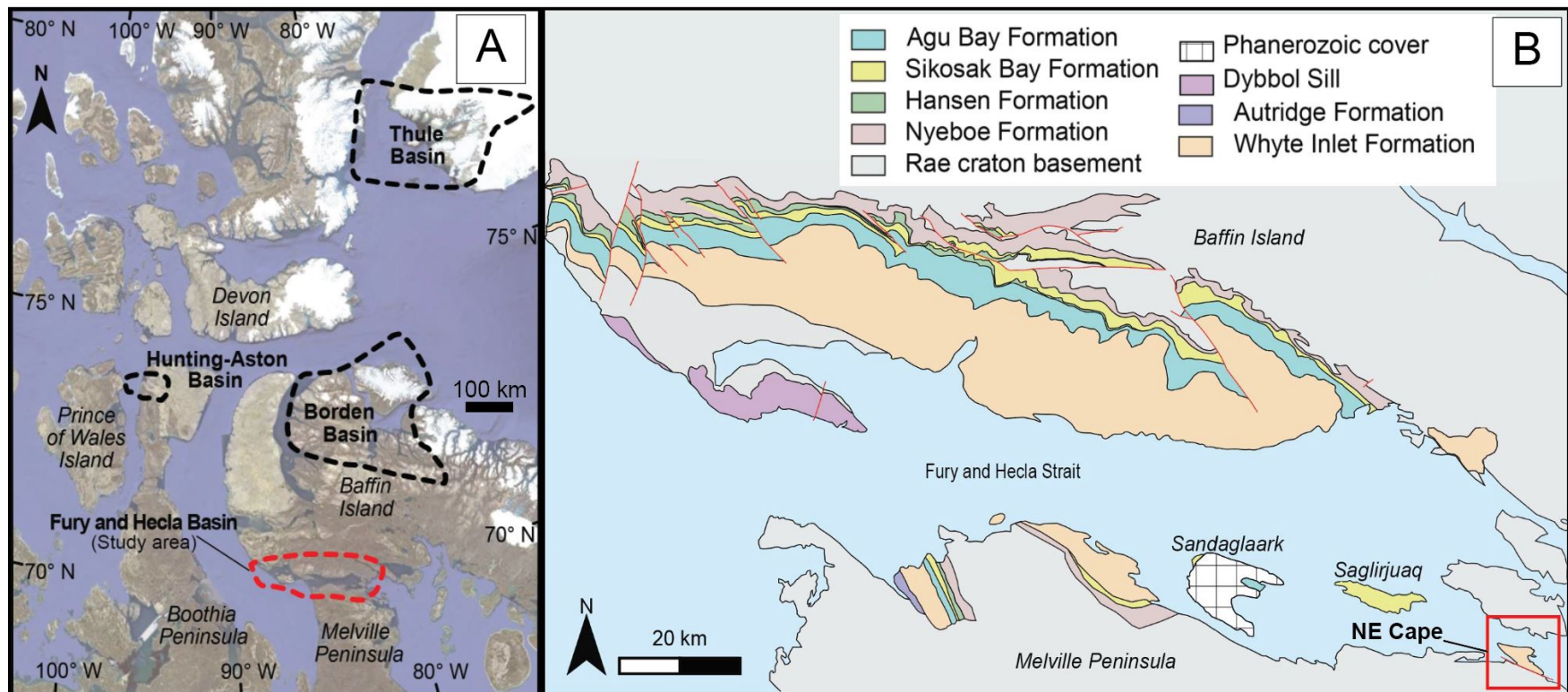
Figure 2-2: Basin-scale maps

Geological sketches showing a) the regional distribution of the Bylot basins, and b) most of the Fury and Hecla Basin (modified after Chandler, 1988). Note that basin outliers farther to the east are not included in the sketch. The northeast cape of Melville Peninsula, the location for a detailed study of the Whyte Inlet Formation, is indicated in panel B with a red box.
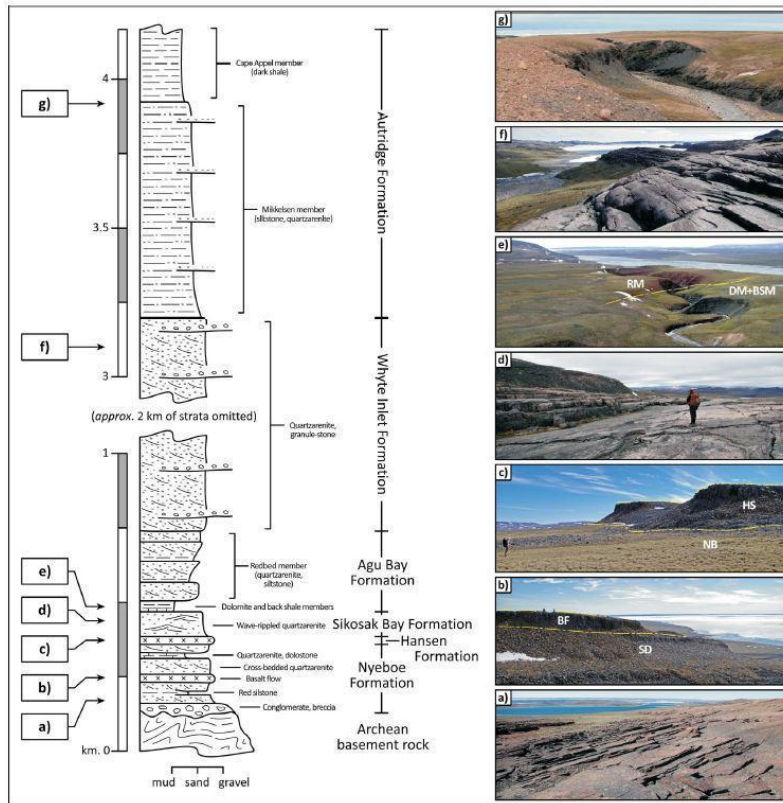
Figure 2-3: General stratigraphic column of the Fury and Hecla Basin

Stratigraphy of the Fury and Hecla Group, which includes a) the Nyeboe Formation (foreground is ~20m wide); b) the basalt flow (BF) in the Nyeboe Formation and sandstone (SD; inukshuks on top of the cliff are ~1.5 m tall); c) the Hansen Formation (HS) and the Nyeboe Formation (NB; geologist is ~1.9 m tall); d) the Sikosak Bay Formation (geologist is ~1.9 m tall); e) the dolostone member (DM), black shale member (BSM) and redbed member (RM) of the Agu Bay Formation (river is ~3 m wide); f) the Whyte Inlet Formation (foreground is ~15 m wide) and g) the Autridge Formation (canyon is ~30 m wide).
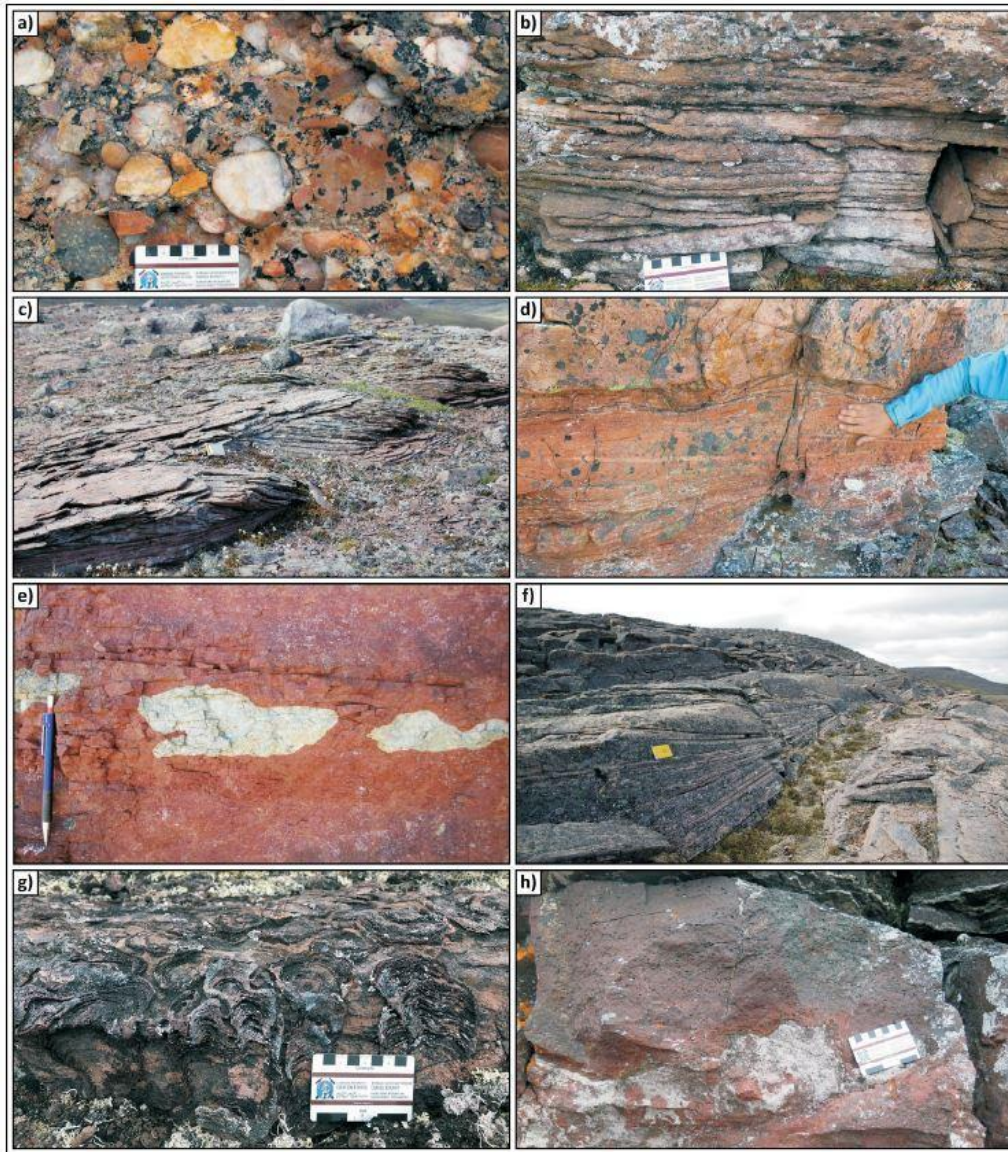
Figure 2-4: Nyeboe Fm photo table

Outcrops of Nyeboe Formation facies: a) quartz-pebble conglomerate; b) planar-stratified sandstone; c) cross-stratified sandstone (exhibiting planar cross sets; compass is ~10 cm long); d) hummocky cross-stratified sandstone; e) planar-stratified heterolithic beds (pencil is ~15 cm long); f) pin-stripe‑laminated sandstone (field notebook is ~20 cm long); g) planar-stratified sandstone and stromatolitic dolostone; h) detail of a basalt flow.
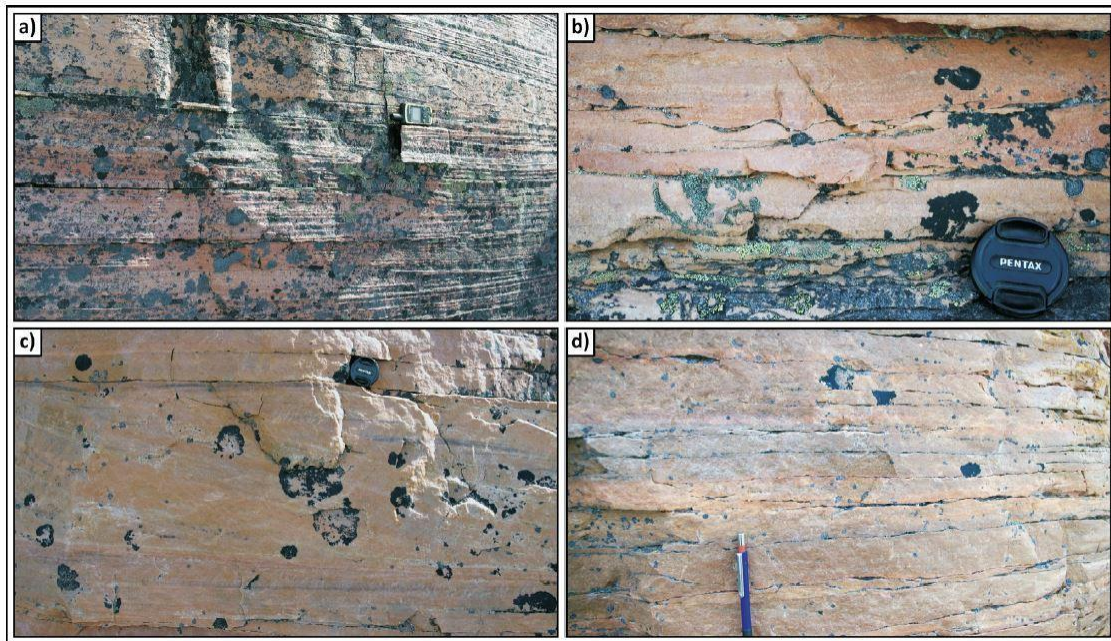
Figure 2-5: Sikosak Bay and Whyte Inlet fms photo table

Outcrops of the a) Sikosak Bay and b‒d) Whyte Inlet formations: a) planar-stratified sandstone with undulatory (wave ripple)forms (satellite messenger is ~15 cm long); b) wave-rippled sandstone (lens cap is ~5 cm across); c) cross-stratified sandstone (lens cap is~5 cm across); d) planar-stratified sandstone (pencil is ~15 cm long).
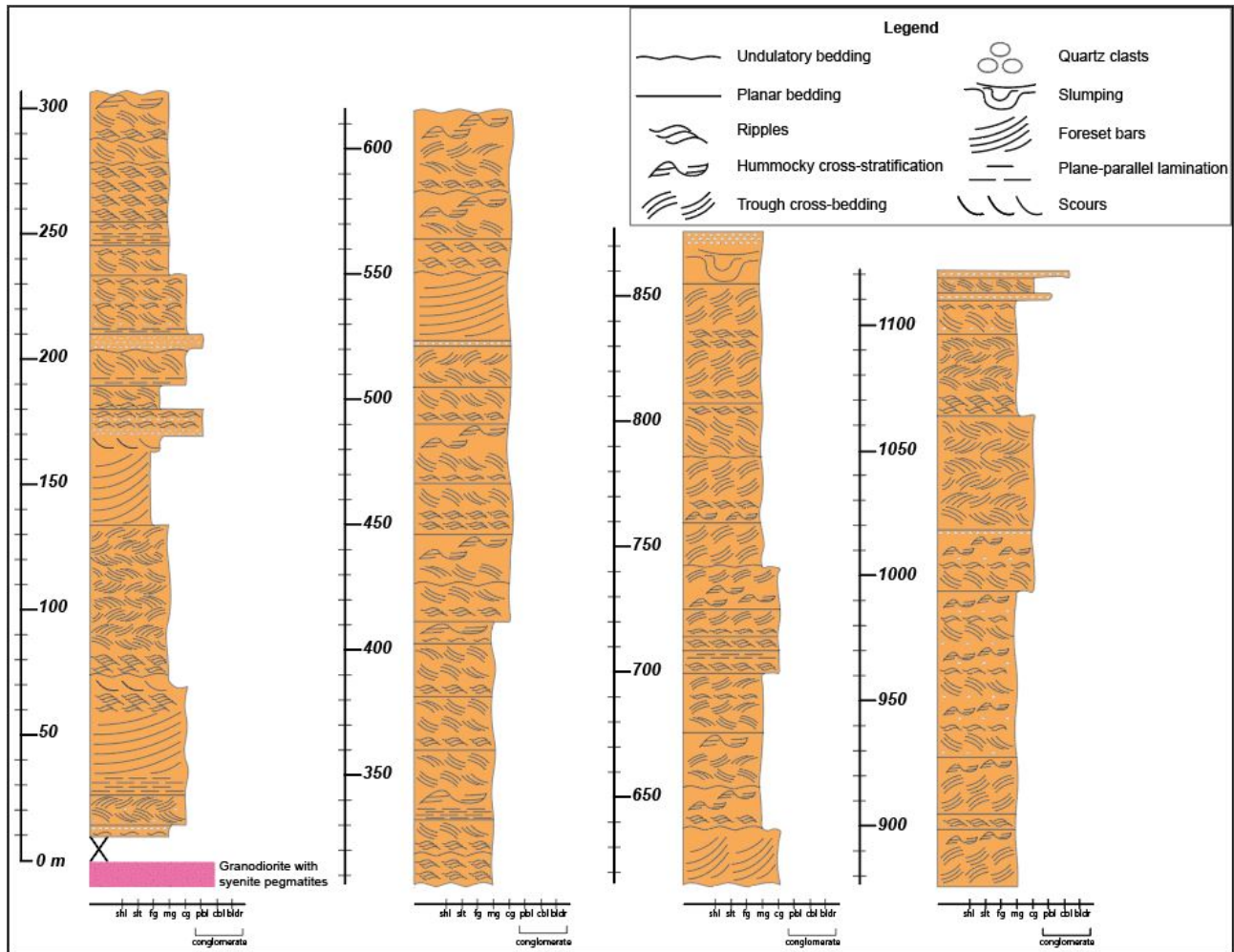
Figure 2-6: NE cape stratigraphic section

Stratigraphic section from the Northeast Cape of Melville Peninsula indicating grain size and sedimentary structures. Stratigraphic section entirely composed of Whyte Inlet Formation. Legend includes sedimentary structures and bedding surfaces.
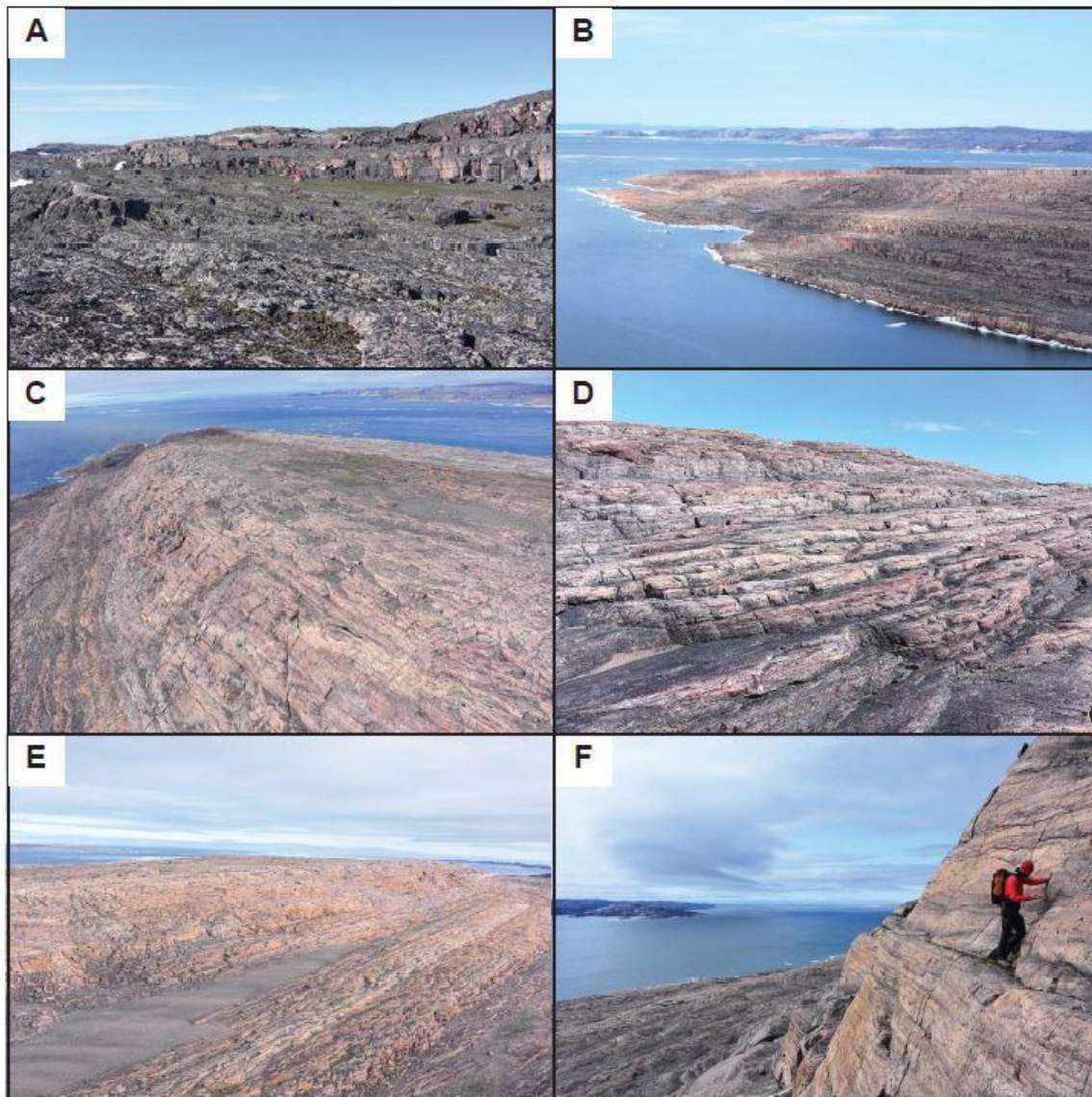
Figure 2-7: NE cape photo table

Photo plate of Northeast Cape exposure of the Whyte Inlet Formation on Melville peninsula:

contact between the basement rocks and overlying sedimentary strata (A); view of the strata from

helicopter (B); along strike aerial view of strata looking west (C); stepwise type exposure typical

of Whyte Inlet strata in this location (D); along strike view of the strata looking east (E); cliff

exposure of the Whyte Inlet Formation looking southeast, basement rock exposure of the Melville

Peninsula seen in background (F).
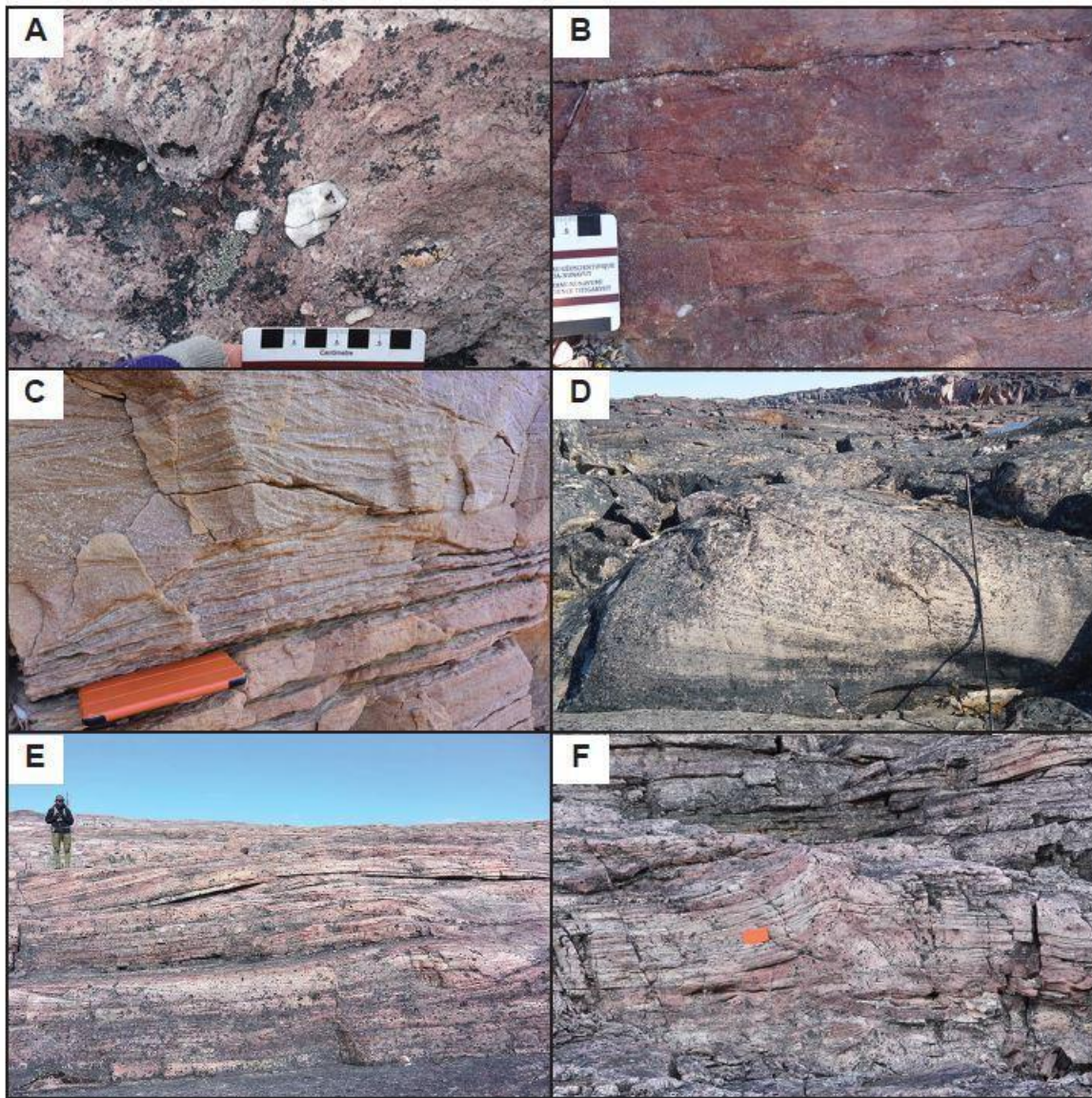
 Figure 2-8: NE cape sedimentary structures photo table

Photo plate indicating sedimentary structures found on the Northeast Cape of the Whyte Inlet
Formation (Fig. 2-2): floating quartz cobbles and pebbles (A); normally graded sedimentary beds
with quartz pebbles concentrated at the base of the bed (B); ripple cross-lamination (C); m-scale
trough cross-bed (D); sand wave clinoform (E); and slump structure (F).

Map centered on 69° 41' 17" N 82° 35' 26" W
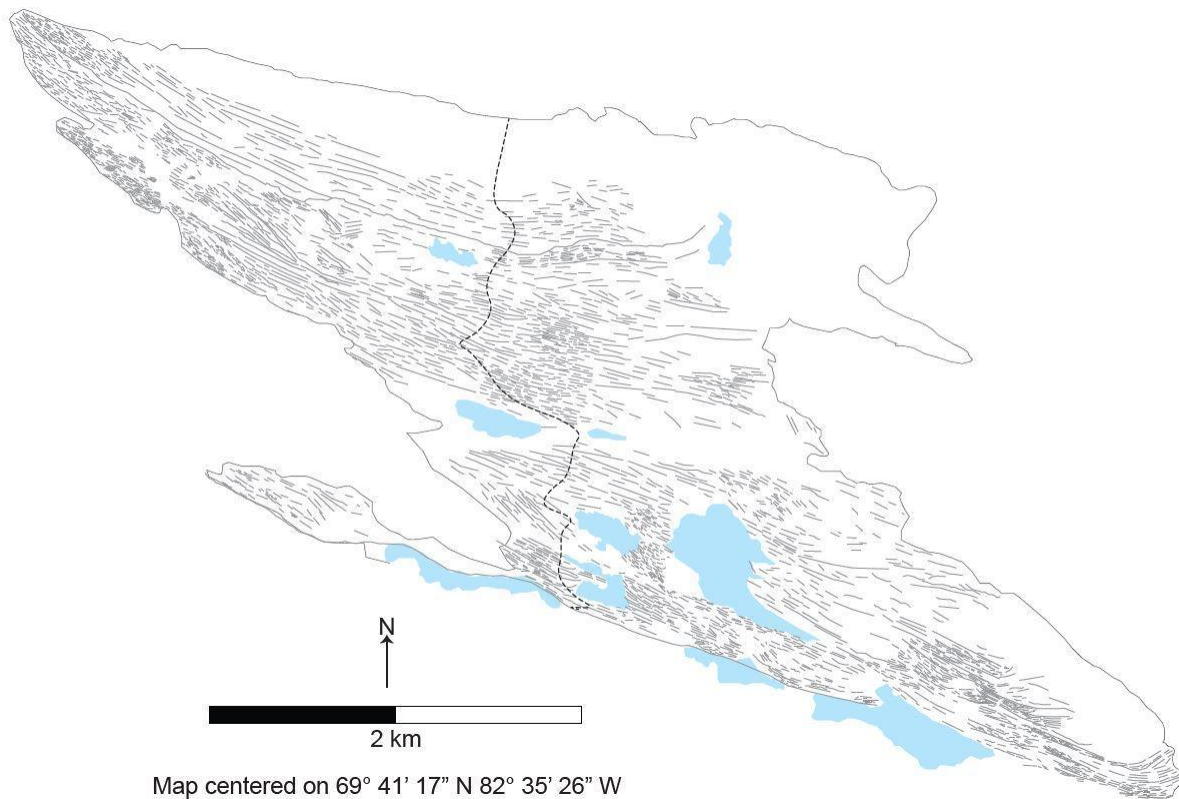
Figure 2-9: Architectural line drawing

Architectural line drawing of any type of bedding surface, such as foreset, from the exceptional exposure of the Whyte Inlet Formation on the Northeast Cape of the Melville Peninsula.Blue indicates standing water. Lines were drawn on detailed satellite photos to infer large trends in the overall sedimentary architecture. Dotted lines indicate traverse to construct the stratigraphic section.
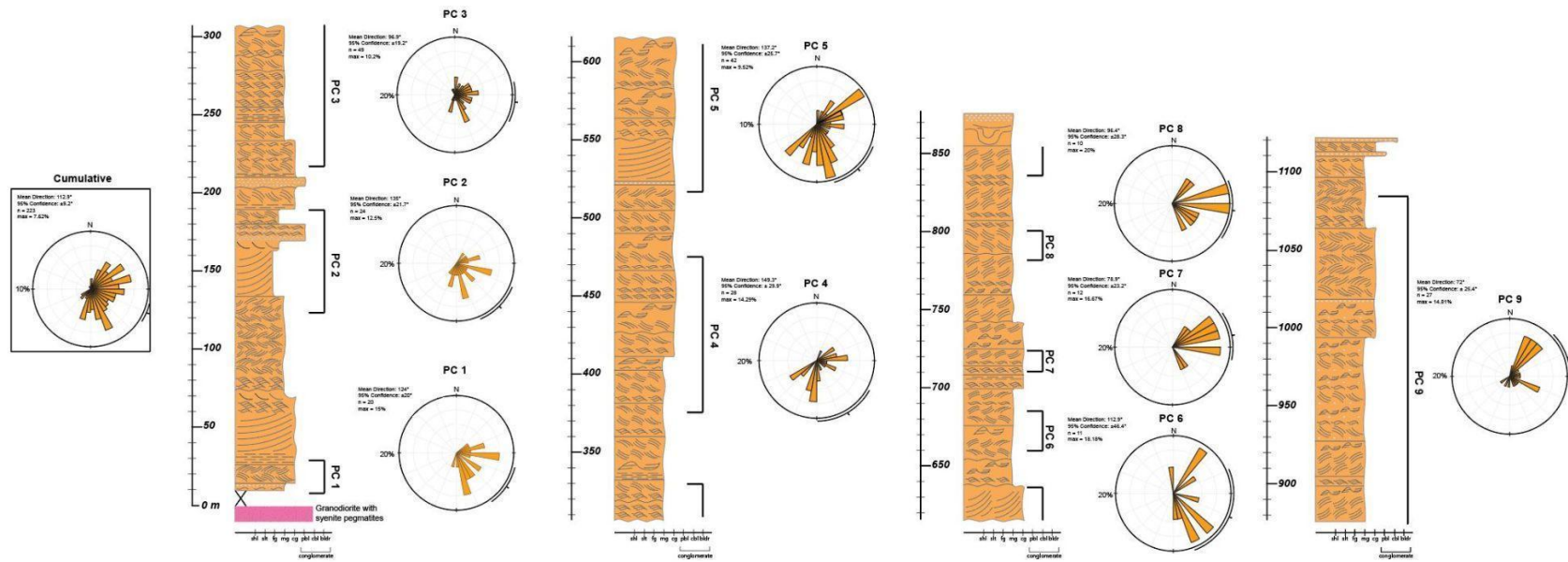
Figure 2-10: NE Cape stratigraphic column

Paleoflows indicated on the stratigraphic section. Cumulative paleoflows compiled on the rose diagram on the left. PC: paleocurrent.

Figure 2-11: NE Cape paleocurrents

Paleoflows indicated on rose diagrams on the left and right. The strata it corresponds to is color coded on traverse and the architectural diagram. Strata young to the north. The rose diagrams on the right are not part of the main traverse and therefore not color-coded. PC: paleocurrent.

2.9   Tables

Paleocurrent	n	Mean direction (degrees)	Max (percentage)
1	20	124	15
2	24	135	12.5
3	48	96.9	10.2
4	28	149.3	14.29
5	42	137.2	137.2
6	11	112.9	18.18
7	12	78.9	16.67
8	10	96.4	20
9	27	72	14.81
10	20	87.2	10
11	20	86.9	15

Table 2-1: Paleocurrent group statistics

Statistics of rose diagrams depicted on Figure 11

2.10 References

Allen, J.R., 1968: The nature and origin of bed-form hierarchies; Sedimentology, v. 10, p. 161‑182.

Berman, R.G., Pehrsson, S.J., Davis, W.J., Ryan, J.J., Qui, H. and Ashton, K.E. 2013: The Arrowsmith orogeny: geochronological and thermobarometric constraints on its extent and tectonic setting in the Rae craton, with implications for pre-Nuna supercontinent reconstruction; Precambrian Research, v. 232, p. 44‑69.

Berne, S., Trentesaux, A., Stolk, A., Missiaen, T., and De Batist, M., 1994, Architecture and long-term evolution of a tidal sand bank: The Middelkerke Bank (southern North Sea); Marine

Geology, v. 121, p. 57‒72.

Blackadar, R.G. 1958: Fury and Hecla Strait map-area; Geological Survey of Canada, map 3-1958.

Blackadar, R.G. 1963: Additional notes to accompany map 3-1958 (Fury and Hecla Strait map-area) and map 4-1958 (Foxe Basin north map-area); Geological Survey of Canada, Paper 62-35, 22 p.

Blackadar, R.G. 1970: Precambrian geology of northwestern Baffin Island, District of Franklin; Geological Survey of Canada, Bulletin 191, 89 p.

Blackadar, R.G. and Lemon, R.R.H. 1963: Admirality Inlet area, Baffin Island, District of Franklin; Geological Survey of Canada, Memoir 328, 84 p.

Bovingdon, P.J., Tinkham, D. and Steenkamp, H.M. 2018: Mafic‒ ultramafic rocks north of Fury and Hecla Strait, Baffin Island, Nunavut; in Summary of Activities 2018, Canada- Nunavut Geoscience Office, p. 63‒74.

Busby-Spera, C.J., And White, J.D.L., 1987: Variation in peperite textures associated withdiffering host-sediment properties; Bulletin of Volcanology, v. 49, p. 765‒775.

Cawood, P.A., Nemchin, A.A., Strachan, R., Prave, T. and Krabbendam, M. 2007: Sedimentary basin and detrital zircon record along East Laurentia and Baltica during assembly and breakup of Rodinia; Journal of the Geological Society, v. 164, p. 257‒275.

Chandler, F.W. 1988: Geology of the Late Precambrian Fury and Hecla Group, northwest Baffin Island, District of Franklin; Geological Survey of Canada, Bulletin 370, 30 p.

Chandler, F.W., Charbonneau, B.W., Ciesielski, A, Maurice, Y.T. and White, S. 1980: Geological studies of the late Precambrian supracrustal rocks and underlying granitic basement, Fury and Hecla Strait area, Baffin Island, District of Mackenzie; Geological Survey of Canada, Current Research, Paper 80-1A, p. 125‒132.

Chandler, F.W. and Stevens, R.D. 1981: Potassium-argon age of the late Proterozoic Fury and Hecla Formation, northwest Baffin Island, District of Franklin; Geological Survey of Canada, Current Research, Paper 81-1A, p. 37‒40.

Clifton, H.E. 2006: A re-examination of facies models for clastic shorelines; in Facies Models Revisited, H.W. Posamentier, R.G.Walker (ed.), SEPM Special Publication, v. 84, p. 293‒337.

Collinson, J.D., Mountney, N.P. and Thompson, D.B. 2006: Sedimentary Structures; Terra Publishing, Harpenden, UK, 292 p.

Covey, M., 1986: The evolution of foreland basins to steady state: evidence form the western Taiwan foreland basin, in Allen, P.A., and Homewood, P.; Foreland Basins: International Association of Sedimentologists, Special Publications, v. 8, p. 77‒90.

Dawes, P.R. 1997: The Proterozoic Thule Supergroup, Greenland and Canada: history, lithostratigraphy and development; Geology of Greenland Survey, Bulletin 174, 150 p.

Ernst, R.E. and Buchan, K.L. 2001: Large mafic magmatic events through time and links to mantle -plume heads; in Mantle Plumes: Their Identification Through Time; Geological Society of America, Special Paper 352, p. 483‒575.

Flemming, B.W., 1980: Sand transport and bedform patterns on the continental shelf between Durban and Port Elizabeth (southeast African continental margin); Sedimentary Geology, v. 26, p. 170‒205.

Gibson, T.M., Shih, P.M., Cumming, V.M., Fischer, W.W., Crockford, P.W., Hodgskiss, M.S.W., Wörndle, S., Creaser, R.A., Rainbird, R.H., Skulski, T.M. and Halverson, G.P. 2017: Precise age of Bangiomorpha pubescens dates the origin of eukaryotic photosynthesis; Geology, v. 46, p. 135‒138.

Goff, J.A., Swift, D.J.P., Duncan, C.S., Mayer, L.A., and Hughes-Clarke, J., 1999: High resolution swath sonar investigation of sand ridge, dune and ribbon morphology in the offshore environment of the New Jersey margin; Marine Geology, v. 161, p. 307‒337.

Greenman, J.W., Patzke, M, Halverson, G.P. and Ielpi, A. 2018: Refinement of the stratigraphy of the late Mesoproterozoic Fury and Hecla Basin, Baffin Island, Nunavut, with a specific focus on the Agu Bay and Autridge formations; in Summary of Activities 2018, Canada-Nunavut Geoscience Office, p. 85‒96.

Greenman, J.W., Rooney, A.D., Patzke, M., Ielpi, A., and Halverson, G.P., 2021: Re-Os geochronology highlights widespread latest Mesoproterozoic (ca. 1090‒1050) cratonic basin development on northern Laurentia; Geology, v. 49, p. 779‒783.

Hahn, K.E., Turner, E.C., Babechuk, M.G. and Kamber, B.S. 2015: Deep-water seep-related carbonate mounds in a Mesoproterozoic alkaline lake, Borden Basin (Nunavut, Canada); Precambrian Research, v. 271, p. 173‒197.

Heaman, L.M., LeCheminant, A.N. and Rainbird, R.H. 1992: Nature and timing of Franklin igneous events, Canada: implications for a Late Proterozoic mantle plume and the breakup of Laurentia; Earth and Planetary Science Letters, v. 109, p. 117‑131.

Herbers, D.S., MacNaughton, R.B., timmer, E.R., Gingras, M.K., and Hubbard, S., 2016: Sedimentology and ichnology of an Early‑Middle Cambrian storm-influenced barred shoreface succession, Colville Hills, Northwest Territories; Bulletin of Canadian Petroleum Geology, v. 64, p. 538‑554.

Hiatt, E.E., Palmer, S.E., Kyser, T.K. and OʹConnor, T.K. 2010: Basin evolution, diagenesis and uranium mineralization in the Paleoproterozic Thelon Basin, Nunavut, Canada; Basin Research, v. 22, p. 302‑323.

Jackson, G.D. 1986: Notes on the Proterozoic Thule Group, northern Baffin Bay; Current Research, Part A, Geological Survey of Canada, Paper 86-1A, p. 541‑552.

Jackson, G.D. and Iannelli, T.R. 1981: Rift-related cyclic sedimentation in the Neohelikian Borden Basin, Northern Baffin Island; in Proterozoic Basins of Canada, F.H.A. Campbell (ed.), Geological Survey of Canada, Paper 81-10, p. 269‑302.

Jackson, G.D. and Berman, R.G. 2000: Precambrian metamorphic and tectonic evolution of northern Baffin Island, Nunavut, Canada; The Canadian Mineralogist, v. 38, p. 399‑421.

Johnson, H. D. 1977: Shallow marine sand bar sequences: an example from the late Precambrian of North Norway; Sedimentology, v. 24, p. 245‑270.

Kah, L.C., Bartley, J.K., and Stagner, A.F., 2009: Reinterpreting a Proterozoic enigma: Conophyton‑Jacutophyton stromatolites of the Mesoproterozoic Atar Group, Mauritania;

in Swart, P.K., Eberli, G.P., and McKenzie, J.A., eds., Perspectives in Carbonate Geology: A Tribute to the Career of Robert Nathan Ginsburg: International Association of Sedimentologists, Special Publication 41, p. 277‑295.

LeCheminant, A.N. and Heaman, L.M. 1989: Mackenzie igneous events, Canada: middle Proterozoic hotspot magmatism associated with ocean opening; Earth and Planetary Science Letters, v. 96, p. 38‑48.

Li, Z. X., Bogdanova, S. V., Collins, A. S., Davidson, A., De Waele, B., Ernst, R. E., Fitzsimons, I.C.W., Fuck, R.A., Gladkochub, D.P., Jacobs, J. Karlstrom, K.E., Lu, S., Natapov, L.M., Pease, V., Pisarevsky, S.A., Thrane, K., Vernikovsky, V., 2008: Assembly, configuration, and break-up history of Rodinia: A synthesis; Precambrian Research, 160(1-2), 179‑210.

Long, D.G.F. 2017: Evidence of flash floods in Precambrian gravel dominated ephemeral river deposits; Sedimentary Geology, v. 347, p. 53‑66.

Long, D.G.F. and Turner, E.C. 2012: Tectonic, sedimentary and metallogenic re-evaluation of basal strata in the Mesoproterozoic Bylot basins, Nunavut, Canada: are unconformity- type uranium concentrations a realistic expectation?; Precambrian Research, v. 214‑215, p. 192‑209.

Loron, C.C., Rainbird, R.H., Turner, E.C., Greenman, J.W. and Javaux, E.J. 2018: Implications of selective predation on the macroevolution of eukaryotes: evidence from Arctic Canada; Emerging Topics in Life Sciences. v. 2 (2). p. 247‑155.

Marconato, A., de Almeida, R.P., Turra, B.B., and dos Santos Fragoso-Cesar, A.R., 2014: Pre-vegetation fluvial floodplains and channel-belts in the Late Neoproterozoic‑Cambrian

Santa B´arbara group (Southern Brazil); Sedimentary Geology, v. 300, p. 49‾61.

Mayr, U., Brent, T.A., de Freitas, T., Frisch, T., Nowlan, G.S. and Okulitch, A.V. 2004: Geology of eastern Prince of Wales Island and adjacent smaller islands, Nunavut; Geological Survey of Canada, Bulletin 547, 88 p.

Mountney, N.P. 2006: Eolian facies; in Facies Models Revisited, H.W. Posamentier and R.G. Walker (ed.), SEPM Special Publication, v. 84, p. 19‾83.

Olson, R.A., 1977, Geology and genesis of zinc-lead deposits within a late Proterozoic dolomite, Northern Baffin Island, N.W.T. [Ph.D. Thesis]: University of British Colombia, 387 p.

Patzke, M., Greenman, J.W., Halverson, G.P., and Iepli, A. 2021: The initiation of the Mesoproterozoic Bylot basins (Nunavut, Arctic Canada) as recorded in the Nyeboe Formation, Fury and Hecla Group; Journal of Sedimentary Research, v. 91, p. 1166‾1187.

Pehrsson, S.J., Eglington, B.M., Evans, D.A.D., Huston, D. and Reddy, S.M. 2016: Metallogeny and its link to orogenic style during the Nuna supercontinent cycle; in Supercontinent Cycles Through Earth History, Z.X. Li, D.A.D.

Rainbird, R.H., Davis,W.J., Pehrsson, S.J.,Wodicka, N., Rayner, N. and Skulski, T. 2010: Early Palaeoproterozoic supracrustal assemblages of the Rae domain, Nunavut, Canada: intracratonic basin development during supercontinent break-up and assembly; Precambrian Research, v. 181, p. 167‾186.

Rainbird, R.H., Rayner, N.M., Hadlari, T., Heaman, L.M., Ielpi, A., Turner, E.C. and MacNaughton, R.B. 2017: Zircon provenance data record the lateral extent of pancontinental, early Neoproterozoic rivers and erosional unroofing history of the

Grenville orogen; Geological Society of America, Bulletin 129, p. 1408‑1423.

Snedden, J.W., and Dalrymple, R.W., 1999: Modern shelf sand bodies: from historical perspective to a unified theory for sand body genesis and evolution, in Bergman, K.M., and Snedden, J.W., eds., Isolated Shallow Marine Sandbodies: Sequence Stratigraphic Analysis and Sedimentologic Interpretation; SEPM, Special Publication 64, p. 13‑28.

Steenkamp, H.M., Bovingdon, P.J., Dufour, F., Généreux, A., Greenman, J.W., Halverson, G.P., Ielpi, A., Patzke, M. and Tinkham, D.K. 2018: New regional bedrock mapping of Precambrian rocks north of Fury and Hecla Strait, northwestern Baffin Island, Nunavut; in Summary of Activities 2018, Canada-Nunavut Geoscience Office, p. 47‑62.

Suter, J.R., 2006: Clastic shelves, in Posamentier, H.W., and Walker, R.G., eds.; Facies Models Revisited: SEPM, Special Publication 84, p. 339‑397.

Stubblefield, W.L., McGrail, D.W., and Kersey, D.G., 1984: Recognition of transgressive and post-transgressive sand ridges on the New Jersey continental shelf, in Tillman, R.W., and Siemers, C.T., eds., Siliciclastic Shelf Sediments: SEPM, Special Publication 34, p. 1‑23.

Takashimizu, Y., and Masuda, F., 2000, Depositional facies and sedimentary successions of earthquake-induced tsunami deposits in Upper Pleistocene incised valley fills, central Japan: Sedimentary Geology, v. 135, p. 231‑239.

Tuke, M.F., Dineley, D.L. and Rust, B.R. 1966: The basal sedimentary rocks in Somerset Island, N.W.T; Canadian Journal of Earth Sciences, v. 3, p. 697‑711.

Turner, E.C. 2009: Mesoproterozoic carbonate systems in the Borden Basin, Nunavut; Canadian Journal of Earth Science, v. 46. p. 915‑938.

Turner, E.C. 2011: Structural and stratigraphic controls on carbonate-hosted base metal mineralization in the Mesoproterozoic Borden Basin (Nanisivik District), Nunavut; Economic Geology, v. 106, p. 1197‒1223.

Turner, E.C. and Kamber, B.S. 2012: Arctic Bay Formation, Borden Basin, Nunavut (Canada): Basin evolution, black shale, and dissolved metal systematics in the Mesoproterozoic ocean; Precambrian Research, v. 208‒211, p. 1‒18.

Turner, E.C., Long, D.G.F., Rainbird, R.H., Petrus, J.A. and Rayner, N.M. 2016: Late Mesoproterozoic rifting in Arctic Canada during Rodinia assembly: impactogens, trans-continental far-field stress and zinc mineralisation; Terra Nova, v. 28, p. 188‒194.

Walker, R.G., and Plint , A.G., 1992: Wave- and storm-dominated shallow marine systems, in Walker, R.G., and James, N.P., eds.; Facies Models: Response to Sea Level Change: Geological Association of Canada, p. 219‒238.

Went, D.J., 2005: Pre-vegetation alluvial fan facies and processes: an example from the Cambro-Ordovician Rozel Conglomerate Formation, Jersey, Channel Islands; Sedimentology, v. 52, p. 693‒713.

Chapter 3

3 The initiation of the Mesoproterozoic Bylot basins (Nunavut, Arctic Canada) as recorded in the Nyeboe Formation, Fury and Hecla Group

Mollie Patzke,[1] J. Wilder Greenman,[2] Galen P. Halverson,[2] and Alessandro Ielpi[1]

[1]Harquail School of Earth Sciences, Laurentian University, Sudbury, Ontario P3E 2C6, Canada

[2]Department of Earth and Planetary Sciences/Geotop, McGill University, Montréal, Quebec H3A 0E8, Canada

3.1 Abstract

Reconstructing Precambrian sedimentary environments over broad cratonic regions often relies on a combination of facies, structural, and provenance analyses. The Mesoproterozoic (ca. 1270−1090 Ma) Fury and Hecla Group, exposed on the Melville Peninsula and northern Baffin Island (Nunavut, Canada), is considered broadly correlative with strata of the Borden, Hunting-Aston, and Thule basins (together referred to as the Bylot basins). We present the results of updated mapping and the first high-resolution sedimentologic and stratigraphic analysis of the lowermost unit in the Fury and Hecla Group, the Nyeboe Formation. The Nyeboe Formation comprises five distinct facies associations: alluvial to fluvial, eolian-backshore, marine-intertidal, marine foreshore to shoreface, and marine-offshore. Thin mafic units are interbedded within the marine shoreface facies and are interpreted to represent volcanic flows. Lateral relationships between facies associations are complex, but generally, facies associations transition from a terrestrial environment at the base to a nearshore marine environment at the top, indicating an

overall transgression. Considering both the along-strike and -dip thickness trends, the presence of mafic volcanic rock units, and possible syndepositional fault orientations crosscutting the deposits, we infer that the Fury and Hecla Group was deposited in a regime of crustal thinning in a half-graben setting. Our results from the Nyeboe Formation suggest a lithostratigraphic correlation to the Nauyat and Adams Sound formations of the Borden Basin. Therefore, this study establishes a geodynamic link between the opening of the Fury and Hecla Basin to the other Bylot basins and contributes to the understanding of a large late-Mesoproterozoic intracontinental-basin system.

3.2   Introduction

Sedimentary facies analysis — the synthesis of the nature, scale, heterogeneity, and physical elements of ancient and modern depositional environments into consistent conceptual models (Walker 2006) — is a cornerstone for the tectonostratigraphic analysis of sedimentary basins. A pillar of facies analysis is that ancient sediments can be compared with deposits and processes from modern environments (i.e.. Collinson et al. 2006; Walker 2006). However, modern and ancient sedimentary environments do not always share similar settings and processes when applied to Precambrian sedimentary records due to the limited influence of the biosphere (Shea 1982; Donaldson et al. 2002; Miall 2014). Despite recent advances in Precambrian basin analysis, including refined methods of understanding depositional architecture over a range of paleodepositional settings (Ielpi and Rainbird 2015; Santos and Owen 2016; Bállico et al. 2017; Lebeau and Ielpi 2017), questions remain regarding the sedimentology of both alluvial and shallow-marine deposits (Long 2011; Eriksson et al. 2013; Davies et al. 2017; McMahon et al. 2017). Few stratigraphic units record rapid vertical and lateral change between both clastic and chemical sedimentary systems such as eolian, fluvial, and marine.

The Canadian Arctic contains exceptionally well-preserved Precambrian sedimentary basins that formed in response to the amalgamation, tenure, and breakup of the Nuna and Rodinia supercontinents (Davidson 2008; Pehrsson et al. 2013; Andersen 2014). Young (1979) first assigned Precambrian strata of the western Canadian Arctic into time-bounded subdivisions, which were then refined by Rainbird et al. (1996). The discovery of the earliest red algal fossil Bangiomorpha pubescens from the Borden and Hunting-Aston basins (Figs. 3-1, 2) sparked recent attention to the Bylot basins of Nunavut and Greenland (Butterfield 2000; Knoll et al. 2013).

The lowest formation of the Fury and Hecla Group, the Nyeboe Formation, records the opening of the Fury and Hecla Basin (Fig. 3-1). Prior studies by Chandler (1988) and Long and Turner (2012) recognized lithological subdivisions and provided the basis for this detailed sedimentological study of the Nyeboe Formation. We present new results including facies, depositional architecture, paleocurrent, and structural analysis of the Nyeboe Formation and synthesize our results into an interpretive block model. Finally, we compare the Nyeboe Formation to similar sandstone units in the region to establish tighter tectonostratigraphic linkages between the early depositional records of the Fury and Hecla and nearby basins.

3.3   Geological setting

The Fury and Hecla Group represents the fill of the eponymous basin in Nunavut, Canada (Fig. 3-1). It comprises sandstone with minor shale, conglomerate, dolostone, and mafic volcanic rocks (Fig. 3-2). Exposures occur over a region roughly 160 km by 50 km wide that straddles the Fury and Hecla Strait between northern Baffin Island and Melville Peninsula (Fig. 3-1). Due to lithological similarities, the Fury and Hecla Basin is correlated to the Borden, Thule, and Hunting-Aston basins located on the arctic islands of Nunavut and Greenland (Blackadar and Fraser, 1960).

Together these basins make up the Bylot basin system (Jackson and Iannelli 1981; Long and Turner 2012, and references therein) (Fig. 3-2).

Basin type and evolution has been interpreted variably over the last ~40 years. Jackson and Iannelli (1981) and Olson (1977) proposed that the Bylot basins formed as aulacogens. Sherman et al. (2002) recognized a shift in deepening direction in the upper stratigraphy and interpreted this to represent deposition in a foreland-basin setting resulting from east-directed compression. Long and Turner (2012) suggested that the Bylot basins opened as intracratonic sag basins. Turner et al. (2016) later proposed that middle and upper strata of the Bylot basins were accommodated in an impactogen that formed in the foreland due to far-field stresses propagated inland from the Grenville Orogen during the formation of Rodinia (ca. 1.1 Ga).

Recent geochemical studies suggest that the Borden Basin was intermittently restricted from the open ocean (Hahn et al. 2015, Hahn and Turner 2017; Gibson et al. 2019; Hodgskiss et al. 2020). Broad chronostratigraphic constraints for the Bylot basins are from basalt found in their lowermost stratigraphy and crosscutting mafic dikes, which have been correlated with the ca. 1270 Ma Mackenzie and ca. 720 Ma Franklin large igneous provinces (LIPs), respectively (Fahrig et al. 1981; Jackson and Iannelli 1981; Chandler 1988; LeCheminant and Heaman 1989; Heaman et al. 1992; Pehrsson and Buchan 1999). The inferred age of ca. 1.2 Ga for the Bylot basins was linked to the presumed Mackenzie-age basalt units in the lower Bylot Supergroup of the Borden Basin (Fahrig et al. 1981; Kah et al. 1999), until more recent studies presented refined ages from black shale units. A U-Pb-Th whole rock age of 1092 ± 59 Ma on black shales of the Arctic Bay Formation (Fig 2.; Turner and Kamber 2012) and Re-Os ages of 1048 ± 12 Ma and 1046 ± 16 Ma of the Arctic Bay and Victor Bay formations (Gibson et al. 2018), respectively, indicate instead

that the middle Bylot Supergroup postdates the Mackenzie event by >200 Myr. Greenman et al.

(2021) reported a Re-Os age of 1087.1 ± 5.9 Ma on organic-rich shale from the Agu Bay

Formation in the Fury and Hecla Basin. This age is consistent with ages reported for the Borden

Basin and indicate widespread black shale deposition of the middle of their stratigraphy of both

basins (Greenman et al. 2021).

The Fury and Hecla Group nonconformably overlies Archean to Paleoproterozoic

crystalline basement of the Rae province in the Laurentian Shield (Chandler et al. 1980; Chandler

1988) and consists of six units: the Nyeboe, Sikosak Bay, Hansen, Agu Bay, Whyte Inlet, and

Autridge formations (Chandler et al. 1980; Chandler 1988) (Fig 1). The Hansen Formation,

previously interpreted as extrusive, is now regarded as a shallowly emplaced sill since it appears to

crosscut strata (Chandler et al. 1980; Steenkamp et al. 2018; Dufour et al. 2020). Exposure of the

Fury and Hecla Group is characterized by hilly ridges and slopes with intervals of blockfield cover

in the east (Fig. 3-3A) to steeper ridges in the central and west (Fig. 3-3B). Outcrops along river

canyons are also present (Fig. 3-3C). The basal Nyeboe Formation contains sandstone, shale,

dolostone, and mafic volcanic rocks (Chandler 1988). Chandler (1988) divided the Nyeboe

Formation into seven stratigraphic members based on lithology from bottom to top: local basal

polymict breccia, red sandstone and shale, quartz conglomerate, a second red sandstone and shale

member, dolomitic quartzarenite and stromatolitic dolomite, altered basalt, and red sandstone. The

Nyeboe Formation passes upward into the mature, more orange-weathering monotonous,

quartzarenite of the Sikosak Bay Formation, although poor exposure precludes determining if the

contact is conformable (Patzke et al. 2018).

Blackadar (1958) characterized the Baffin Island exposure of the Fury and Hecla Group as a south-southeast-dipping homocline. The homocline was recently recognized as part of a broad west-northwest-plunging syncline with the hinge axis located in the Fury and Hecla Strait, and a broad, northwest-plunging anticline on the Melville Peninsula (Greenman et al. 2020; Their figure 2). Timing of deformation is poorly constrained.

3.4   Methods

This study integrates sedimentary facies analysis and stratigraphic logging and is corroborated by paleocurrent analysis and petrography. Fieldwork was conducted in the Fury and Hecla Strait region during the summers of 2018 and 2019, and outcrops were accessed through foot traverses supported by helicopter. Using the geological map of Chandler (1988) and Google Earth satellite imagery as references, field relationships between different rocks units were assessed. Chandler′s (1988) seven-member division lacks detail and is abandoned in favor of a facies-association approach owing to the complex internal stratigraphy and lateral facies changes observed in the unit. We define facies association (FA) as a suite of facies that characterize a specific depositional environment (Collison 1969; Reading and Levell 1996). Bed-by-bed, decimeter-scale stratigraphic logging and facies analysis focused on identifying sedimentary structures following the guidelines of Collinson et al. (2006) and Mountney (2006). Five stratigraphic logs of the Nyeboe Formation were measured, spanning 780 m of stratigraphy (Fig. 3 -4). Thickness is estimated and is not meant to represent depositional thickness as strata may have been affected by compaction or erosion after its lithification. Sometimes, satellite imagery was used in combination with field data (dip) to understand thickness using basic trigonometry. Stratigraphic column WG1901 (Fig. 3-4) is a partial log adopted from Greenman et al. (2020;

Their figure 3). Paleocurrent data were collected from the dip-direction of the strata of 81 trough cross-beds, and eight foresets of macroforms exposed in three dimensions at five sites, following general guidelines of Collinson et al. (2006) and Eastwood et al. (2012). Paleocurrent measurements were plotted and analyzed using the OpenStereo software. This dataset is limited to 89 measurement due to time constraints and is not intended to provide a full-scale basin-analysis interpretation. Descriptions of facies in the field were coupled with petrographic observations, which included analysis of grain morphology (sphericity, rounding) and visual estimation of composition and texture (i.e., first-order modal percentage of quartz, feldspar, and lithic grains, and type of matrix and cement); observations were made on thin sections of 15 sandstone samples using a standard petrographic microscope. In sum, we recognized 14 facies in the Nyeboe Formation and grouped them into five facies associations (Table 3-1).

3.5   Results

3.5.1 The Nyeboe Formation

The Nyeboe Formation ranges in thickness from 43 m to 400 m (from estimates based on combined field and satellite-imagery data) and accounts for ~15% of the total thickness of the Fury and Hecla Group. On Baffin Island, the Nyeboe Formation thickens to the west except for one anomalous 158-m-thick section east of the main basin (section BI4; Figs. 3-1, 4). On the Melville Peninsula, the Nyeboe Formation thickens to the northwest (Fig. 3-1). We measured five partial stratigraphic sections of the Nyeboe Formation (WG1901, BI1-4) ranging in thickness from 43 to 400 m (Figs. 3-1, 4).

The Nyeboe Formation comprises sandstone, conglomerate, shale, and dolostone lithologies. In addition to the sedimentary rocks, mafic volcanic rocks are exposed in individual flows ranging in thickness from 2 to 4 m (Fig. 3-5A) near the top of the Nyeboe Formation. On the Melville Peninsula, an ~2-m-thick red-weathering basalt occurs ~250 m stratigraphically above the base of the formation (Greenman et al. 2020). Chandler (1988) described three distinct mafic flows, but we observed only two flows in the western part of the basin. These flows are exposed as units of 2 to 4 m thick discrete units, ~400 and ~650 m stratigraphically above the base of the formation, respectively. At various locations across the basin, single mafic volcanic units are reported ~250 to 350 m stratigraphically above the base of the formation (Chandler 1988), but we were unable to determine if these flows are separate, laterally discontinuous events or a continuation of one of the flows identified at the first section (Fig. 3-4).

The contacts between the individual basalt-flow units and the bounding strata are often recessive (Fig. 3-5A). However, a thin (~5 cm) peperite, consisting of distinct reddish pink quartzarenite with rusty colored globular chips (0.5 to 2 cm) of mafic fragments, indicating subaqueous emplacement on a wet substrate, was recognized below the mafic rocks at one outcrop in the western part of the basin stratigraphically near the top of the Nyeboe Formation (Fig. 3-5B; cf. Busby-Spera and White 1987). The contact between the rust-colored basalt and the underlying pink quartzarenite is covered by felsenmeer, and the peperite is not observed elsewhere. The Nyeboe Formation basalts are pillowed and commonly include amygdules composed of prehnite and pumpellyite (Chandler 1988) (Figs. 3-5C, D).

The availability of suitable outcrops to measure paleocurrents was limited, especially in the marine strata, and therefore much of the paleocurrent dataset is concentrated in the central part of

the mapped Nyeboe Formation. Paleocurrent indicators from trough cross-stratified fluvial strata (Figs. 3-6a, 7) indicate dispersal predominantly to the west, and slightly west-southwest (Fig. 3-6b). Marine facies yield more dispersed paleocurrent readings (Fig. 3-6c). Another eight measurements were collected from one outcrop of large-scale inclined strata in deposits that are also considered marine in origin upper part of the Nyeboe Formation (Chandler 1988; Patzke et al. 2018; Figs. 3-6, 7). Trough cross-strata from the section BI4 transect (Fig. 3-1C), which represents the most eastern exposure of the Nyeboe Formation, indicate northwest transport (n = 10), orthogonal to the dominantly southwestward vector indicated by measurements elsewhere (Fig. 3-6d). Paleoflow data from this study are overall consistent with the measurements collected by Chandler (1988).

3.5.2 Large-scale structural relationships

Evidence for brittle deformation of the Fury and Hecla Group can be subdivided into three categories based on fault orientation and estimated offset (Fig. 3-1). Offsets were estimated based on the difference in thickness of strata where fault repetition occurs based on mapping relationships (Chandler, 1988). A group of faults on the north side of the basin with a strike of ~115° and apparent stratigraphic throw of at least ~300−500 m is subparallel to the axis of basin. These faults displace the basement rocks just below the unconformity with the Fury and Hecla Group, and the Nyeboe, Sikosak Bay, Hansen. Similarly oriented faults are also found in the central and eastern part of the basin (purple faults in Fig. 3-1). Another group of faults with a strike of ~130° and apparent stratigraphic throw of 500−700 m displaces the Nyeboe, Sikosak Bay, Hansen, and rarely the Agu Bay formations. The latter faults are found in the western part of the basin (blue faults in Fig. 3-1). Notably, this group of faults is not seen in basement rocks on the

periphery of the basin. A third group of faults displaces the entire Fury and Hecla Group (e.g., faults striking ~335° and ~020°; red faults in Fig. 3-1; Chandler 1988; Steenkamp et al. 2018). These faults are coaxial with the 720 Ma Franklin dikes (Heaman et al. 1992; Buchan and Ernst 2013).

3.5.3 Facies associations

Combinations of the 14 facies (Table 3-1) were grouped into five different facies associations (FAs): (1) alluvial to fluvial; (2) eolian-backshore; (3) marine-intertidal; (4) wave-dominated marine shelf; and (5) marine offshore-transition (Figs. 3-8−3-12).

3.5.3.1 FA1: Alluvial to Fluvial Facies Association

3.5.3.1.1   Description

Lithology of FA1 ranges from medium-grained quartzarenite to boulder-scale, extraformational and intraformational conglomerate. Quartzarenite grains are subangular and moderately spherical, whereas conglomerate clasts are rounded and nonspherical and occur together with an interspersed sandy matrix. Petrographically, FA1 shows highly compacted, medium-grained quartzarenite with indentations and pressure-solution seams (Fig. 3-13). Bed thickness ranges from 0.25 m to 1.2 m, and the internal stratification of the beds is better developed in the finer-grained fractions (see Table 1). Most beds of FA1 exhibit planar geometry with scoured erosional bases. Texturally immature strata of this FA include breccia (Cbr; Fig. 3-8E), polymict conglomerate (Cpy; Fig. 3-8F), trough cross-stratified sandstone and quartz monomict conglomerate (Stc; Fig. 3-8A-C), and massive sandstone (Sma). Most grain populations are

mature, particularly in planar-cross-stratified sandstones (Sps) and plane-parallel-stratified sandstones (Spc; Fig. 3-8; Table 1).

3.5.3.1.2   Occurrence

FA1 overlies the nonconformity between the Fury and Hecla Group and the Archean to Paleoproterozoic basement granitoids. It occurs in sections WG1901, BI1, BI3, and BI4, where it reaches accumulated thicknesses of 5 m, 21 m, 59 m, and 7 m, respectively. Accumulated thicknesses are determined by summing all intervals of the FA in each section. Sections WG1901 and BI4 also contain, respectively, 28-m- and 26-m-thick intervals that are interbedded with FA4. Regional erosional relief on the nonconformity is inferred from estimates of the FA thickness within covered intervals, estimated at up to 15 m if the covered interval is assumed to consist of sedimentary strata. In section BI3, FA1 stratigraphically overlies FA2 and shoreface FAs. FA1 can be followed along strike for up to 10 km (inferred from satellite imagery) and grades upward into the FA2 or shoreface FA through well-defined, fining-upward trends. Anomalously, section BI3 contains a second interval of FA1 in the upper part of the Nyeboe Formation.

3.5.3.1.3   Interpretation

Based on its sedimentology and stratigraphic position next to other FAs, stacks of planar- and trough-cross-stratified sandstones and conglomerates (Stc, Sps, Spc) are interpreted to represent deposition in pre-vegetation river channels as bars and fills nearing a marine shoreline (Bridge 2006; Muhlbauer et al. 2020). Polymictic conglomerate and massive sandstone (Cpy, Sma) facies are inferred to record outbuilding of small-scale alluvial fans (Went 2005). The breccia (Cbr) represents scree-slope deposition (Went 2005). Notably, Cpy also occurs in upper part of section BI3 (Fig. 3-4). Textural immaturity and unidirectional or bidirectional, mildly

dispersed paleoflow directions (Fig. 3-6) suggest that alluvial to fluvial deposits in the Nyeboe

Formation experienced short-lived WSW-ward transport before deposition in a terrestrial setting

(Collinson 1996; Scherer and Lavina 2006).

3.5.3.2 FA2: Eolian-Backshore Facies Association

3.5.3.2.1   Description

The lithology of FA2 is defined by siltstone to coarse-grained quartzarenite and mudstone.

In outcrop, grains also exhibit a frosted texture. Sandstone beds in FA2 range from 0.5 m to 2 m in

thickness, and their internal stratification is well defined by continuous pinstripe lamination

(Fryberger et al. 1992), i.e., marked and repetitive grain-size segregation. Petrographically, FA2

exhibits compacted, subangular to subrounded, fine- to coarse-grained quartzarenite (Fig. 3-13).

These beds are bounded by planar depositional surfaces, and their internal pinstripe lamination

defines asymptotic planar cross-stratification (Sas), with localized erosional reactivation surfaces

(Fig. 3-9A). Bottomsets of the pinstripe cross-stratified deposits also display adhesion warts (Fig.

3-9C; Table 1). Thin (2 to 5 cm), plane-parallel beds (Sps) of quartzarenite occur locally in

sections BI1 and BI3. Mudstones in this association ranges from 0.05 m to 1 m in thickness. These

beds are bounded by planar depositional surfaces and contain desiccation cracks on bed surfaces

(Mrd; Fig. 3-9D).

3.5.3.2.2   Occurrence

FA2 is found in sections BI1 and BI3, where it attains accumulated thicknesses of 42 m and

49 m, respectively. This association overlies FA1 and is overlain by FA4. In section BI3, facies

from this and the alluvial to fluvial FAs are interbedded. FA2 can be followed along strike for < 25

km (based on mapping relationships) and occurs in the middle of the Nyeboe Formation, thickening towards the western parts of the basin. A broad coarsening-upward trend is observed in FA2 in section BI1.

3.5.3.2.3   Interpretation

Asymptotic, low-angle cross-stratification (Sas) and pinstripe lamination suggests migration of low-relief dunes in an eolian origin, specifically with alternations in air-flow strength and associated deposition of grain-fall and grain-flow laminae (Mountney and Thompson 2002; Mountney 2006). The occurrence of adhesion warts (Sas) on the bottomsets of the cross-strata suggest that wind blew sand over damp surfaces in the interdune regions (Sharp 1963; Fryberger et al. 1992; Mountney 2006), which is common in dune fields close to the groundwater table (Hilbert et al. 2015). Minimal relative thickness of the eolian bedsets and their simple geometry (i.e., absence of complex, compound cross-stratification) suggest deposition of small-scale dunes (Chakraborty 1991). Mudstone beds with desiccation cracks (Mrd) indicate the accumulation of fine-grained sediments in shallow ephemeral ponds. Plane-parallel beds (Sps) may indicate reworking of sand in very shallow water (Chakraborty 2001). FA2 is interpreted to represent the development of a small-scale eolian dune field with ephemeral interdune ponds in an eolian-backshore setting, consistent with its occurrence between terrestrial (FA1) and shallow-marine deposits (FA4) (Hilbert et al. 2015).

3.5.3.3 FA3: Marine-Intertidal Flat Facies Association

3.5.3.3.1   Description

Lithology of FA3 is characterized by dolomite-cemented fine-grained to medium-grained quartzarenite and, locally, by impure dolostone with interspersed quartz grains. Quartz grains are rounded and moderately spherical. Sandstone beds in this FA range from 0.05 m to 0.15 m in thickness, having undulatory bounding surfaces, show well-defined internal stratification, and commonly contain vugs (Fig. 3-10A). Stratification is often marked by wrinkled surfaces implying the influence of microbial mats (Noffke 2009) (Figs. 3-10B, F). Multiple cross-stratification styles are observed: herring-bone cross-stratification (*Shb;* Fig. 3-10E), trough cross-stratification (*Stc;* Fig. 3-10G), plane-parallel stratification (*Sps;* Fig. 3-10C) and planar cross-stratification (*Spc;* Table 1). In addition, symmetrically rippled sandstone is observed (*Ssr;* Fig. 3-10C. FA3 also contains a thin (8 cm) bed of dolomitic, symmetric, columnar stromatolites (*Dst;* Fig. 3-10D).

3.5.3.3.2   *Occurrence*

FA3 is found in sections WG1901 and BI2, where it reaches accumulated thicknesses of 46 m and 35 m, respectively. FA4 forms the upper and lower bounds of FA3. The marine-intertidal association can be followed along strike for < 3 km, where it narrows considerably and eventually pinches out to the west. FA3 is found in the upper part of the Nyeboe Formation and occurs only in the central part of the basin. Recurring fining-upwards cycles are observed in section BI2 (Fig. 3-4). Chandler (1988) also reported these facies (Nyeboe Formation member 5) in the central part of the basin.

3.5.3.3.3   *Interpretation*

Dolomite-cemented sandstone with microbial laminae suggest deposition in an environment with locally limited clastic supply or waters supersaturated with carbonate (Grotzinger and James 2000). Cross-stratified sandstone facies (*Stc, Ssr*) are interpreted to have

deposited under subcritical flows, while supercritical regimes are locally recorded by facies *Spc* and *Sps*. In conjunction with the other facies, opposing, bidirectional stratification is interpreted as herring-bone cross-stratification (*Shb*), which suggests that this FA was deposited in a tidally influenced environment, subject to bidirectional flows (Dalrymple and Choi 2007), while symmetrical ripple forms (*Ssr*) indicate wave winnowing. Ubiquitous wrinkled surfaces are interpreted to be microbially induced (Noffke 2009) and indicate that colonization of the sedimentary substrate by microbial mats was not limited to the dolostone stromatolite bioherms. Columnar morphology of the stromatolites suggests deposition in a moderately high-energy environment. Stromatolites occur only locally, possibly due to a localized paleo-topographic high formed due to faulting, and/or protection from wave winnowing, may have caused the area to be clastic-starved (Nichols 2009; Cattaneo and Steel 2003). FA3 is interpreted to represent an intertidal, shallow-water environment.

3.5.3.4 FA4: Wave-Dominated, Marine-Shelf Facies Association

3.5.3.4.1   Description

Lithology of FA4 ranges from fine-grained to coarse-grained subarkose to quartzarenite that contains minor quartz-pebble stringers. Sandstone is physically mature (i.e., with subrounded to well rounded and highly spherical grain morphology and no matrix). Petrographically, FA4 exhibits compaction and pressure solution seams (Figs. 3-13E, F). Beds from FA4 range from 0.1 cm to 3 m in thickness, and their internal stratification is well developed (Table 3-1). Most beds of FA4 exhibit planar geometry. Oscillatory flows produced several facies: hummocky cross-stratified sandstone (Shc) and symmetrically rippled sandstone (Ssr). Trough-cross-stratified sandstone (Stc), plane-parallel-stratified sandstone (Sps) and planar-cross-stratified sandstone

(Spc) also contribute to FA4 (Figs. 3-11B, C; Table 1), indicating that wave winnowing alternated with unidirectional upper-flow-regime flows. Thin, discontinuous (< 8 m along strike) quartz-pebble interbeds (10 cm to 25 cm thick) with rounded and highly spherical clasts commonly form the base of sandstone cross-stratified beds. Near the top of the Nyeboe Formation, larger-scale macroforms (sensu Galloway 2002) have also been observed (Fig. 3-11A). These macroforms display large, inclined beds (ca. 20° dip angle) that define individual foresets that are 3 m to 5 m thick and can be followed along strike for 8 m to 12 m. Internally, the foresets contain stacked sets of planar and hummocky cross-stratified sandstone (Sps, Shc; Fig. 3-12C) with symmetrical ripple topography (Ssr) along foreset boundaries and atop the macroform (Fig. 3-12B).

3.5.3.4.2   *Occurrence*

This FA occurs in each measured section and represent the most laterally and vertically extensive FA in the Fury and Hecla Group. Accumulated thicknesses are 6 m to 237 m in the measured sections and constitute the bulk of the Nyeboe Formation. Section WG1901 and BI4 contain, respectively, a 28-m- and 26-m-thick transitional zone with the alluvial to fluvial FA. FA4 typically overlies the FA1 and FA2. In section BI2, FA4 is interbedded with FA3, and in section BI3 this association is interbedded with FA5. The marine-shoreface FA can be traced along strike for > 25 km (based on mapping relationships) and is overlain by similar (i.e., wave-dominated, marine-shelf) deposits belonging to the Sikosak Bay Formation, though the nature of this contact is not fully understood due to poor exposure (Fig. 3-1). FA4 mostly occurs in the upper part of the Nyeboe Formation. Section BI4 contains coarsening-upward packages on FA4 bounded by finer-grained deposits of FA5 (Fig. 3-4). By comparison, in the western part of the basin and on the Melville Peninsula, no upward grain-size trend is observed.

3.5.3.4.3   Interpretation

Sedimentary structures mostly produced by wave-induced oscillatory flows and unconfined unidirectional flows suggest that FA4 experienced reworking in a storm-influenced, wave-dominated, clastic marine shelf environment (Suter 2006). Hummocky cross-stratified sandstone (Shc) indicates deposition near the lower shoreface during storm events (Clifton 2006; Dumas and Arnott 2006). Continuous wave oscillation generated symmetrically rippled sandstone (Ssr) on both the upper and lower shoreface (Allen 1968). The cross-stratified sandstone facies (Stc, Spc) are interpreted to be the product of migrating dune bedforms (possibly part of compound sand bars) that formed on the upper shoreface (Dalrymple et al. 1990). The plane-parallel-stratified sandstone facies (Sps) was deposited where water was shallowest and/or attained the highest flow strength on the shelf, e.g., foreshore to upper shoreface (Galloway and Hobday 1996). Accordingly, the sporadic quartz-pebble stringers flooring sandstone cross-strata represent down-slope transport of coarser material during storms or locally developed pebbly foreshores (Aigner 1985; Hart and Plint 1995). In this context, the macroforms are interpreted as foreset bars shaped by a combination of drift currents, wave winnowing, and storms (Suter 2006). Similar foreset bars in other successions have been interpreted as a product of shore-parallel currents (longshore drift) due to oblique angle of wave attack against the coastline (Stubblefield et al. 1984; Hart and Plint 1995; Herbers et al. 2016).

3.5.3.5 FA5: Marine-Offshore-Transition Facies Association

3.5.3.5.1   Description

The lithology of FA5 ranges from mudstone to medium-grained quartzarenite. Mudstone beds range from 3 to 10 cm in thickness, and their internal stratification is faintly defined by plane-parallel lamination or is massive (Mpr). These beds are bounded by planar depositional surfaces (Fig. 3-11A; Table 3-1). Quartzarenite is physically mature (i.e., with well-rounded and highly spherical grain morphology with no matrix). Petrographically, this FA shows compacted, subrounded to rounded, fine- to medium-gained quartzarenite with pressure-solution seams (Figs. 3-13G, H). Sandstone beds are 3–50 cm thick, and their internal structures are well developed. These beds are bounded by undulatory surfaces and contain hummocky cross-stratification and symmetrical ripples (Shc, Ssr; Figs. 3-11C, D). FA5 contains many of the same facies as the FA4 (presumably due to their spatial proximity on the marine shelf) but is identified as a separate FA primarily based on the mud interbeds.

3.5.3.5.2   *Occurrence*

FA5 was observed only in section BI4, where its cumulative thickness is 17 m. However, this facies is likely more prevalent than this sole occurrence suggests, as it is also present in subcrops and poorly exposed areas overlain by broken, red mudstone throughout the basin. FA5 is bounded by gradational transitions with the wave-dominated marine-shelf FA.

3.5.3.5.3   *Interpretation*

Intercalation of mudstone and texturally mature sandstone suggests that tranquil conditions favorable to the settling of fine-grained sediments alternated with higher-energy flow capable of entraining sand. Specifically, mudstone (Mpr) is interpreted to represent settling of fine-grained material below the influence of storm waves (Dalrymple 1992), and its plane-parallel lamination is interpreted at least in part as a feature related to compaction (Collinson et al. 2006). Hummocky

cross-stratification (Shc) and symmetrically rippled sandstone (Ssr) were formed when storm waves impacted the substrate and transported sand from the shoreface (Dott and Bourgeois 1982; Cheel and Leckie 1993). Therefore, FA5 is interpreted to represent the offshore-transition zone of a clastic marine shelf.

3.6   Discussion

3.6.1 Depositional evolution

Detailed facies analysis of the Nyeboe Formation records considerable lithological variability both spatially and temporally throughout the opening of the Fury and Hecla Basin (Figs. 3-14, 15). While the lateral extents of the FAs are not defined, they are based on additional mapping data, which is separate than the locations of the measured stratigraphic columns (Steenkamp et al., 2018). Basal alluvial to fluvial strata preserved in the central area of the basin correspond with basin inception and the establishment of a subaerial drainage systems (Fig. 3-14A). Alluvial to fluvial systems pass up-section into eolian-backshore or coastal to shallow-marine strata across the entire study area. The general pattern of deepening depositional environments up section (N to S; Fig. 3-4) corresponds to the inferred topographic gradient from north to south (Fig. 3-14). FA2 represents local beach-dune fields (Nichols 2009) that are laterally limited and interpreted to have been protected from wave erosion by local coastal promontories (Fig. 3-14B). Strata belonging to FA3 record clastic starvation, indicating either a transgression (e.g., South and Talbot 2000) or a shielding from clastic influx, e.g., from compounding sand bars forming beach barriers in front of embayments (Roep et al. 1998; Köykkä and Lamminen 2011; Kirk and Lauder 2000) (Figs. 3-14A, B). In this scenario, the high-energy effects of storm-derived

wave-winnowing were dissipated by the longshore bars, protecting the upper shoreface while also stabilising an intertidal lagoon (e.g., Herbers et al. 2016). Whereas this interpretation for lagoonal sedimentation is preferred, we cannot rule out the possibility that paleotopography may have controlled FA distribution. An intraformational conglomerate located in the northcentral part of the basin (section BI3; Fig. 3-4) records local, renewed alluvial- fan and/or fluvial scree-slope deposition in the middle stratigraphy of the Nyeboe Formation. We infer that these intraformational clasts imply lithification and subsequent renewed uplift and erosion coeval with Nyeboe deposition. The coarse-grained conglomerate wedge may be fault-bounded and therefore likely records localized fault-controlled topographic steepening in the basin′s catchment and progradation of proximal terrestrial systems (Blair and Bilodeau 1988; Fidolini et al. 2013).

Lateral relationships between FAs are complex, as illustrated in the northern part of the study area on Baffin Island (Fig. 3-15). However, strata of the wave-dominated marine-shelf facies association (FA4) form the bulk of the Nyeboe Formation and record the establishment of a shallow, wave-winnowed clastic sea (Johnson and Baldwin 1996; Went 2013) (Fig. 3-14C). Finer grained interbeds (*Mrd)* in the eastern area of the basin are inferred to be contemporaneous with the aforementioned FA4 deposition in the west, and suggest that the basin deepened, at least in part, to the east due to differential progradation and subsidence (Macquaker and Taylor 1996; Ghinassi 2007). We attribute these mudstones to more rapid subsidence in this eastern part of the basin and retreat of the clastic shelf (Muto and Steel 2002; Cattaneo and Steel 2003; Blair and Bilodeau 1988) (Fig. 3-14C). Our depositional model depicts the development of a predominantly clastic, transgressive shelf with mafic volcanics occurring in the middle of the stratigraphy. The mafic volcanics suggest ongoing rifting throughout the deposition on the Nyeboe Formation.

Facies and depositional trends can be compared with sediment dispersal data from fluvial and marine strata. Paleoflow indicators from fluvial strata are directed towards the west-southwest and west-northwest and are subparallel to the basin-bounding faults (red faults on Fig. 3-1), suggesting the establishment of an axial drainage system consistent with the lateral distribution of the facies (Figs. 3-6, 14A). The axial flow runs perpendicular to the alluvial fans, like Badwater basin in Death Valley (Ielpi, 2018). Our paleoflow indicators, which suggest axial drainage, likely records the minor localized fluvial activity, and are broadly consistent with the west-trending pan-continental sediment dispersal recorded in Proterozoic Laurentian basins (e.g., Athabasca and Thelon basins; Rainbird and Young 2009; Ielpi et al. 2017). Paleoflow data derived from marine facies are limited, but they suggest a polymodal paleocurrent that generally points to the west, parallel to the basin-bounding faults (Figs. 3-1, 6, 12, 14). Given sedimentological evidence of longshore bars (Herbers et al. 2016), we infer that these data record longshore drift, rather than dispersal in the actual down-dip direction. Stacked bedforms containing hummocky cross-stratification (in the eastern part of the basin) indicate that storms played a role in developing longshore bars (Herbers et al. 2016). The longshore bars may also have provided a topographic barrier that allowed the development of intertidal lagoons (Fig. 3-14B).

3.6.2 Opening of the Fury and Hecla Basin

Onset of a predominantly clastic transgressive shelf with mafic volcanism reflects crustal stretching due to faulting (Morgan and Ramberg 1987; Allen and Allen 2005) (Fig. 3-14). Deposition of thick shoreface-dominated successions, including FA4 and FA5, is consistent with a sustained and quasi-steady state between accommodation and sediment supply (Covey 1986). Our suggested scenario is also consistent with slow rates of crustal relaxation or thermal sagging in the

aftermath of a thermal pulse (Armitage and Allen 2010). Westward-thickening mafic volcanic flows first appear in the middle strata of the Nyeboe Formation, and therefore a delay can be inferred between the onset of basin-forming tectonism and lava extrusion.

Fahrig et al. (1981) reported that 16 paleomagnetic poles in the Nauyat Formation basalt in the Borden Basin were consistent with the Mackenzie LIP. Chandler (1988) similarly inferred that the mafic volcanic flows in the lower Fury and Hecla Group were related to the Mackenzie LIP based on geography and inferred stratigraphic relationships. The inferred Mackenzie igneous plume centre is on Victoria Island, ~1000 km to the west of the present-day Nyeboe Formation exposure (Buchan and Ernst 2013). The closest Mackenzie age-dated dikes trend ESE and are located on the Melville Peninsula, ~130 km south of the Fury and Hecla Group exposure (Buchan and Ernst 2013) and are oriented similarly to the trend of the faults parallel to the northern margin of the Fury and Hecla Basin. Therefore, it seems likely that the origin of the Fury and Hecla Basin was coeval with the Mackenzie event, though this hypothesis still requires geochronological confirmation.

The depositional framework illustrated above, trends in stratigraphic thickness, and structural setting are used to infer possible tectonic controls on sedimentation. More proximal FAs (alluvial-fluvial) are spatially associated with a cluster of faults that offset basement rocks, and the lowest strata of the Fury and Hecla Group that strike of ~115° (purple faults in Fig. 3-1). Since the terrestrial-proximal facies are interpreted to record basin inception, we hypothesize that south-dipping normal faults striking at ~115° are associated with the opening of the Fury and Hecla Basin (Fig. 3-14A). While we do not have enough structural data to concretely identify which faults were most important for basin initiation, we postulate that faults striking ~115° were initiated syndepositionally and subsequently reactivated. Other faults offset younger units of the

Fury and Hecla Group and are hypothesized to be related to renewed tectonism and subsidence of the basin and/or deformation after the deposition of the Nyeboe Formation (Fig. 3-1). Shallower-water depositional environments, such as FA2 and shallow-water, intertidal marine FAs, are localized in the west and central parts of the study area, whereas deeper-water depositional environments, such as the wave-dominated strata, are ubiquitous but thicken towards the east (Fig. 3-14). We infer that these facies trends imply deeper-water conditions in the eastern part of the study area (Fig. 3-14C) and are related to differential throw along the basin-initiating normal faults, as is commonly observed in fault-bounded extensional basins (Gawthorpe and Leeder 2000; Ghinassi 2007). This reconstruction infers a higher sedimentation rate closer to the faults, and notably counters the inferred westward-deepening direction for the Fury and Hecla Group strata above the Nyeboe Formation (Chandler 1988; Greenman et al. 2018).

Considering the paleogeography, we propose that a half-graben model is the most consistent with the observed distribution of FAs in the basin. Lateral facies-association distribution and paleoflows to the west record axial drainage parallel to the master fault of the half-graben (Gawthorpe and Leeder 2000). Master faults of the half-graben are interpreted to be the same orientation as the ~115° fault traces in the center and located on the north side of the basin (i.e., purple faults; Figs. 3- 1, 14). Both the basement rocks and the Fury and Hecla strata on the Melville Peninsula are crosscut by an undated fault system that strikes ~115°, the same direction as the basin axis (Spratt et al. 2013). However, these faults cannot be genetically related to early basin -forming events because they do not affect the lowest strata of the Fury and Hecla Group. Rather, if this Melville Peninsula fault system was established before basin formation, it may have contributed to the crustal anisotropy that controlled the orientation of the basin. In our interpretation of a half-graben setting, the principal deepening direction of the basin would have

been to the south. Here, we speculate an alluvially influenced domain in the northern part of the

basin, including the conglomerate wedge in section BI3, from a river-dominated domain observed

in section WG1901 (Fig. 3-4). Whereas the distinction of alluvial-fan from very proximal fluvial

strata may be ambiguous, our interpretation is rooted in the relative abundances of tractional vs.

mass-flow deposits. The scenario presented here is, accordingly, consistent with the presence of

proximal, alluvial to fluvial facies (FA1) mapped in the northern study area, which record footwall

unroofing and erosion (Mortimer and Carrapa 2007) (Fig. 3-14). Subsequent footwall-scarp

retreat, resulting in a decrease in topographic gradient, and continued subsidence led to the

establishment of marine, wave-dominated clastic sedimentation (Fig. 3-14). Differential fault

offset and subsidence in the basin caused the deeper-water deposition in the east (Gawthorpe and

Leeder 2000; Ghinassi 2007). In contrast to the stratigraphically lower and terrestrial-proximal

FAs, these marine deposits show no relationship to the faults, indicating that they were either

inactive or buried by this time.

3.6.3 Comparison with the Borden and Other Basins

The depositional model developed in this study for the Nyeboe Formation provides a basis

for considering correlations with basal stratigraphic units in other Bylot basins. The Borden Basin

(Fig. 3-1) contains a series of three, NW-SE-trending grabens on northern Baffin Island and Bylot

Island (Jackson and Iannelli 1981). The lowermost Nauyat Formation is 240 m to 430 m thick,

thickens to the south, and comprises predominantly quartzarenite with minor conglomerate,

subarkose, shale, stromatolitic dolostone, and up to seven mafic volcanic-flow units that, like the

Nyeboe basalts, have been linked to the Mackenzie igneous event (Jackson and Iannelli 1981;

Fahrig et al. 1981; Chandler and Stevens 1981; Long and Turner; 2012). Jackson and Iannelli

(1981) noted that a thin conglomerate unit often overlies the basement contact. The Nauyat volcanic units have a sharp, altered contact with the underlying rocks and often an erosional top, though basalt fragments are seldom found in the overlying sandstone. Long and Turner (2012) suggested that these flows are subaqueous owing to the observation of pillow structures, hyaloclastite, and lack of diagnostic characteristics that would otherwise indicate a subaerial origin. Although Jackson and Iannelli (1981) originally interpreted the siliciclastic units of the Nauyat Formation as fluvial in origin, Long and Turner (2012) proposed a marine setting based on a sedimentological analysis. Volcanic rocks of the Nauyat Formation disappear to the east, where the overlying Adams Sound Formation directly rests directly on basement (Jackson and Iannelli 1981).

The Adams Sound Formation is composed of quartzarenite, conglomerate, and shale (Jackson and Iannelli 1981). Long and Turner (2012) interpreted the Adams Sound Formation to be predominantly shallow marine in origin, although basal braided-river deposits have also been described at one location (Long and Turner 2012). Paleocurrents from the Nauyat and Adams Sound formations are dispersed but overall indicate west to northwest paleoflow (Jackson and Ianellli 1981; Long and Turner 2012). The similarities in lithology (mostly sandstone, with minor conglomerate, shale, isolated stromatolitic carbonate, and several basalt-flow units), depositional environments (basal fluvial passing into nearshore-marine), and paleocurrent trends (broadly westward) suggest a lithostratigraphic correlation between the Nyeboe Formation in the Fury and Hecla Basin and the Nauyat‒Adams Sound formations in the Borden Basin.

Recently acquired Re-Os ages of 1048 ± 12 Ma on the Arctic Bay Formation in the Borden Basin (Gibson et al. 2019) and 1087.1 ± 5.9 Ma on the Agu Bay Formation in the Fury and Hecla Basin (Greenman et al. 2021) indicate that most of the Bylot and Fury and Hecla stratigraphy is >

200 Myr younger than the Mackenzie-related basalts near the base of each succession. These ages imply that a major unconformity must separate the lower and middle stratigraphy in each basin (Turner et al. 2016; Gibson et al. 2019; Greenman et al. 2021). Whereas the location of the unconformity is not yet evident in either case, it follows that the lowermost strata in both successions constitute a tectonostratigraphic package distinct from the overlying strata. Whereas the Re-Os ages on the Arctic Bay and Agu Bay formations (Fig. 3-2) imply that these units may be geodynamically related due to their lithologic similarity but not temporally correlative, a chronostratigraphic correlation between the lower units can be postulated based on the inferred age of the basalt flows in both basins. We speculate that both the basal Bylot Supergroup and the Fury and Hecla Group were deposited in basins that opened because of modest crustal stretching related to the Mackenzie large igneous event.

While these lower tectonostratigraphic packages share many similarities, one important difference is that the Nauyat Formation of the Borden Basin contains much thicker mafic flows than the Nyeboe Formation, despite their similar distance from the inferred plume head centered beneath Victoria Island ~1000 km to the east (Baragar et al. 1996). Given that the lower, mixed sandstone-basalt package in the Borden Basin is thicker than its counterpart in the Fury and Hecla Basin, the most likely explanation for this difference is that the former experienced a greater degree of crustal stretching. However, heterogeneity in plume dynamics may have also played a role. This also highlights the discrepancy that the Borden Basin was interpreted to have opened as a sag basin, contradictory to our interpretation that the Fury and Hecla Basin opened in a half-graben setting related to the Mackenzie large igneous event (i.e., faulting due to crustal stretching; Turner and Kamber 2012). Structural refinements in the Bylot basins are necessary to disentangle the tectonic history in more detail and reconcile apparent discrepancies between their initiation.

Owing to the same similarities in lithostratigraphy (and particularly the occurrence of basal conglomerate overlain by nearshore-marine sandstone hosting mafic-flow units), the correlation proposed above could also be tentatively extended to the Nares Strait and Smith Sound groups, laterally equivalent units constituting the basal Thule Supergroup (Fig. 3-1; Dawes 1997). The basal Aston Formation in the little-studied Hunting-Aston basin (Fig. 3-1) is a 600- to 1300-m-thick unit composed of sandstone and minor stromatolitic dolostone exposed on Somerset and Prince of Wales islands (Tuke et al. 1966; Stewart 1987; Mayr et al. 2004) and has likewise been interpreted as nearshore-marine in origin (Long and Turner 2012). However, the Aston Formation lacks terrestrial facies, precluding tighter analogies to the Nyeboe Formation.

3.7   Conclusions

We present a detailed sedimentological study on the sandstone dominated Nyeboe Formation, which forms the base of the Fury and Hecla Group in northeastern Nunavut. We identified five facies associations in the Nyeboe Formation: fluvial to alluvial, eolian-backshore, marine-intertidal, wave-dominated marine shelf, and marine offshore-transition. The Nyeboe Formation broadly records a transgression from a terrestrial to a wave-dominated, marine clastic shelf setting. We postulate faults striking ~115° located in the central area of the basin, which offset only the lower formations of the Fury and Hecla Group stratigraphy and appear to be related to thicker successions of the alluvial to fluvial facies association, may be associated with opening of the basin. Based on field relationships between facies associations and fault structures, we infer that the Nyeboe Formation was accommodated in a half-graben, fault-bounded on the north side (present coordinates). Initial faulting along the basin master faults was related to the establishment of topographic gradients decreasing to the south and progradation of alluvial to fluvial systems.
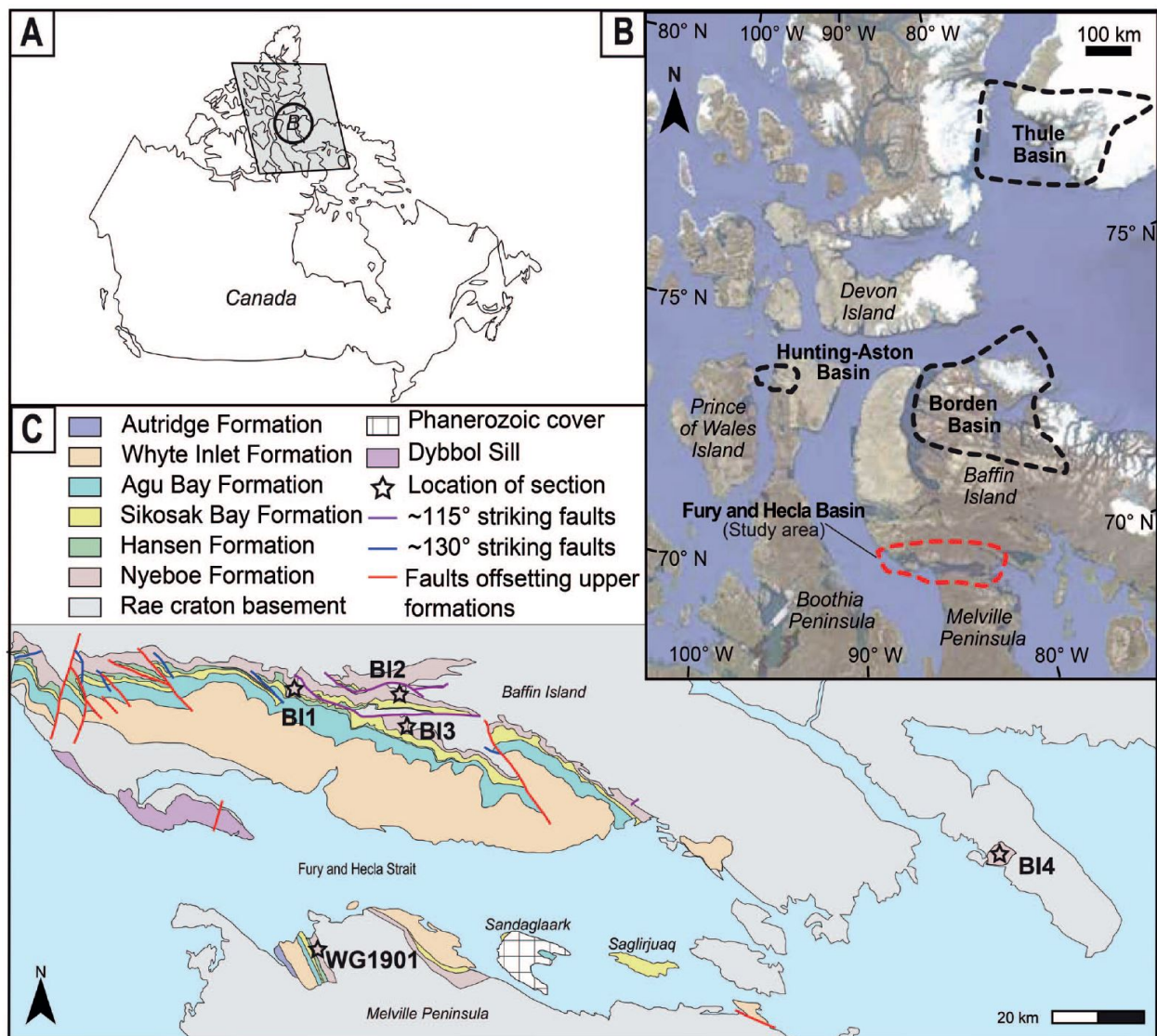
Transgression and sediment supply resulted in varied depositional paleogeography including nearshore- to deep-marine domains, backshore dune fields, and intertidal lagoons built along the coast. Eventually, most of the basin transitioned into a mature, wave-dominated coastal environment with longshore bars. Sedimentary structures and paleocurrent indicators suggest a component of longshore drift due to an oblique angle of wave attack to the coastline. Although paleocurrent data points are limited, westward sediment dispersal indicated by the fluvial paleocurrent data is consistent with the pattern observed across Laurentia throughout much of the Proterozoic, suggesting that the Fury and Hecla Basin might have acted as a sink for far-travelled detritus from the east. Mafic basalt flows in the middle of the Nyeboe Formation stratigraphy imply that the thermal event responsible for the Mackenzie large igneous province played a role in the initial opening of the Fury and Hecla Basin (and presumably the other Bylot basins). Finally, our results suggest strong correlation potential between the Nyeboe Formation and the Nauyat and Adams Sound formations in the Borden Basin, and possibly the Nares Strait and Smith Sound groups in the Thule Basin (Fig. 3-1B). The hypotheses formulated here about correlations to other strata in the Bylot basins contributes towards a refinement of the tectonostratigraphic and paleogeographic frameworks for the Mesoproterozoic strata of Laurentia.

3.8   Acknowledgements

3.9   Figures

Figure 3-1: Regional and study area maps

Geographic and geological setting of this study including A) the location of the study area and B) geographic sketch of the Bylot basins. C) Geological sketch of the Fury and Hecla Basin (from Chandler 1988; Greenman et al. 2018; Patzke et al. 2018; Greenman et al. 2020). Faults are classified into three groups based on their location, orientation, and offset. Locations of the stratigraphic sections of Figure 4 are also reported.
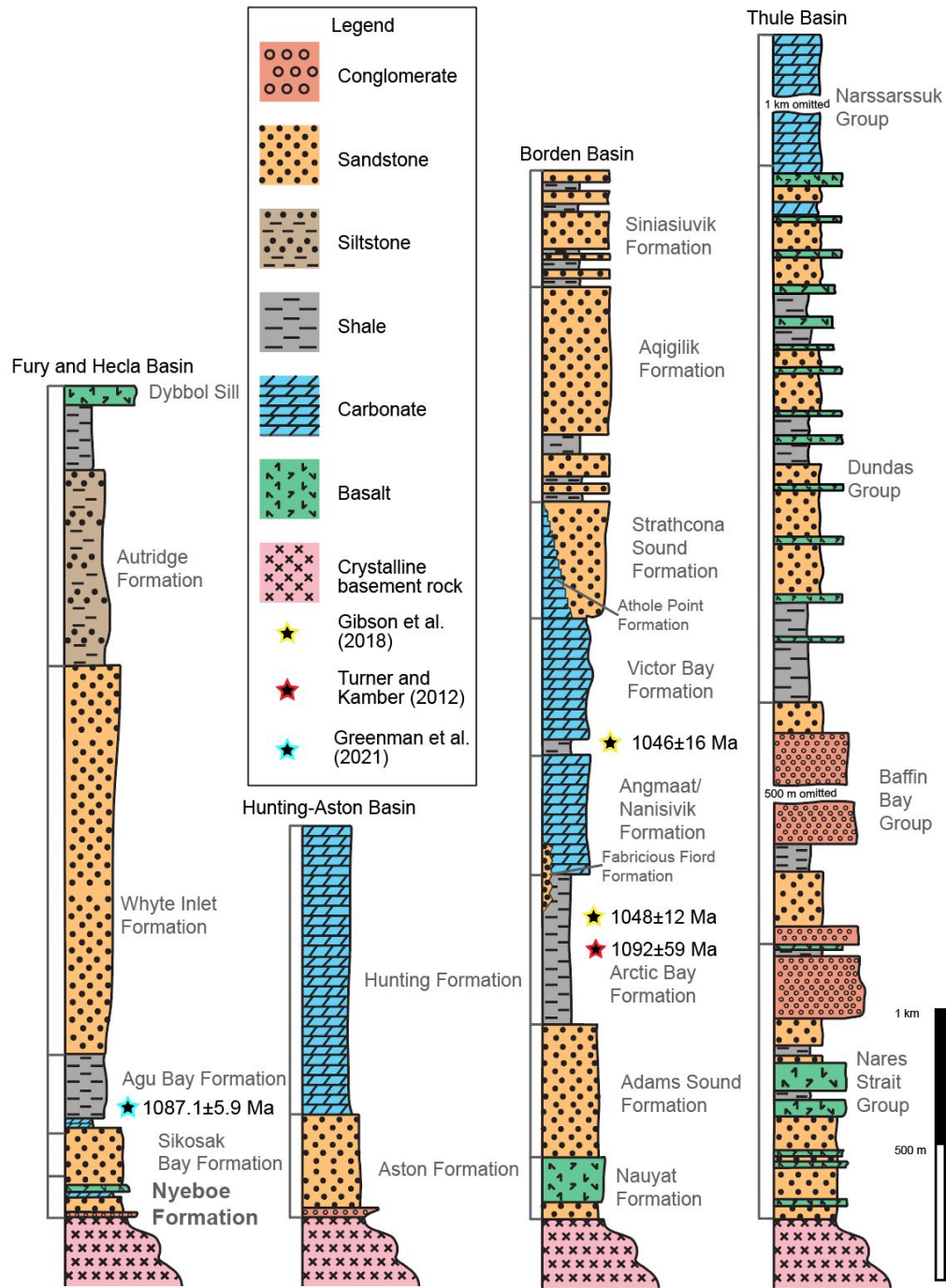
Figure 3-2: Bylot basins stratigraphic columns

Generalized lithostratigraphy of the Bylot basins, after Long and Turner (2012) and Greenman et al. (2020). The bounding lines to the left indicate formation contacts (labels to the right of the

column). Note the clastic-dominated nature of the Fury and Hecla Basin when compared to the

nearby Hunting-Aston and Borden basins. The Hansen Formation is omitted from the Fury and

Hecla Group due to its inconsistent stratigraphic position. In the Borden Basin, the Iqqittuq and

Ikpiarjuk carbonate-dominated formations are also omitted from the stratigraphy for simplicity.
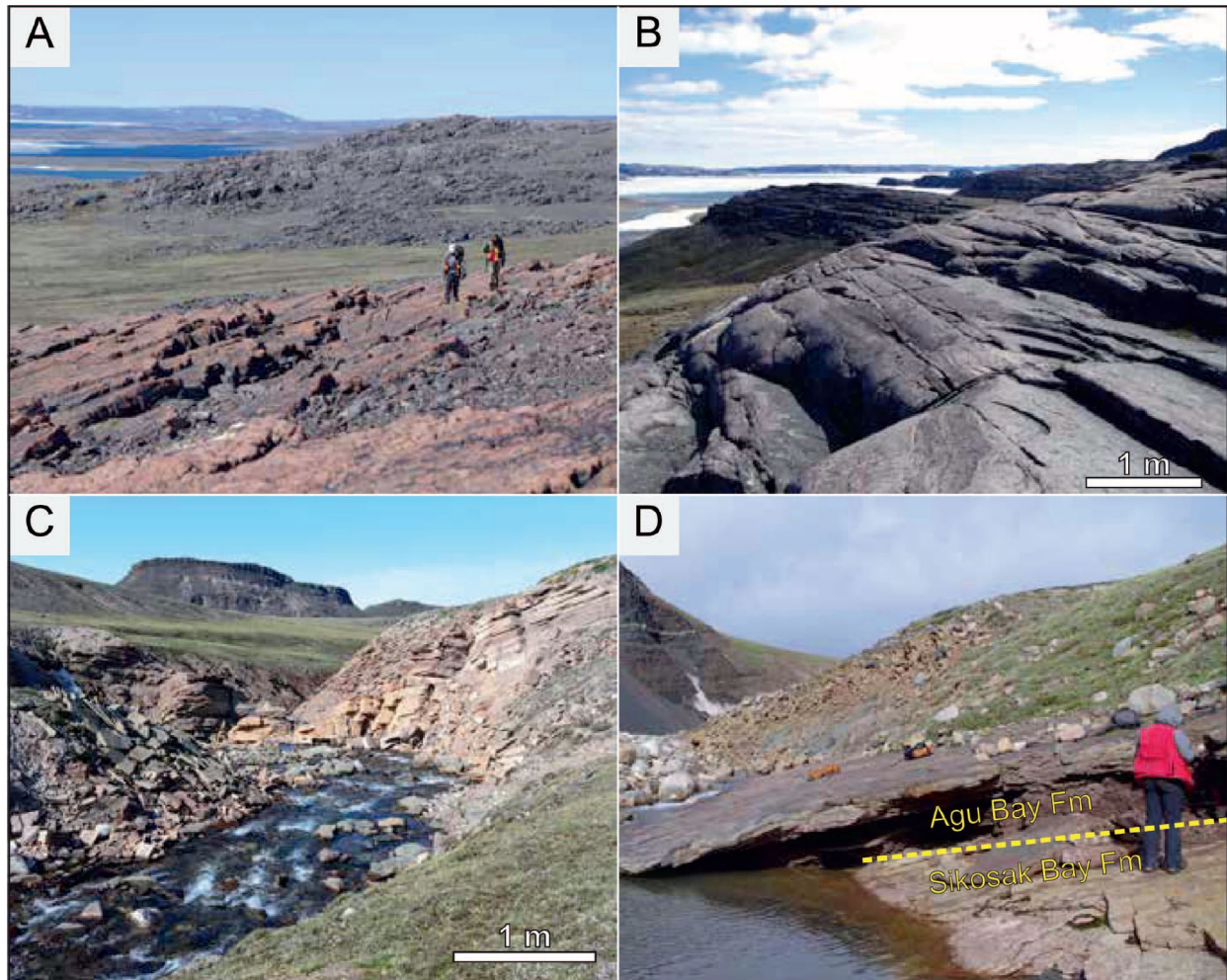
Figure 3-3: Typical exposure photo plate

Typical exposures of the Fury and Hecla Group in the homonymous basin. Geologists for scale in

parts A and C are about 1.7 m tall. A) Hillslope exposures common in the eastern part of the basin.

Photo from section BI4. B) Cliff exposure common in the western part of the basin. C) Canyon

exposure of the lower strata on the Melville Peninsula. D) Upper contact of the Nyeboe Formation

with the Sikosak Bay Formation in the central part of the basin. The Agu Bay Formation is visible

along cliffs in the background.
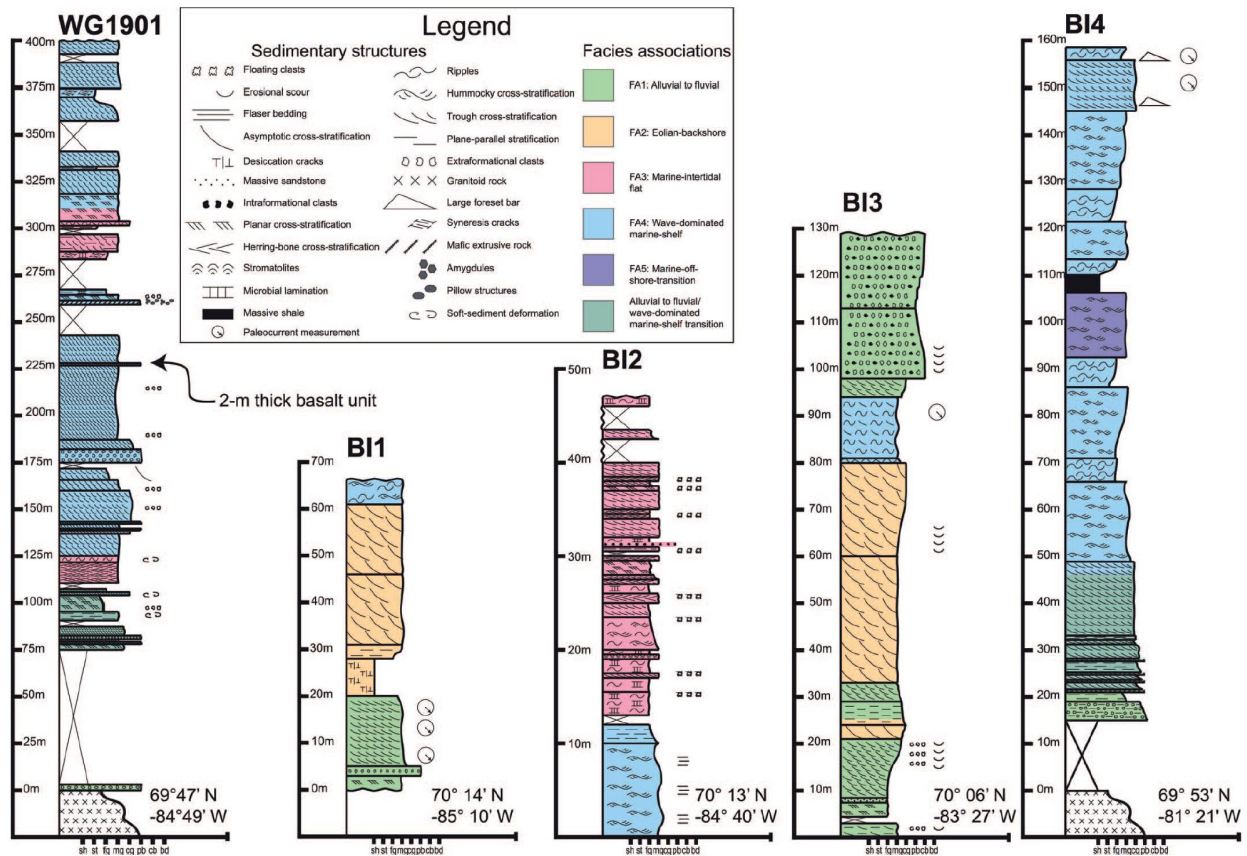
Figure 3-4: Nyeboe Formation stratigraphic columns

Stratigraphic sections of the Nyeboe Formation measured in this study. Sections are organized left

to right from west to east. Locations of sections are indicated by stars in Figure 1. Stratigraphic

columns are not hung on a datum; they represent different strata of the overall Nyeboe Formation.
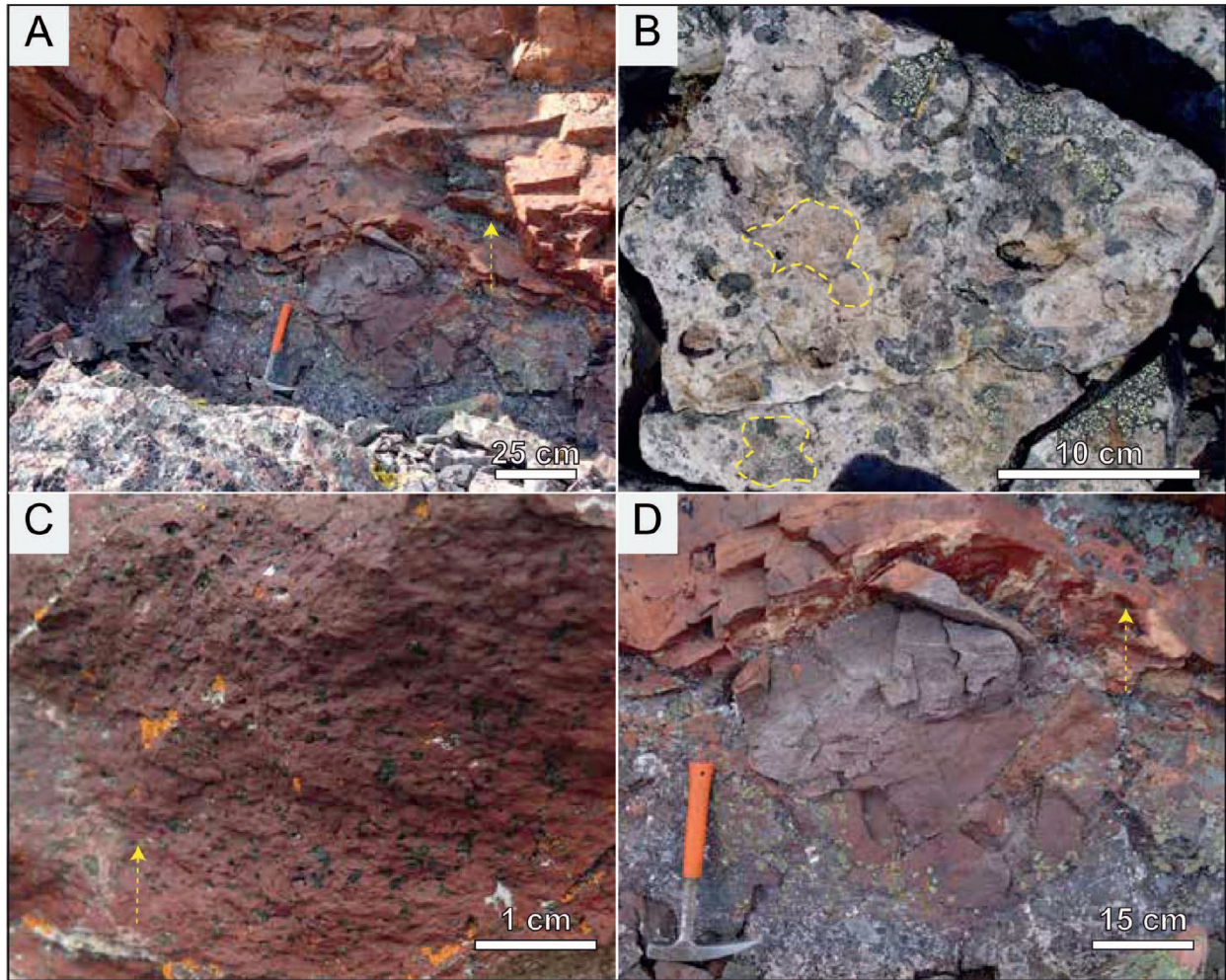
Figure 3-5: Nyeboe Formation mafic unit photo table

Field photos of the Nyeboe Formation's mafic volcanic unit. A). Exposure of rusty-colored basalt on the Melville Peninsula. B–D) Details of a quartzarenite with peperite texture along the contact with a volcanic unit (B), amygdules (C), and pillow structure (D).
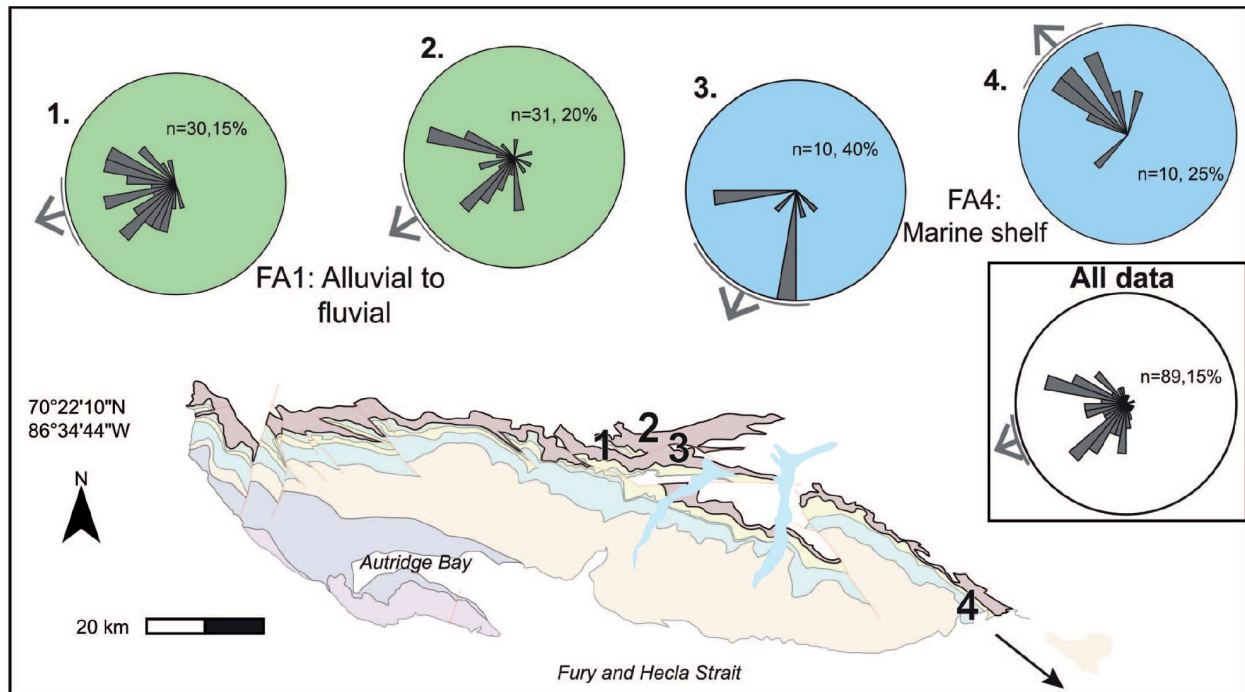
Figure 3-6: Nyeboe Formation paleocurrents

Summary of the paleocurrent data collected from cross-beds in the Nyeboe Formation. Rose diagrams summarize measurements from various locations, as indicated by numbers on the sketch map. Green diagrams represent FA1 fluvial facies indicators, and blue diagrams represent FA4 marine facies indicators. The rose diagram in the lower right corner with all data also includes measurements of macroform-accretion dip directions from section BI4 (see Figure 8). See also Figures 1 and 4 for formation colors.
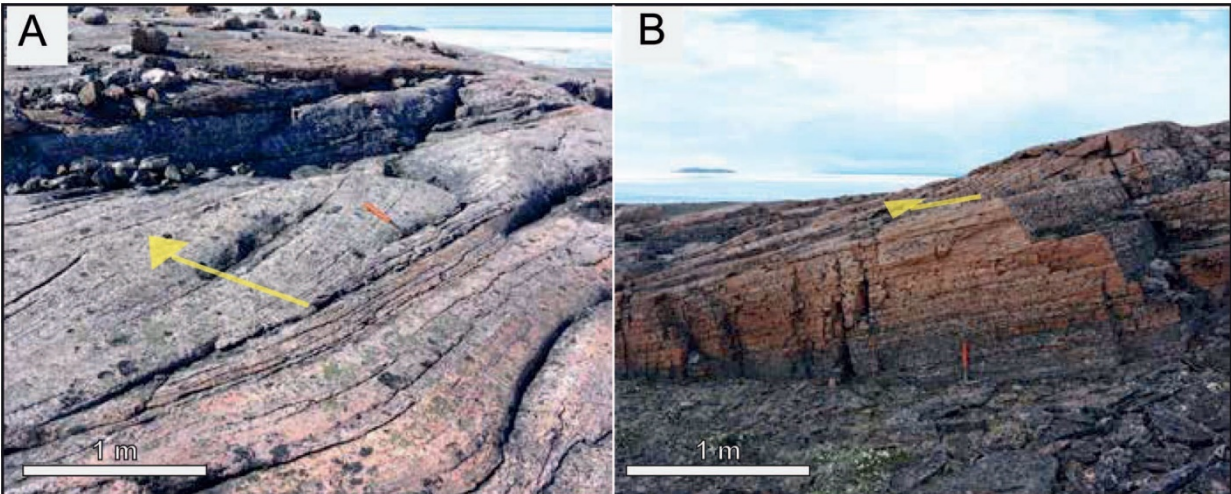
Figure 3-7: Paleocurrent photo table

Field photo examples of A) trough cross-beds and B) foresets used to determine paleocurrent data.

Arrows indicate paleocurrent direction. Hammer is 20 cm in length.
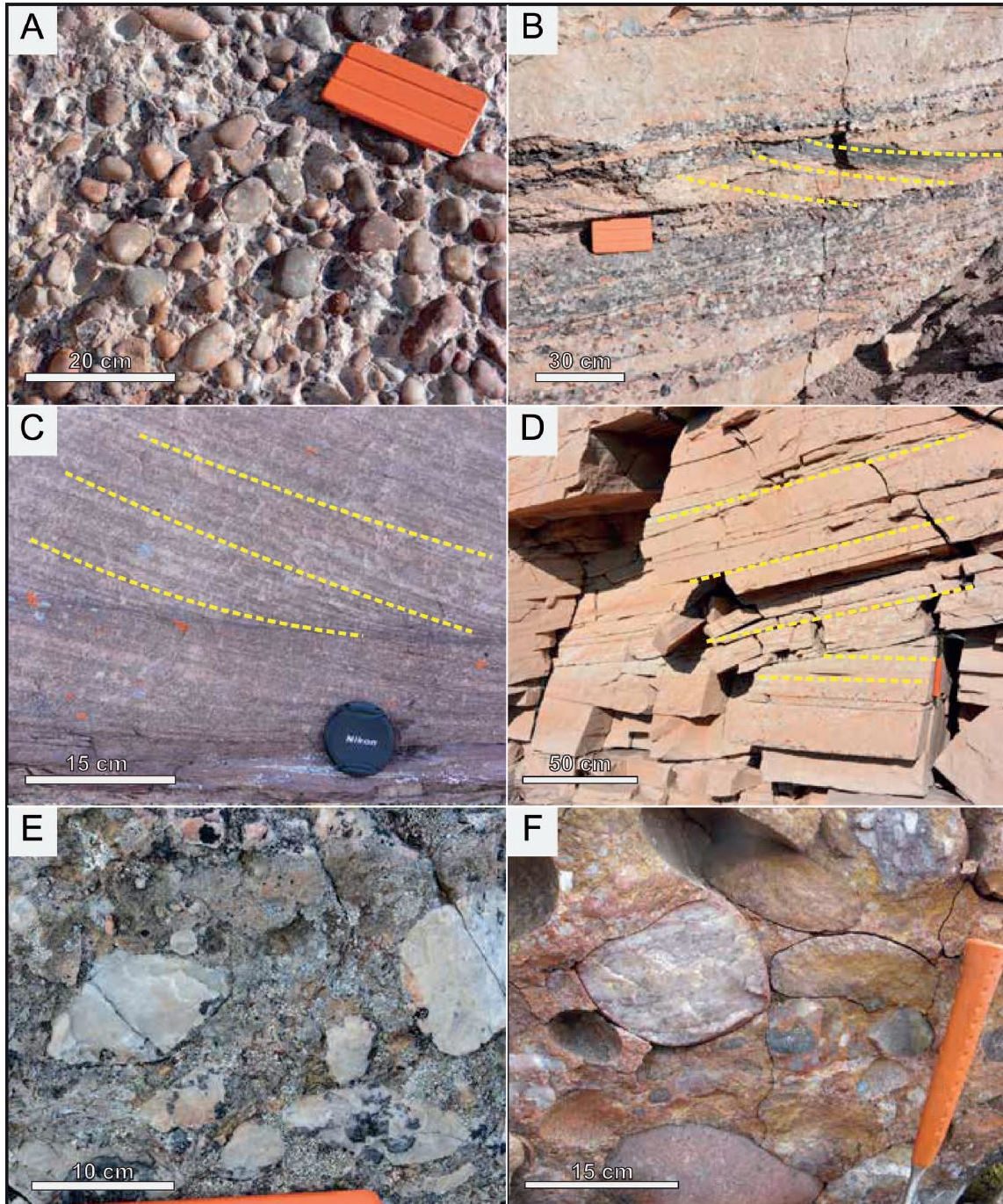
Figure 3-8: Terrestrial alluvial to fluvial FA1 photo table

Field exposures of alluvial to fluvial facies association 1 (FA1) of the Nyeboe Formation. Dashed

lines trace stratification. A) Poorly sorted and relatively massive extraformational conglomerate,

facies *Spc*. B) Normally graded, extraformational pebble-clast conglomerate and medium-grained

sandstone with trough cross-stratification, facies *Stc.* C) Ungraded, medium-grained sandstone with trough cross-stratification, facies *Stc.* D) Normally graded, medium-grained sandstone with plane-parallel stratification overlain by normally graded, medium-grained planar cross-stratified sandstone, facies *Sps* and *Spc.* E) Breccia with polymict, angular clasts, facies *Cbr.* F) Cobble- to boulder-grade, polymict conglomerate, facies *Cpy.*
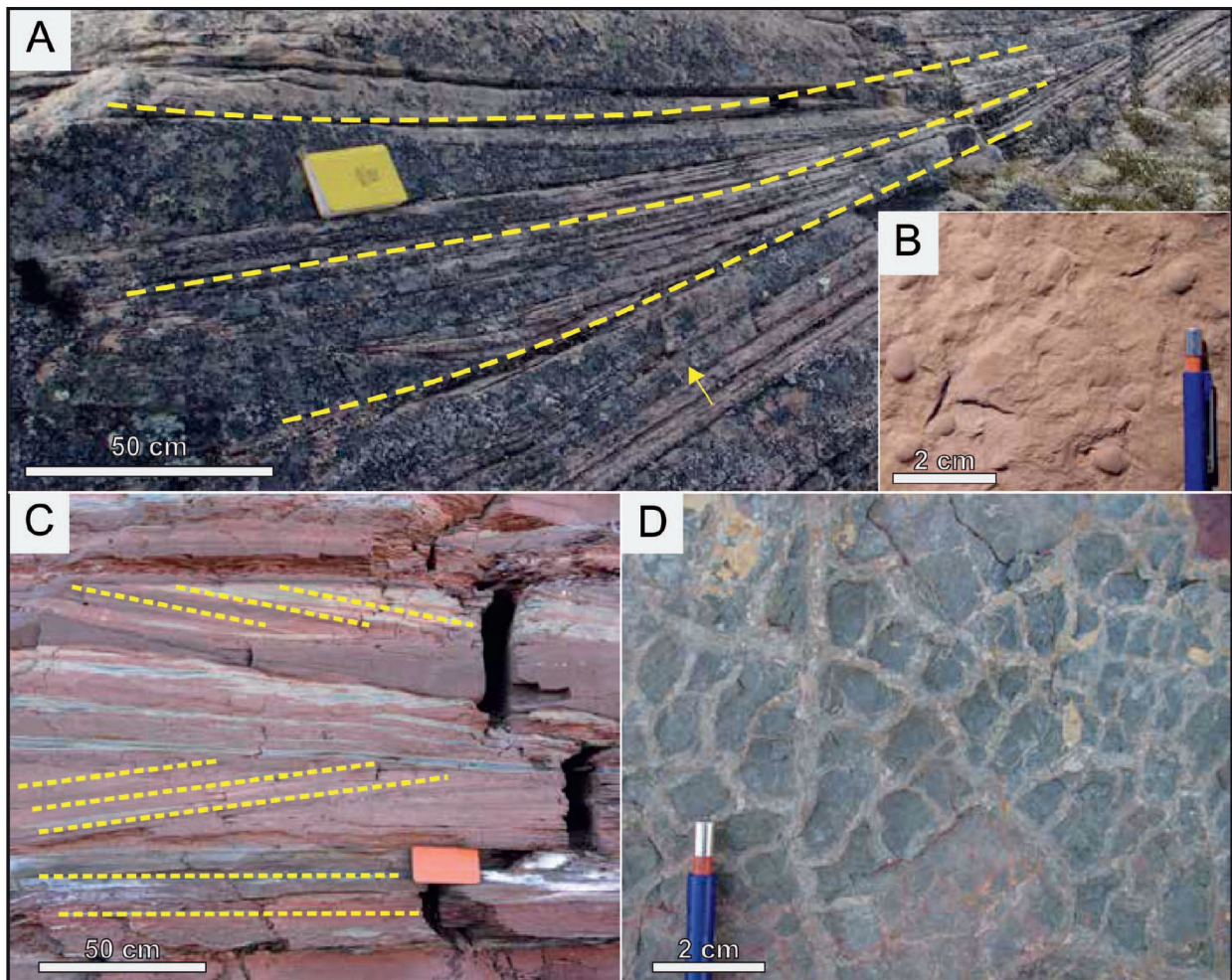
Figure 3-9: Backshore eolian FA photo table

Field photos of eolian-backshore facies association (FA2) identified in section BI3. A) Field photograph of the bedset with dashed lines indicating asymptotic cross-stratification and an arrow to show the reactivation surface. B) Detail of a surface bearing adhesion warts in plan view, facies

Sas. C) Planar and cross-stratified siltstone, facies *Mpr*. D) Mudstone stratum top (seen in plan

view) with polygonal desiccation cracks, facies *Mrd*.
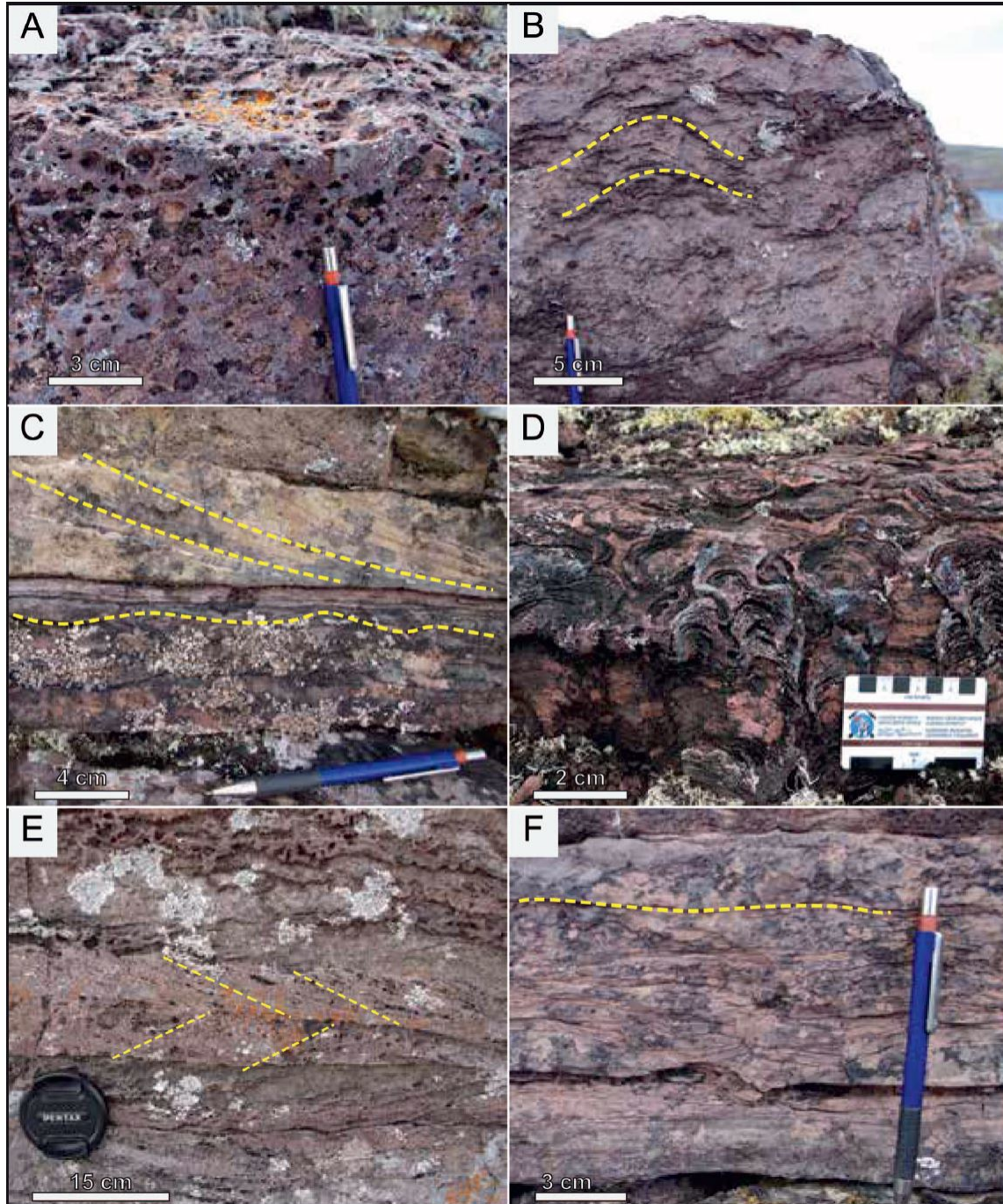
Figure 3-10: Intertidal-marine FA photo table

Field photos of the intertidal-marine facies association (FA3) of the Nyeboe Formations. Dashed lines denote stratification planes. A) Vuggy texture seen throughout the intertidal facies. B) Evidence for microbial build-up and microbially induced wrinkling. C) Symmetrically rippled sandstone, facies *Ssr,* overlain by trough cross-strata, facies *Stc.* D) Stromatolitic dolostone, facies *Dst*. E) Herring-bone cross-stratified sandstone with dolomitic cement, facies *Shb*. F) Wrinkled texture developed in sandstone.
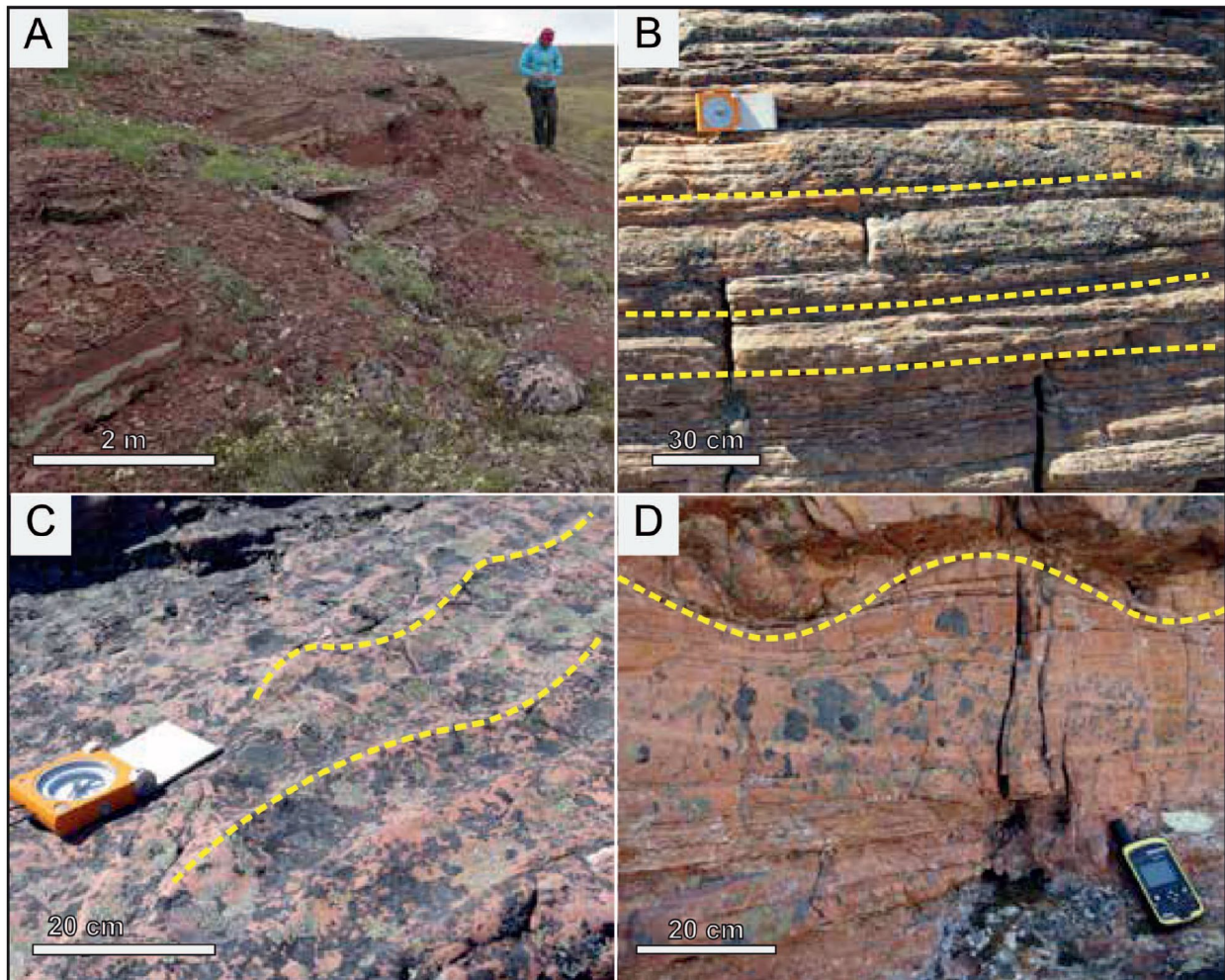
Figure 3-11: Marine shelf and offshore-transition photo table

Field photos from the marine shelf (FA4) and offshore-transition (FA5). Yellow lines denote characteristic features of A) plane-parallel-laminated mudstone, facies *Mpr*; (B) plane-parallel-

laminated sandstone, facies *Sps* (C) symmetrically rippled sandstone, facies *Ssr*; and (D) hummocky cross-stratified sandstone, possibly emphasized by sedimentary loading, facies *Shc*.
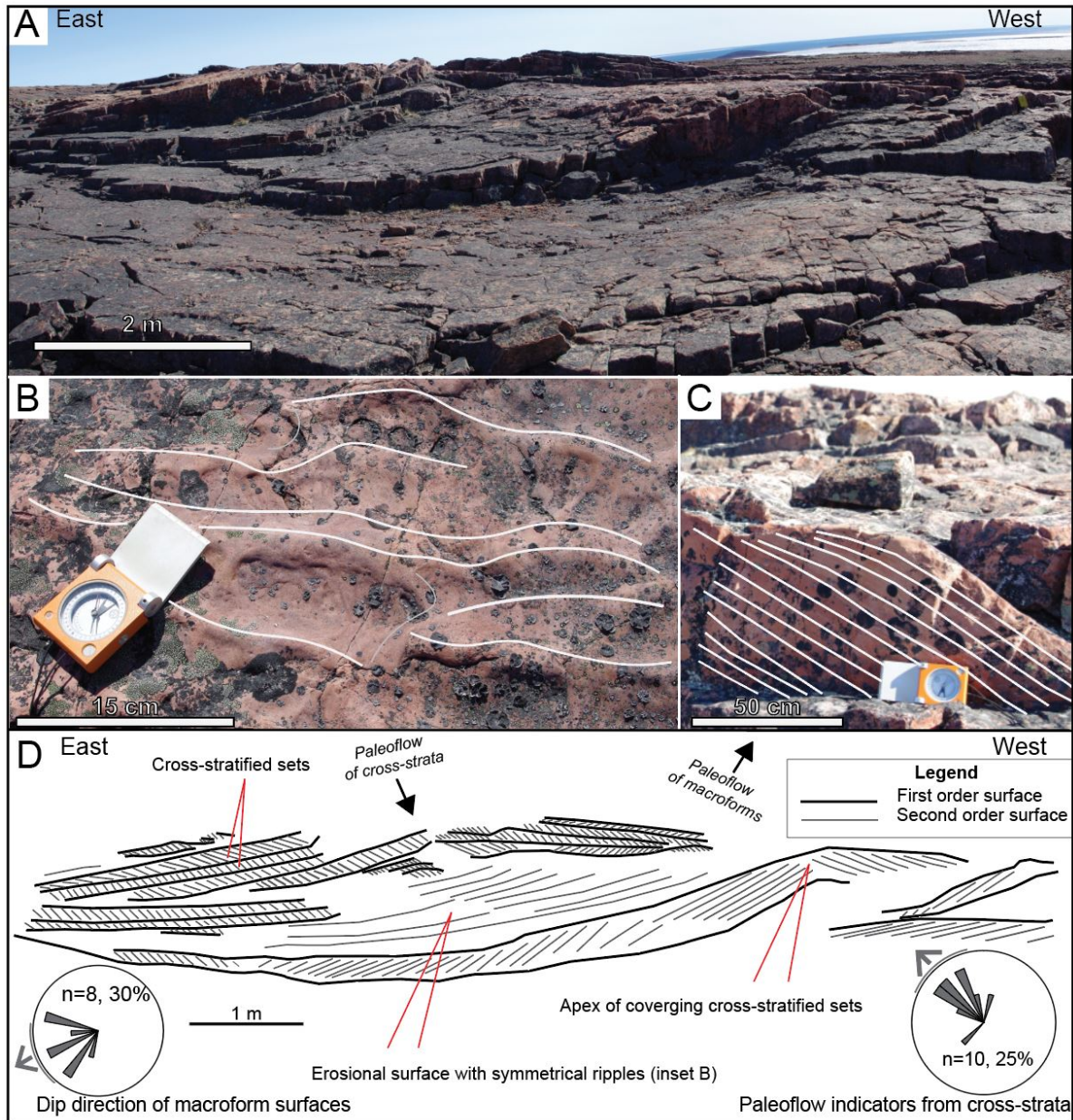
Figure 3-12: Architecture of cross-stratified sandstone

Field photos and annotations showing architectural features of cross-stratified sandstone strata.

A–D) Large foreset bar identified in section BI4 including: A) a panoramic photo of the sediment

body; B) details of symmetrical ripples (white lines) with a sub-orthogonal interference pattern

(gray lines), facies Ssr; C) high-angle planar cross-bed set with white lines indicating stratification;

and D) line drawing showing the main stratification features of the exposure in Part A.
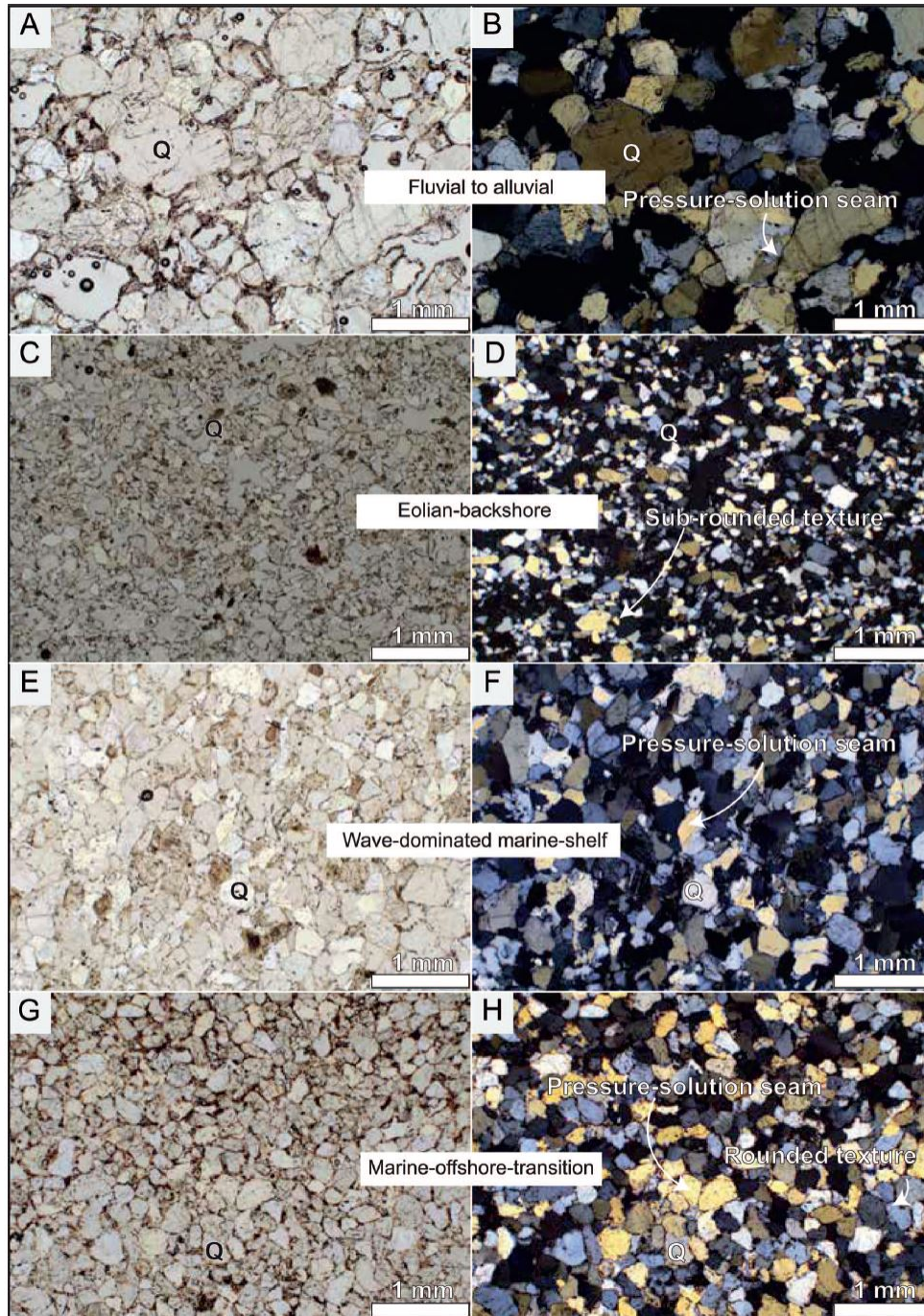
Figure 3-13: Thin-section petrography photo table

Plane light (left panels) and cross-polarized (right panels) thin-section photographs of the sandstone-dominated facies associations. A, B) Fluvial to alluvial facies association. C, D) Backshore-marine facies association. E, F) Wave-dominated marine-shelf facies association. G, H) Offshore transition of the marine-shelf facies association.
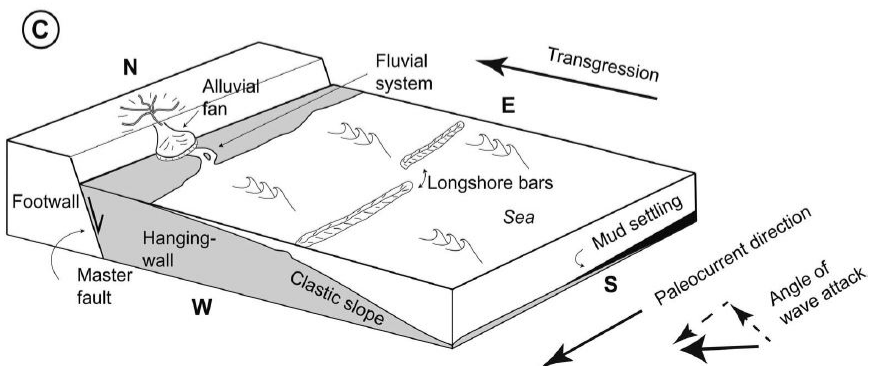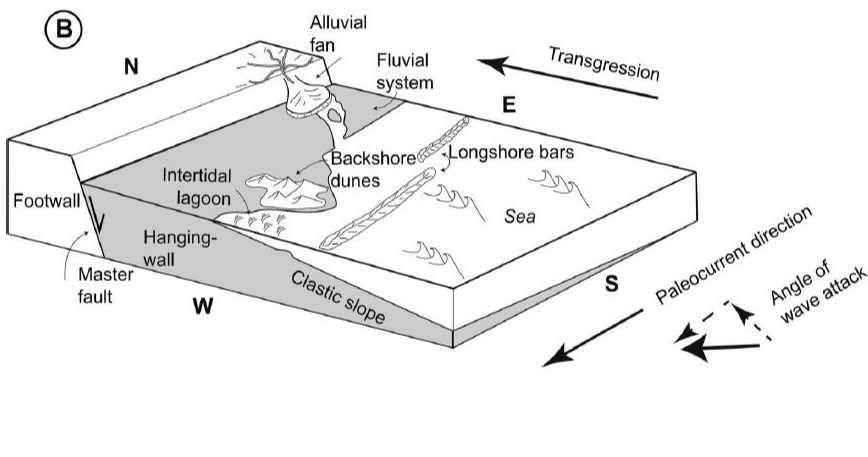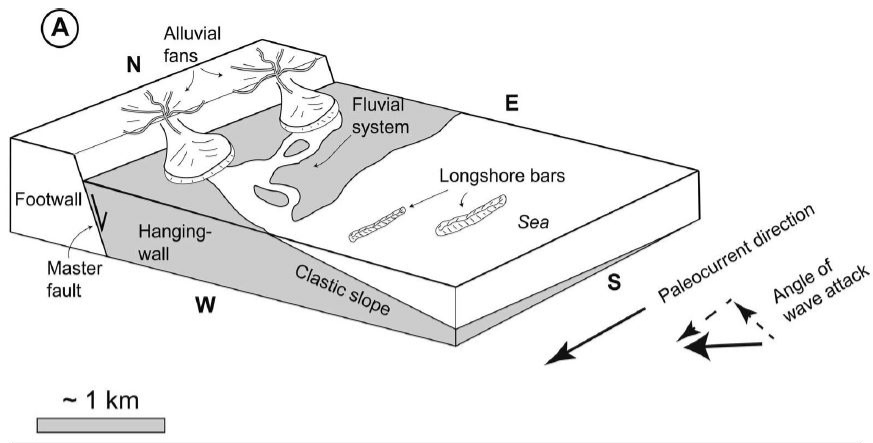
Figure 3-14: Block diagram

Block-diagram models showing the salient relationship between depositional paleo-environments, paleo-topography, faulting, and sediment dispersal during the time of progressive deposition of the Nyeboe Formation, including A) basin inception, B) establishment of coastal complexes of lagoons and backshore dunes, and C) eventual transgression of sandy, wave-influenced marine realm.
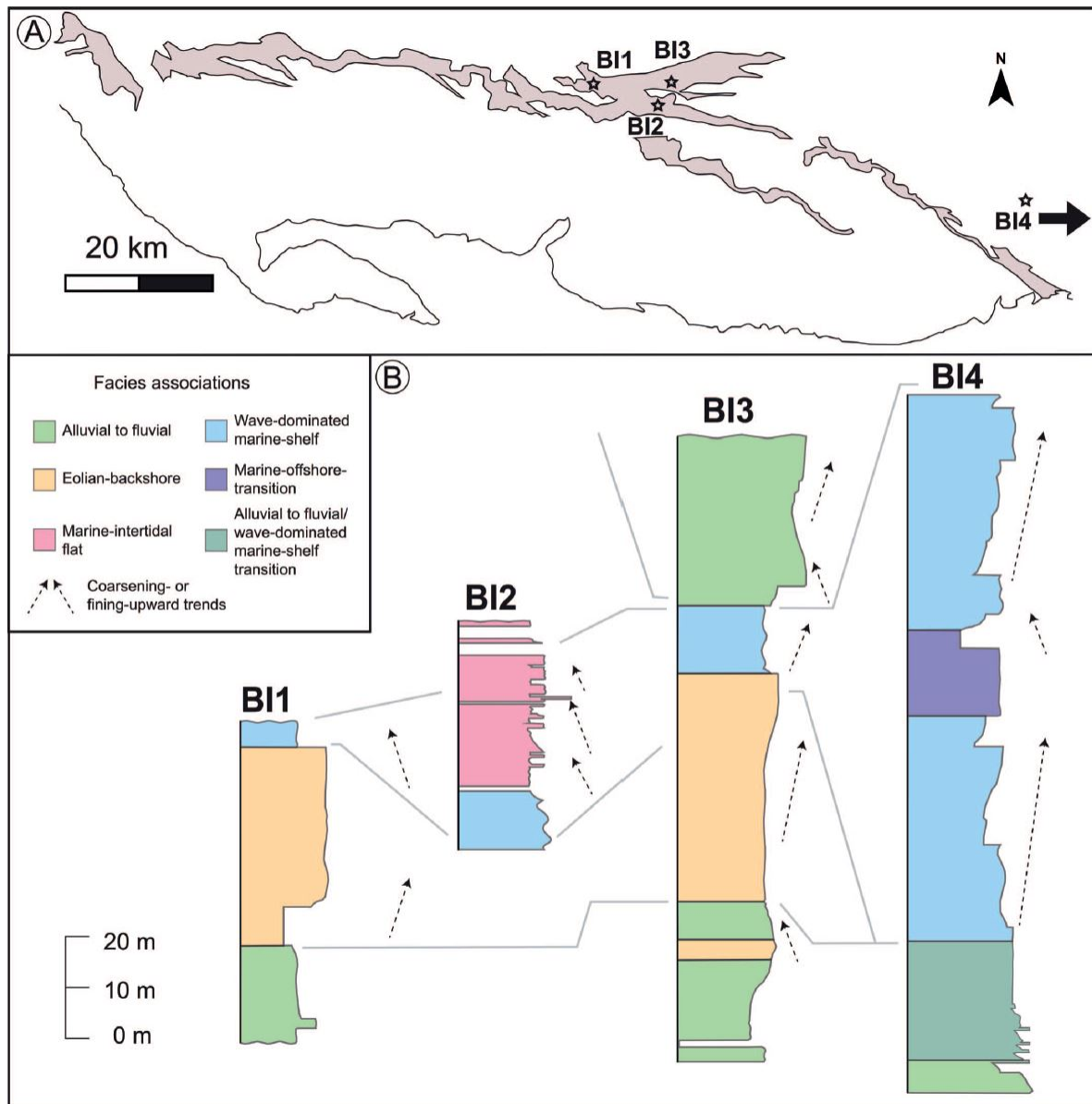
Figure 3-15: Lateral changes in facies

Lateral changes of facies associations on the Baffin Island exposure of the Nyeboe Formation. Simplified stratigraphic sections with inferred fining- and coarsening-upward sequences are shown on a A) map and then B) correlated to show lateral distribution of depositional environments. This correlation is not hung any a specific horizon and therefore approximated based on depositional environment represented.

3.10 Tables

Code	Description	Interpretation
Cbr	**Angular-clast conglomerate and breccia**. Disorganized, angular pebble- to cobble-size conglomerate and breccia, medium-grained sandstone to granule matrix, with a clast-supported, structureless aspect. Crude bedding defines m-thick units.	Proximal deposition operated by short-travelled mass flows (Blair and McPherson 1998; Talling et al. 2012). Clast-supported aspect and crude bedding suggest depositional freezing.
Cpy	**Polymictic conglomerate**. Disorganized, normally graded deposits with pebble- to boulder-grade, extraformational and intraformational, rounded framework clasts, and medium-grained sandstone to granules matrix. The deposit is clast-supported, and crude bedding defines > 1-m-thick units.	Proximal deposition by cohesive debris flows, with intraformational clasts likely derived from gravitational failure of nearby deposits (Talling et al. 2012).
Stc	**Trough cross-stratified quartz monomict conglomerate and sandstone**. Normally graded medium-grained sandstone to cobble-grade, extraformational subrounded framework clasts, and medium-grained sandstone matrix. The deposit is clast-supported; cobbles floor intra-set scour surfaces; finer-grained fractions exhibit trough cross-stratification. Bedding defines units 30 cm to 2 m	Deposition of sand and gravel by tractional waterflows in the subcritical regime. The trough cross-stratification indicates accretion and progradation of 3D dunes, likely in confined channels (Miall 1978; Plint 1983; Bridge 2006).

	thick.	
Spc	**Planar-stratified quartz monomict conglomerate and sandstone**. Normally graded deposits with fine-grained sandstone to pebble- to cobble-grade, extraformational subrounded framework clasts, and medium-grained sandstone to granule matrix. The deposit is clast-supported and organized in units 10 cm to 150 cm thick.	Deposition of sand and gravel by tractional waterflows in the supercritical regime. The planar stratification likely formed as bedload sheet migrated downstream (Feary 1984; Bennett and Bridge 1995; Collinson 1996; Bridge 2006).
Sma	**Massive sandstone**. Ungraded, structureless medium- to coarse-grained sandstone, flooring erosional surfaces. Organized in 1sets 0 cm to 3 m thick.	Depositional freezing of bedload-dominated underflows (Mulder and Syvitski 1995; Reading and Collinson 1996; Myrow et al. 2002; Plink-Björklund and Steel 2004).
Shc	**Hummocky cross-stratified sandstone**. Ungraded or normally graded medium- to coarse-grained sandstone, in places with flaggy lamination, exhibiting low-angle cross-stratification defining sinusoidal geometries (with amplitude of 10 cm to 100 cm). In some exposures, loading may emphasize the increase the angle of the stratification. Organized in sets 20 cm to 3 m thick.	Sand winnowing by interacting storm-wave agitation and relaxation flows (Greenwood and Sherman 1986; Arnott and Southard 1990).
Ssr	**Symmetrically rippled sandstone**. Ungraded medium-grained sandstone exhibiting symmetrical	Sand winnowing by subcritical-flow-regime, oscillatory flows in ripple-bed configuration (Harms et al. 1975; Miall 1978; Plint

	ripples. Organized in units 5 cm to 50 cm thick.	1983).
Sps	**Plane-parallel stratified sandstone**. Ungraded or normally graded fine- to medium-grained sandstone, exhibiting planar stratification. Organized in units 5 cm to 8 m thick.	Deposition of sand by tractional waterflows in the supercritical regime. The planar stratification likely formed as bedload sheet and traction carpets migrated downstream (Miall 1977; Cant and Walker 1976).
Sas	**Asymptotic, pinstripe cross-stratified sandstone.** Medium-grained sandstone exhibiting pinstripe cross-stratification (i.e., asymptotic cross-stratification with laminae defined by sharp grain-size segregation), and siltstone with adhesion warts. Organized in sets 5 cm to 1.25 m thick.	Sand winnowing and deposition by air flows. The cross-stratification likely formed from migration of aeolian dunes (Sharp 1963; Fryberger et al. 1992; Mountney 2006). The adhesion structures are a product of wind blowing sand over damp interdune surfaces (Mountney 2006).
Sdr	**Dolomitic ripple cross-laminated sandstone**. Ungraded or normally graded fine- to medium-grained sandstone with dolomitic cement, often microbially laminated and wrinkled, exhibiting symmetrical ripples. Organized in units 5 cm to 10 cm thick.	Deposition (and early cementation?) of sand by (oversaturated?) water flows in the subcritical regime and in ripple-bed configuration (Miall 1985). Colonization of the substrate by microbial communities, which likely caused the wrinkled appearance (Noffke 2009).
Shb	**Herringbone cross-stratified sandstone**. Normally graded fine-grained sandstone with dolomitic cement, exhibiting herringbone cross-stratification. Organized in sets 8 cm to 15 cm thick.	Sand deposition by polarly reversing water flows in the subcritical regime, and in ripple-bed configuration (Takashimizu and Masuda 2000; Amajor 1984).
Mrd		

	Red mudstones with desiccation cracks. Ungraded or normally graded mudstone to very fine-grained sandstone. Organized in units 5 cm to 100 cm thick.	Deposition of sand by subcritical-flow-regime water flows, interposed with settling of fines in standing water. The polygonal desiccation cracks likely formed from periodic wetting-drying cycles (Marconato et al. 2014), and thus indicates periodic exposure.
Mpr	**Plane-parallel-stratified red mudstone to siltstone**. Ungraded to normally graded mudstone to siltstone, either structure-less or exhibiting planar laminations. Organized in sets 3 cm to 10 cm thick.	Deposition of sand by diluted, supercritical-flow-regime waterflows in the plane-bed configuration and interposed fallout of silt fractions (Miall 1977).
Dst	**Stromatolitic dolostone**. Isopachously laminated, columnar stromatolites. Bioherms are ~5 cm in diameter. Mounds have 0.25 m to 0.3 m synoptic relief.	Accretion of microbial bioherms in agitated, clastic-starved, oversaturated-water marine shoals (Kah et al. 2009).

Table 3-1: Sedimentary facies in the Nyeboe Formation

Description and interpretation of the sedimentary facies recognized in Nyeboe Formation (after Collinson et al. 2006).

3.11 References

Aigner, D.K., 1985, Storm depositional systems: dynamic stratigraphy in modern and ancient shallow-marine sequences, lecture Notes in Earth Sciences, Berlin, Springer-Verlag, v. 3, 174 p.

Allen, J.R., 1968, The nature and origin of bed-form hierarchies: Sedimentology, v. 10, p. 161–182.

Allen, P.A., And Allen, J.R., 2005, Basin Analysis: Principles and Applications, Blackwell Publishing, v. 2, 547 p.

Amajor, L.C., 1984, Sedimentary facies analysis of the Ajali sandstone (upper Cretaceous), southern Benue Trough: Journal of Mining and Geology, v. 21, p. 171–176.

Andersen, T., 2014, The detrital zircon record: Supercontinents, parallel evolution－Or coincidence?: Precambrian Research, v. 244, p. 279–287.

Armitage, J.J., And Allen, P.A. 2010, Cratonic basins and the long-term subsidence history of continental interiors, Geological Society of London Journal, v. 167, p. 61–70.

Arnott, R.W., And Southard, J.B., 1990, Exploratory flow-duct experiments on combined-flow bed configurations, and some implications for interpreting storm-event stratification: Journal of Sedimentary Petrology, v. 60, p. 211–219.

Bállico, M.B., Scherer, C.M.S., Mountney, N.P., Souza, E.G., Chemale, F., Pisarevsky, S.A., And Reis, A.D., 2017, Wind-pattern circulation as a palaeogeographic indicator: Case study of the 1.5–1.6 Ga Mangabeira Formation, São Francisco Craton, Northeast Brazil: Precambrian Research, v. 298, p. 1–15.

Baragar, W.R.A., Ernst, R.E., Hulbert, L., And Peterson, T., 1996, Longitudinal Petrochemical
        Variation in the Mackenzie Dyke Swarm, Northwestern Canadian Shield: Journal of
        Petrology, v. 37, p. 317‒359.

Bennett, S.J., And Bridge, J.S., 1995, The geometry and dynamics of low-relief bed forms in
        heterogeneous sediment in laboratory channel, and their relationship to water flow: Journal
        of Sedimentary Research, v. A65, p. 29‒39.

Blackadar, R.G., 1958, Fury and Hecla Strait map-area: Arctic, v. 11, p. 156‒163.

Blair, T.C., And Bilodeau, W.L., 1988, Development of tectonic cyclothems in rift, pull-apart, and
        foreland basins: Sedimentary response to episodic tectonism: Geology, v. 16, p. 517‒520.

Blair, T.C., And Mcpherson, J.G., 1998, Recent debris-flow processes and resultant form and
        facies of the Dolomite alluvial fan, Owens Valley, California: Journal of Sedimentary
        Research, v. 68, p. 800‒818.

Buchan, K.L., And Ernst, R.E., 2013, Diabase dyke swarms of Nunavut, Northwest Territories and
        Yukon, Canada: Geological Survey of Canada, Open File 7464, scale 1:3,000,000.

Busby-Spera C.J., And White, J.D.L., 1987, Variation in peperite textures associated with
        differing host-sediment properties. Bulletin of Volcanology, v. 49, p. 765‒775.

Butterfield, N.J., 2000, Bangiomorpha pubescens n. gen., n. sp.: implications for the evolution of
        sex, multicellularity, and the Mesoproterozoic/Neoproterozoic radiation of eukaryotes:
        Paleobiology, v. 26, p. 386‒404.

Bridge, J.S., 2006, Fluvial facies models: recent developments, in Posamentier, H.W., and Walker,
        R.G., eds., Facies Models Revisited: SEPM, Special Publication 84, p. 85‒170.

Cattaneo, A., And Steel, R.J., 2003, Transgressive deposits: A review of their variability: Earth-Science Reviews, v. 62, p. 187‒228.

Cant, D.J., And Walker, R. G., 1976, Development of a braided-fluvial facies model for the Devonian Battery Point Sandstone, Québec: Canadian Journal of Earth Sciences, v. 13, p. 102‒119.

Chakraborty, T., 1991, Sedimentology of a Proterozoic erg: the Venkatpur Sandstone, Pranhita-Godavari Valley, south India: Sedimentology, v. 38, p. 301‒322.

Chakraborty, C., 2001, Lagoon-tidal flat sedimentation in an epeiric sea: Proterozoic Bhander Group, Son Valley, India: Geological Journal, v. 36, p. 125‒141.

Chandler, F.W., Charbonneau, B.W., Ciesielski, A, Maurice, Y.T., And White, S., 1980, Geological studies of the late Precambrian supracrustal rocks and underlying granitic basement, Fury and Hecla Strait area, Baffin Island, District of Mackenzie: Geological Survey of Canada, Current Research, v. 80, p. 125‒132.

Chandler, F.W., And Stevens, R.D., 1981, Potassium-argon age of the late Proterozoic Fury and Hecla Formation, northwest Baffin Island, District of Franklin: Geological Survey of Canada, Current Research, v. 81, p. 37‒40.

Chandler, F.W., 1988, Geology of the Late Precambrian Fury and Hecla Group, Northwest Baffin Island, District of Franklin: Geological Survey of Canada, Bulletin 370, p. 26‒32.

Cheel, R.J., And Leckie, D.A., 1993, Cross-stratification: Sedimentology Review, p. 103‒122.

Clifton, H.E., 2006, A re-examination of facies models for clastic shorelines, in Posamentier, H.W., and Walker, R.G., eds., Facies Models Revisited: SEPM, Special Publication 84, p.

293‒337.

Collinson, J.D., 1969, The Sedimentology of the Grindslow Shales and the Kinderscout Grit: A Deltaic Complex in the Namurian, of Northern England: Journal of Sedimentary Petrology, v. 39, p. 194‒221.

Collinson, J.D., 1996, Alluvial sediments, in Reading, H.G., Sedimentary Environments: Processes, Facies, and Stratigraphy, p. 37‒82.

Collinson, J.D., Mountney, N.P., And Thompson, D.B., 2006, Sedimentary Structures: Enfield, U.K., Terra Publishing, 292 p.

Covey, M., 1986, The evolution of foreland basins to steady state: evidence form the western Taiwan foreland basin, in Allen, P.A., Homewood, P., Foreland Basins: International Association of Sedimentologists Special Publications, v. 8, p. 77‒90.

Dalrymple, R.W., Knight, R.J., Zaitlin, B.A., And Middleton, G.V., 1990, Dynamics and facies model of a macrotidal sand-bar complex, Cobequid Bay-Salmon River Estuary (Bay of Fundy): Sedimentology, v. 37, p. 577‒612.

Dalrymple, R.W. 1992, Tidal Depositional Systems, in Walker, R.G., and James, N.P., Facies Models: Response to Sea-Level Change: Geological Association of Canada, p. 195‒218.

Dalrymple, R.W., And Choi, K., 2007, Morphologic and facies trends through the fluvial‒marine transition in tide-dominated depositional systems: A schematic framework for environmental and sequence-stratigraphic interpretation: Earth-Science Reviews, v. 81, p. 135‒174.

Davidson, A., 2008, Late Paleoproterozoic to mid-Neoproterozoic history of northern Laurentia: An overview of central Rodinia: Precambrian Research, v. 160, p. 5‒22.

Davies, N.S., Shillito, A.P., And Mcmahon, W.J., 2017, Short-term evolution of primary sedimentary surface textures (microbial, abiotic, ichnological) on a dry stream bed: modern observations and ancient implications: Palaios, v. 32, p. 125‒134.

Dawes, P.R., 1997, The Proterozoic Thule Supergroup, Greenland and Canada: history, lithostratigraphy and development: Geology of Greenland Survey Bulletin, v. 174, 152 p.

Donaldson, J.A., Eriksson, P.G., And Altermann, W. 2002, Actualistic vs. non-actualistic conditions in the Precambrian sedimentary record: reappraisal of an enduring discussion in Altermann, W., Corcoran, P.L., eds., Precambrian sedimentary environments: a modern approach to ancient depositional systems, Special publication of the international association of sedimentologists, v. 33, p. 3‒14.

Dott, R.H., And Bourgeois, J. 1982, Hummocky stratification: Significance of its variable bedding sequences: Geological Society of America Bulletin 93, p. 663‒680.

Dufour, F., Stevenson, R., And Halverson, G.P. 2020, Timing of emplacement of mafic rocks of the Fury and Hecla Group and younger mafic intrusions, northwestern Baffin Island, Nunavut: Summary of Activities 2019, Canada-Nunavut Geoscience Office, p. 27‒36.

Dumas, S., And Arnott, R.W.C. 2006, Origin of hummocky and swaley cross-stratification‒ The controlling influence of unidirectional current strength and aggradation rate: Geology, v. 34, p. 1073‒1076.

Eastwood, E. N., Kocurek, G., Mohrig, D., And Swanson, T. 2012, Methodology for reconstructing wind direction, wind speed and duration of wind events from aeolian cross-strata: Journal of Geophysical Research: Earth Surface, v. 117, F03035, p. 1‒20.

Eriksson, P.G., Banerjee, S., Catuneanu, O., Corcoran, P.L., Eriksson, K.A., Hiatt, E.E., Laflamme, M., Lenhardt, N., Long, D.G.F., Miall, A.D., Mints, M.V., Pufahl, P.K., Sarkar, S., Simpson, E.L., And Williams, G.E. 2013, Secular changes in sedimentation systems and sequence stratigraphy: Gondwana Research, v. 24, p. 468‒489.

Fahrig, W.F., Christie, K.W., And Jones, D.L. 1981, Paleomagnetism of the Bylot basins: Evidence for Mackenzie continental tensional tectonics; Proterozoic Basins of Canada: Geological Survey of Canada Paper, v. 81, p. 303‒312.

Feary, D. A. 1984, The Boambolo Formation-a Silurian prograding fan-delta sequence in southeastern New South Wales, Australia: Sedimentary Geology, v. 39, p. 169‒195.

Fidolini, F., Ghinassi, M., Aldinucci, M., Billi, P., Boaga, J., Deiana, R., And Brivio, L. 2013, Fault-sourced alluvial fans and their interaction with axial fluvial drainage: An example from the Plio-Pleistocene Upper Valdarno Basin (Tuscany, Italy): Sedimentary Geology, v. 289, p. 19‒39.

Fryberger, S.G., Hesp, P., And Hastings, K. 1992, Aeolian granule ripple deposits, Namibia: Sedimentology, v. 39, p. 319‒331.

Galloway, W. E., And Hobday, D. K. 1996, Fluvial Systems in Galloway, W.E., Hobday, D.K., eds., Springer-Verlag Berlin Heidelberg, Terrigenous Clastic Depositional Systems, p. 60‒90.

Galloway, W. E. 2002, Paleogeographic Setting and Depositional Architecture of a Sand-
        Dominated Shelf Depositional System, Miocene Utsira Formation, North Sea Basin:
        Journal of Sedimentary Research, v. 72, p. 476‑490.

Gawthorpe, R.L., And Leeder, M.R. 2000, Tectono-sedimentary evolution of active extensional
        basins: Basin Research, v. 12, p. 195‑218.

Ghinassi, M. 2007, The effects of differential subsidence and coastal topography on high-order
        transgressive‑regressive cycles: Pliocene nearshore deposits of the Val d'Orcia Basin,
        Northern Apennines, Italy: Sedimentary Geology, v. 202, p. 677‑701.

Gibson, T.M., Shih, P.M., Cumming, V.M., Fischer, W.W., Crockford, P.W., Hodgskiss, M.S.W.,
        Wörndle, S., Creaser, R.A., Rainbird, R.H., Skulski, T.M., And Halverson, G.P. 2018,
        Precise age of Bangiomorpha pubescens dates the origin of eukaryotic photosynthesis:
        Geology, v. 46, p. 135‑138.

Gibson, T.M., Wörndle, S., Crockford, P.W., Hao Bui, T., Creaser, R.A., And Halverson, G.P.
        2019, Radiogenic isotope chemostratigraphy reveals marine and nonmarine depositional
        environments in the late Mesoproterozoic Borden Basin, Arctic Canada: Geological
        Society of America Bulletin, v. 131, p. 1965‑1978.

Greenman, J.W., Patzke, M, Halverson, G.P., And Ielpi, A. 2018, Refinement of the stratigraphy
        of the late Mesoproterozoic Fury and Hecla Basin, Baffin Island, Nunavut, with a specific
        focus on the Agu Bay and Autridge formations: Summary of Activities 2018, Canada-
        Nunavut Geoscience Office, p. 85‑96.

Greenman, J.W., Patzke, M., Halverson, G.P., And Ielpi, A. 2020, Updated stratigraphy of the Fury and Hecla Group of Melville Peninsula and northwestern Baffin Island, Nunavut: Summary of Activities 2019, Canada-Nunavut Geoscience Office, p. 37‒50.

Greenman, J.W., Rooney, A.D., Patzke, M., Ielpi, A., And Halverson, G.P., 2021, Re-Os geochronology highlights widespread latest Mesoproterozoic (ca. 1090‒1050) cratonic basin development on northern Laurentia: Geology, v. 49, , p. 779‒783.

Greenwood, B., And Sherman, D.J. 1986, Hummocky cross-stratification in the surf zone: flow parameters and bedding genesis: Sedimentology, v. 33, p. 33‒45.

Grotzinger, J.P., And James, N.P. 2000, Precambrian carbonates: Evolution of understanding in Grotzinger, J.P., James, N.P., eds., Sedimentation and Diagenesis in the Evolving Precambrian World, SEPM Special Publication 67, p. 3‒19.

Hahn, K.E., Turner, E.C., Babechuk, M.G., And Kamber, B.S. 2015, Deep-water seep-related carbonate mounds in a Mesoproterozoic alkaline lake, Borden Basin (Nunavut, Canada): Precambrian Research, v. 271, p. 173‒197.

Hahn, K.E., And Turner, E.C. 2017, Composition and history of giant carbonate seep mounds, Mesoproterozoic Borden Basin, Arctic Canada: Precambrian Research, v. 293, p. 150‒173.

Harms, J.C., Southard, J.B., And Walker, R.G. 1975, Depositional environments as interpreted from sedimentary structures and stratification sequences: SEPM Short Course, v. 9, 249 p.

Hart, B.S., And Plint, G. 1995, Gravelly shoreface and beachface deposits: Special Publication of the International Association of Sedimentologist in Plint, G., Sedimentary Facies Analysis: A Tribute to the Research and Teaching of Harold G. Reading, v. 22, p. 75‒99.

Heaman, L.M., Lecheminant, A.N., And Rainbird, R.H. 1992, Nature and timing of Franklin igneous events, Canada: implications for a Late Proterozoic mantle plume and the breakup of Laurentia: Earth and Planetary Science Letters, v. 109, p. 117‒131.

Herbers, D. S., Macnaughton, R. B., Timmer, E. R., Gingras, M. K., And Hubbard, S. 2016, Sedimentology and ichnology of an Early-Middle Cambrian storm-influenced barred shoreface succession, Colville Hills, Northwest Territories: Bulletin of Canadian Petroleum Geology, v. 64, p. 538‒554.

Hilbert, N.N., Guedes, C.C.F., And Giannini, P.C.F. 2015, Morphologic and sedimentologic patterns of active aeolian dune-fields on the east coast of Maranhão, northeast Brazil: Earth Surface Processes and Landforms, v. 41, p. 87‒97.

Hodgskiss, M.S.W., Sansjofre, P., Kunzmann, M., Sperling, E.A., Cole, D.B., Crockford, P.W., Gibson, T.M., And Halverson, G. P. 2020, A high-TOC shale in a low productivity world: The late Mesoproterozoic Arctic Bay Formation, Nunavut: Earth and Planetary Science Letters, v. 544, p. 1¬‒14.

Ielpi, A., And Rainbird, R.H. 2015, Architecture and morphodynamics of a 1.6 Ga fluvial sandstone: Ellice Formation of Elu Basin, Arctic Canada: Sedimentology. v. 62, p. 1950‒1977.

Ielpi, A., Rainbird, R.H., Ventra, D., Ghinassi, M. 2017, Morphometric convergence between Proterozoic and post-vegetation rivers: Nature Communications, v. 8, p. 15250.

Ielpi, A. Morphodynamics of meandering streams devoid of plant life: Amargosa River, Death Valley, California. GSA Bulletin 2018; 131 (5-6): 782‒802.

Jackson, G.D., And Iannelli, T.R. 1981, Rift-related cyclic sedimentation in the Neohelikian Borden Basin, Northern Baffin Island in Campbell, F.H.A., ed., Proterozoic Basins of Canada: Geological Survey of Canada, Paper 81-10, p. 269‒302.

Johnson, H.D. And Baldwin, C.T. 1996, Shallow Clastic Seas in Reading, H.G., 3 ed., Sedimentary environments: processes, facies and stratigraphy, p. 232‒280.

Kah, L.C., Bartley, J.K., And Stagner, A.F. 2009, Reinterpreting a Proterozoic enigma: Conophyton‒Jacutophyton stromatolites of the Mesoproterozoic Atar Group, Mauritania in Swart, P.K., Eberli, G.P., McKenzie, J.A., eds., Perspectives in Carbonate Geology: A Tribute to the Career of Robert Nathan Ginsburg: Special Publication 41 of the International Association of Sedimentologists, p. 277‒295.

Kah, L.C., Sherman, A.G., Narbonne, G.M., Knoll, A.H., And Kaufman, A.J. 1999, ^{13}C stratigraphy of the Proterozoic Bylot Supergroup, Baffin Island, Canada: Implications for regional lithostratigraphic correlations: Canadian Journal of Earth Sciences, v. 36, p. 313‒322.

Kirk, R.M., And Lauder, G.A. 2000, Significant coastal lagoon systems in the South Island, New Zealand: Coastal processes and lagoon mouth closure: Science for Conversation, v. 146, 46 p.

Knoll, A.H., Wörndle, S., Kah, L.C. 2013, Covariance of microfossil assemblages and microbialite textures across an upper Mesoproterozoic carbonate platform: Palaios, v. 28, p. 453‒470.

Köykkä, J., And Lamminen, J. 2011, Tidally influenced clastic epeiric sea at a Mesoproterozoic continental margin, Rjukan Rift Basin, southern Norway: Precambrian Research, v. 185, p. 164‑182.

Lebeau, L.E., And Ielpi, A. 2017, Fluvial channel-belts, flood basins, and aeolian ergs in the Precambrian Meall Dearg Formation (Torridonian of Scotland): Inferring climate regimes from pre-vegetation clastic rock records: Sedimentary Geology, v. 357, p. 53‑71.

Lecheminant, A.N., And Heaman, L.M. 1989, Mackenzie igneous events, Canada: Middle Proterozoic hotspot magmatism associated with ocean opening: Earth and Planetary Science Letters, v. 96, p. 38‑48.

Long, D.G.F. 2011, Architecture and depositional style of fluvial systems before land plants: a comparison of Precambrian, early Paleozoic and modern river deposits in Davidson, S.K., Leleu, S., North, C.P., eds., From River to Rock Record: The Preservation of Fluvial Sediments and their Subsequent Interpretation: SEPM Special Publication 97, p. 37‑61.

Long, D.G.F., And Turner, E.C. 2012, Tectonic, sedimentary and metallogenic re-evaluation of basal strata in the Mesoproterozoic Bylot basins, Nunavut, Canada: Are unconformity-type uranium concentrations a realistic expectation?: Precambrian Research. v. 214‑215, p. 192‑209.

Macquaker, J.H.S., And Taylor, K.G. 1996, A sequence-stratigraphic interpretation of a mudstone -dominated succession: The Lower Jurassic Cleveland Ironstone Formation, UK: Journal of the Geological Society, v. 153, p. 759‑770.

Marconato, A., De Almeida, R.P., Turra, B.B., And Dos Santos Fragoso-Cesar, A.R. 2014, Pre-vegetation fluvial floodplains and channel-belts in the Late Neoproterozoic‑Cambrian Santa Bárbara group (Southern Brazil): Sedimentary Geology, v. 300, p. 49-61.

Mayr, U., Brent, T.A., De Freitas, T., Frisch, T., Nowlan, G.S. And Okulitch, A.V. 2004, Geology of eastern Prince of Wales Island and adjacent smaller islands, Nunavut: Geological Survey of Canada, Bulletin 547, 88 p.

Mcmahon, W. J., Davies, N. S., And Went, D. J. 2017, Negligible microbial matground influence on pre-vegetation river functioning: Evidence from the Ediacaran-Lower Cambrian Series Rouge, France: Precambrian Research, v. 292, p. 13‑34.

Miall, A.D. 1977, A review of the braided-river depositional environment: Earth-Science Reviews, v. 13, p. 1-62.

Miall, A.D. 1978, Paleocurrents and Basin Analysis: Geoscience Canada, v. 5, p. 160‑161.

Miall, A.D. 1985, Architectural-element analysis: A new method of facies analysis applied to fluvial deposits: Earth-Science Reviews, v. 22, p. 261‑308.

Miall, A.D. 2014, Updating uniformitarianism: stratigraphy as just a set of ʺfrozen accidentsʺ in Smith, D.G., Bailey, R.J., Burgess, P.M., Fraser, A.J., eds., Strata and Time: Probing the Gaps in Our Understanding: Geological Society of London Special Publication 404, p. 11‑36.

Morgan, P., And Ramberg, I. B. 1987, Physical changes in the lithosphere associated with thermal relaxation after rifting: Tectonophysics, v. 143, p. 1‑11.

Mortimer, E., And Carrapa, B. 2007, Footwall drainage evolution and scarp retreat in response to increasing fault displacement: Loreto fault, Baja California Sur, Mexico: Geology, v. 35, p. 651.

Mountney, N. P., And Thompson, D. B. 2002, Stratigraphic evolution and preservation of aeolian dune and damp/wet interdune strata: an example from the Triassic Helsby Sandstone Formation, Cheshire Basin, UK: Sedimentology, v. 49, p. 805‒833.

Mountney, N.P. 2006, Eolian facies in Posamentier, H.W., and Walker, R.G., eds., Facies Models Revisited: SEPM, Special Publication 84, p. 19‒83.

Muhlbauer, J.G., Fedo, C.M. And Moersch, J.E. 2020, Architecture of a distal pre‒vegetation braidplain: Cambrian middle member of the Wood Canyon Formation, southern Marble Mountains, California, USA: Sedimentology, v. 67, p. 1084‒1113.

Mulder, T., And Syvitski, J.P.M. 1995, Turbidity currents generated at river mouths during exceptional discharges to the world oceans: The Journal of Geology, v. 103, p. 285‒299.

Muto, T., And Steel, R. J. 2002, In defense of shelf‒edge delta development during falling and lowstand of relative sea level: The Journal of Geology, v. 110, p. 421‒436.

Myrow, P.M., Fischer, W., And Goodge, J.W. 2002, Wave‒Modified Turbidites: Combined‒Flow Shoreline and Shelf Deposits, Cambrian, Antarctica: Journal of Sedimentary Research, v. 72, p. 641‒656.

Nichols, G. 2009, Sedimentology and Stratigraphy. Wiley-Blackwell, 2 ed., v. 2, 432 p.

Noffke, N. 2009, The criteria for the biogeneicity of microbially induced sedimentary structures (MISS) in Archean and younger, sandy deposits: Earth-Science Reviews, v. 96, p.

173‒180.

Olson. R.A. 1977, Geology and genesis of zinc-lead deposits within a late Proterozoic dolomite, Northern Baffin Island, N.W.T. [PhD Thesis]: University of British Colombia, 387 p.

Patzke, M., Greenman, J.W., Ielpi, A., And Halverson, G.P. 2018, Sedimentology of the sandstone -dominated units in the Fury and Hecla Basin, Northern Baffin Island, Nunavut: Summary of Activities 2018, Canada-Nunavut Geoscience Office, p. 75‒84.

Pehrsson, S.J., And Buchan, K.L. 1999, Borden dykes of Baffin Island, Northwest Territories: a Franklin U-Pb baddeleyite age and a paleomagnetic reinterpretation: Canadian Journal of Earth Sciences, v. 35, p. 65‒73.

Pehrsson, S.J., Berman, R.G., And Davis, W.J. 2013, Paleoproterozoic orogenesis during Nuna aggregation: A case study of reworking of the Rae craton, Woodburn Lake, Nunavut: Precambrian Research, v. 232, p. 167‒ 188.

Plink-Björklund, P., And Steel, R.J. 2004, Initiation of turbidity currents: outcrop evidence for Eocene hyperpycnal flow turbidites: Sedimentary Geology, v. 165, p. 29‒52.

Plint, A.G. 1983, Facies, environments and sedimentary cycles in the Middle Eocene, Bracklesham Formation of the Hampshire Basin: evidence for global sea-level changes?: Sedimentology, v. 30, p. 625‒653.

Rainbird, R.H., Jefferson, C.W., And Young, G.M. 1996, The early Neoproterozoic sedimentary Succession B of northwestern Laurentia: Correlations and paleogeographic significance: Geological Society of America Bulletin, v. 108, p. 454‒470.

Rainbird, R.H., And Young, G. 2009, Colossal Rivers, Massive Mountains and Supercontinents: Earth Magazine, v. 54, p. 52‒61.

Reading, H.G., And Collinson, J.D. 1996, Clastic coasts in Reading, H.G., ed., Blackwell Scientific Publications, Sedimentary Environments: Processes, Facies and Stratigraphy, p. 154‒231.

Reading, H.G. And Levell, B.K. 1996, Controls on the sedimentary record in Reading, H.G., ed., Blackwell Scientific Publications, Sedimentary Environments: Processes, Facies and Stratigraphy, p. 5‒36.

Roep, T.B., Dabrio, C.J., Fortuin, A.R., And Polo, M.D. 1998, Late highstand patterns of shifting and stepping coastal barriers and washover-fans (late Messinian, Sorbas Basin, SE Spain): Sedimentary Geology, v. 116, p. 27‒56.

Santos, M.G.M., Owen, G. 2016 Heterolithic meandering-channel deposits from the Neoproterozoic of NW Scotland: Implications for palaeogeographic reconstructions of Precambrian sedimentary environments: Precambrian Research, v. 272, p. 226‒243.

Scherer, C.M.S., And Lavina, E.L.C. 2006, Stratigraphic evolution of a fluvial‒eolian succession: The example of the Upper Jurassic‒ Lower Cretaceous Guará and Botucatu formations, Paraná Basin, Southernmost Brazil: Gondwana Research, v. 9, p. 475‒484.

Sharp, R.P. 1963, Wind ripples: The Journal of Geology, v. 71, p. 617‒636.

Sherman, A.G., James, N.P., And Narbonne, G.M. 2002, Evidence for reversal of basin polarity during carbonate ramp development in the Mesoproterozoic Borden Basin, Baffin Island: Canada Journal of Earth Sciences, v. 39, p. 519‒538.

Shea, J.H. 1982, Twelve fallacies of uniformitarianism: Geology, v. 10, p. 455‒460.

South, D., And Talbot, M. 2000, The sequence stratigraphic framework of carbonate diagenesis within transgressive fan-delta deposits: Sant Llorenç del Munt fan-delta complex, SE Ebro Basin, NE Spain: Sedimentary Geology, v. 138, p. 179‒198.

Spratt, J., Jones, A.G., Corrigan, J.D., And Hogg, C. 2013, Lithospheric geometry revealed by deep-probing magnetotelluric surveying, Melville Peninsula, Nunavut: Geological Survey of Canada Current Research 2013-12, 14 p.

Steenkamp, H.M., Bovingdon, P.J., Dufour, F., Généreux, C., Greenman, J.W., Ielpi, A., Patzke, M., And Tinkham, D. 2018, New regional mapping of Precambrian rocks north of Fury and Hecla Strait, northwestern Baffin Island, Nunavut: Summary of Activities 2018, Canada-Nunavut Geoscience Office, p. 47‒62.

Stewart, W.D. 1987, Late Proterozoic to early Tertiary stratigraphy of Somerset Island and northern Boothia Peninsula, District of Franklin, NWT: Geological Survey of Canada, Paper 83-26, scale 1:250,000.

Stubblefield, W.L., Mcgrail, D.W., And Kersey, D.G. 1984, Recognition of transgressive and post-transgressive sand ridges on the New Jersey continental shelf in Tillman, R.W., Siemers, R.T., eds., Siliciclastic Shelf Sediments: SEPM Special Publications 34, p. 1‒23.

Suter, J.R. 2006, Clastic shelves in Posamentier, H.W., and Walker, R.G., eds., Facies Models Revisited: SEPM, Special Publication 84, p. 339‒397.

Takashimizu, Y., And Masuda, F. 2000, Depositional facies and sedimentary successions of earthquake-induced tsunami deposits in Upper Pleistocene incised valley fills, central

Japan: Sedimentary Geology, v. 135, p. 231‒239.

Talling, P.J., Masson, D.G., Sumner, E J., And Malgesini, G. 2012, Subaqueous sediment density flows: Depositional processes and deposit types: Sedimentology, v. 59, p. 1937‒2003.

Tuke, M.F., Dineley, D.L. And Rust, B.R. 1966, The basal sedimentary rocks in Somerset Island, N.W.T: Canadian Journal of Earth Sciences, v. 3, p. 697‒711.

Turner, E.C., And Kamber, B.S. 2012, Arctic Bay Formation, Borden Basin, Nunavut (Canada): Basin evolution, black shale, and dissolved metal systematics in the Mesoproterozoic ocean; Precambrian Research, v. 208, p. 1‒18.

Turner, E.C., Long, D.G.F., Rainbird, R.H., Petrus, J.A., And Rayner, N.M. 2016, Late Mesoproterozoic rifting in Arctic Canada during Rodinia assembly: impactogens, trans-continental far-field stress and zinc mineralisation: Terra Nova, v. 28, p. 188‒194.

Walker, R.G. 2006, Introduction in Posamentier, H.W., and Walker, R.G., eds., Facies Models Revisited: SEPM, Special Publication 84, p. 1‒17.

Went, D.J. 2005, Pre-vegetation alluvial fan facies and processes: an example from the Cambro-Ordovician Rozel Conglomerate Formation, Jersey, Channel Islands: Sedimentology, v. 52, p. 693‒713.

Went, D.J. 2013, Quartzite development in early Palaeozoic nearshore marine environments: Sedimentology, v. 60, p. 1036‒1058.

Young, G.M. 1979, Correlation of middle and upper Proterozoic strata of the northern rim of the North Atlantic craton: Transactions of the Royal Society of Edinburgh, v. 70, p. 323‒336.

Chapter 4

4 Detrital zircon provenance of the Fury and Hecla Group: Refining the tectono-depositional framework of the Mesoproterozoic Bylot basins (Arctic Laurentia)

Mollie Patzke[1], J. Wilder Greenman[2], Robert H. Rainbird[3], Galen P. Halverson[2], Alessandro Ielpi[1]

[1]Harquail School of Earth Sciences, Laurentian University, Sudbury, Ontario P3E 2C6, Canada

[2]Department of Earth and Planetary Sciences, McGill University, Montréal, Quebec H3A 0E8, Canada

[3]Geological Survey of Canada, 601 Booth Street, Ottawa, Ontario K1A 0E8, Canada

4.1   Abstract

Intracratonic basins that developed during supercontinent amalgamation are abundant in the Precambrian record but poorly understood. The Bylot basins of Arctic Canada and Greenland include the Fury and Hecla, Borden, Thule, and Aston-Hunting basins, which together record widespread intracratonic sedimentation on northern Laurentia during the late Mesoproterozoic. New Re-Os ages from the Fury and Hecla and Borden basins have constrained much of their deposition to ca. 1090−1040 Ma, which is ca. 200 Myr younger than had long been assumed. Here we report the first detrital zircon data from the Fury and Hecla Group, which provides new insight on the subsidence evolution and paleogeographic context of the Bylot basins. Seven samples spanning the Fury and Hecla Group record zircon U-Pb age populations ranging from ca. 3350 to ca. 1695 Ma. Ages display a bimodal probability density distribution attributed to extensive zircon

-growth events around ca. 2700 (e.g., Rae cratonization) and ca. 1900 Ma (e.g., Snowbird and Trans-Hudson orogenesis, Taltson magmatism). Compared to the Bylot Supergroup of the Borden Basin detrital-age record, the Fury and Hecla Group shows similar age peaks but different distributions in the lower and upper strata, and notably it lacks a younger ca.1.1 Ga age population. Due to the difference in depositional and detrital ages, we test the hypothesis of sedimentary recycling into the Fury and Hecla Basin (and Borden Basin) from older supracrustal successions. Detrital geochronology from the ca. 1.9 Ga Amer Group, 600 km to the southwest, shows overlap with the Fury and Hecla Group. However, only one formation in the Fury and Hecla Group shows east directed paleocurrents. Therefore, we suggest Amer Group age-equivalent source strata located east of the Fury and Hecla Basin may be undiscovered or since eroded away. We posit that the Borden Basin received recycled sediment from different sources than the Fury and Hecla Basin. Our results further our understanding of the role of recycling in intracratonic basins developed during supercontinent amalgamation.

4.2   Introduction

Detrital zircon geochronology provides summaries of geologic history that can capture entire supercontinent cycles (Cawood et al., 2013). Since the 1990s, sedimentary provenance based on detrital mineral geochronology has proved to be a powerful tool to understand the complex relationships between crustal and surface processes, and the mechanisms of continental assemblage, tenure, and breakup (Rainbird et al., 1992; Rainbird et al., 2010; Cawood et al., 2013; Pehrsson et al., 2013; Rainbird et al., 2017). Detrital geochronology contributes to the understanding of basin formation and evolution by linking sources of detritus to their sinks (Dickinson, 1988; Fedo et al. 2003; Surpless et al., 2018; Wang et al., 2019). The statistical

analysis of detrital-age spectra also provides insight into the geodynamic setting of continents and their basins (Cawood et al., 2012; Reimink et al., 2021). Sedimentary provenance is, therefore, a key component of basin analysis, and helps unravel the complex histories and paleogeographic context of supercontinents and the unroofing of Earth's largest orogens. The Precambrian geology of North America broadly records three cycles of supercontinent assembly and breakup related to: Mesoarchean to Neoarchean cratonization and rifting (Bleeker, 2003; Pehrsson et al., 2013); Paleoproterozoic to Mesoproterozoic orogenic events that led to the assembly, growth, and partial breakup of Nuna (Zhao et al., 2002; Evans and Mitchell, 2011); and the late Mesoproterozoic to early Neoproterozoic assembly and breakup of Rodinia (Li et al., 2008; Cawood and Pisarevsky, 2017). Proterozoic sedimentary basins of North America highlight a complex history of basin development in response to subsequent events of crustal flexure, thermal sag, and rift to drift (Rainbird and Young, 2009; Rainbird et al., 2010; Rainbird et al., 2012; Gumsley et al., 2017).

The Mesoproterozoic assembly of Rodinia and the associated Grenvillian Orogeny characterize one of the largest continental crust- and zircon forming events in Earth's history (Moecher and Samson, 2006), yet questions remain concerning its evolution (Li et al., 2008; Evans et al., 2009; Hynes and Rivers, 2010; Bradley, 2011; Cawood et al., 2016). The supercontinent Rodinia assembled from 1300−900 Ma (Li et al., 2008). Certain craton-scale tectonic events are important to intracratonic basin development, such as the Bylot basins. The Bylot basins consist of the Thule, Aston-Hunting, Borden and Fury and Hecla basins (Olson,1977; Jackson and Iannelli, 1981; Long and Turner, 2012; Fig. 4-1A−B). The Mackenzie Large Igneous Province (LIP; LeCheminant and Heaman, 1989), centered on Victoria Island, was emplaced in northern Laurentia at ca.1270 Ma, at the onset of the Rodinia assembly. The emplacement of the Mackenzie

LIP is inferred to be contemporaneous to the opening of the Bylot basins in northern Laurentia (Fahrig et al., 1981). The lowest formations (e.g., Nyeboe Formation in the Fury and Hecla Group, and the Nauyat Formation in the Borden Basin) contains basalt units attributed to the Mackenzie LIP based on paleomagnetic data (Fahrig et al., 1981). Later, the eastern flank of Laurentia was affected by the multi-phase Grenville Orogeny. The Shawinigan phase of the Grenvillian Orogeny occurred from 1220−1160 Ma (McLelland et al., 2013). Tectonic convergence dominated throughout the amalgamation of Rodinia but crustal weakening, thinning and extension of intracratonic basins at ca. 1090-1030 Ma took place at the Midcontinent Rift (Swanson-Hysell et al., 2019), Amundsen Basin (Rainbird et al., 2020) and Bylot basins (Greenman et al., 2021). This relaxation phase is notably concurrent with the 1090−980 Ma Ottawan phase of the Grenvillian Orogeny, which affected the eastern and southern flank of Laurentia (Hynes and Rivers, 2010). Simultaneous extension during contraction is possibly related to mantle upwelling centered at the Midcontinent Rift (Greenman et al., 2021). Combining the known depositional ages with detrital geochronology of penecontemporaneous basins can help constrain the unroofing and sediment pathways of the Grenvillian Orogen.

This study focuses on the Bylot basins of eastern arctic Canada and western Greenland. Prior to this study, detrital zircon data only existed from the Borden Basin (Turner et al., 2016), limiting the extent to which tectono-depositional models could be tested. We present the first complete detrital zircon U-Pb geochronology dataset for the Fury and Hecla Group, collected with a sensitive high-resolution ion microprobe (SHRIMP). We employ provenance analysis as a tool to reveal the depositional evolution of the Fury and Hecla Basin and the broader paleogeography of the Bylot basins.

4.2.1 Potential source regions

The Rae craton records a complex history of Archean crustal accretion, with several zircon-forming events spanning from 3.0 to 2.6 Ga (Pehrsson et al., 2013). Orogenic events that affected the interior or margins of the Rae craton include the ca. 2.5 Ga MacQuoid, ca. 2.3 Ga Arrowsmith, ca. 2.0 Ga Thelon, ca. 1.9 Ga Taltson and Snowbird, and ca. 1.85 Ga Trans-Hudson events (St. Onge et al., 2006; Berman et al., 2007; Berman, 2010; Berman et al., 2013; Pehrsson et al., 2013). All of these events are recorded in the detrital age spectra of supracrustal suites deposited atop the Rae Craton during the 2.3‒1.8 Ga interval, at which Laurentia assembled (Berman et al., 2010, Rainbird et al., 2010; Partin et al., 2014) and are recorded prominently in intracratonic basins post-dating the assembly of Laurentia in both the Slave (e.g., Elu and Kilohigok; Rainbird and Davis, 2022; McCormick, 1992) and Rae cratons (e.g., Athabasca, Thelon, Baker Lake; Rainbird et al., 2006; Rainbird and Davis, 2007; Rainbird et al., 2007).

4.3   Geological Setting

Stratigraphic correlations have been postulated among the Bylot basins since early studies (Jackson and Iannelli, 1981; Chandler, 1988; Long and Turner, 2012). However, until recently, correlations between the Fury and Hecla Basin and other basins have mostly been at the basin scale rather than formation-scale due to mismatching lithologies and limited age controls. The Nyeboe Formation of the Fury and Hecla Group and the Nauyat and Adams Sound formations of the Bylot Supergroup of the Borden Basin can be linked based on similarities in sedimentary facies (Patzke et al., 2021). An initial U-Pb-Th whole rock black shale age on the Arctic Bay Formation 1092 ± 59 Ma first indicated that the basin had a history that significantly post-dated the Mackenzie event

(Turner and Kamber, 2012).Higher resolution Re-Os black shale ages of 1048 ± 12 Ma on the Arctic Bay Formation and 1046 ± 16 Ma on the Victor Bay Formation confirmed that the majority of the Bylot Supergroup was deposited at least 200 Myr after the Mackenzie emplacement (Fig. 4-2; Gibson et al., 2018). Similarly, a new Re-Os age of 1087 ± 6 on black shale of the Agu Bay Formation of the Fury and Hecla Group implies post-Mackenzie basin reactivation in the Fury and Hecla Basin (Fig. 4-2; Greenman et al., 2021).

Turner et al. (2016) showed a small contribution of Grenvillian detrital zircons (ca.1100 Ma) (n=5) in the upper Bylot Supergroup, and spectra displayed prominent detrital-age peaks of ages overlapping with the ca. 2900−2500 Ma assemblage of the Superior, Rae and Hearne cratons) and ca. 1900−1700 Ma crustal thickening that accompanied the Trans-Hudson orogeny. Combined with previous studies (Knight and Jackson, 1994; Sherman et al., 2001; Sherman et al., 2002; Turner 2009; Turner 2011; Turner and Kamber, 2012), these detrital zircon data corroborated that the Borden Basin experienced a complex history of compression and extension. Turner et al. (2016) reconciled the formation of the Bylot basins during a time of convergence related to the assembly of Rodinia and the Grenvillian orogeny by postulating an impactogen model where basins formed due to the propagation of far-field stresses related, in this case, to the collision of Amazonia and Laurentia (Sengor, 1995; Turner et al., 2016). More recently, Greenman et al. (2021) proposed a 1090−1050 Ma crustal thinning event, related to the Midcontinent rift, that resulted in basin rejuvenation, transgression, and penecontemporaneous shale deposition in the Bylot basins and Amundsen Basin.

The Fury and Hecla Group represents the fill of the namesake basin and is divided into six formations (Fig. 4-1C−D). The lowermost, fluvial- to nearshore marine deposited, Nyeboe

Formation records basin opening in a half-graben setting, with a topographic high horst to the

bounding the basin to the north, and paleocurrent indicators suggesting an overall southwest-ward

sediment dispersal (Fig. 4-3A; Patzke et al., 2021). The orientation of the basin is parallel to deep-

seated faults on the Melville Peninsula (Spratt et al., 2013). The 70−400 m thick Nyeboe

Formation contains subaqueous emplaced mafic flows attributed to the ca. 1270 Ma Mackenzie

LIP (Fahrig et al., 1981; Chandler, 1988; LeCheminant and Heaman, 1989). The conformable

transition into the overlying ca. 300 m thick Sikosak Bay Formation records nearshore-marine

deposition (Fig. 4-3B; Chandler, 1988; Long and Turner, 2012; Patzke et al., 2018). The Hansen

Formation is a mafic sill that crosscuts the Nyeboe and Sikosak Bay formations (Chandler, 1988;

Steenkamp et al., 2018; Dufour et al., 2020). Then there is a disconformable contact to the <500 m

thick Agu Bay Formation which contains minor dolostone, black shale, and red siltstone with

interbedded sandstone (Greenman et al., 2018). The overlying Whyte Inlet Formation comprises

some 3 km of monotonous shallow-marine sandstone (Fig. 4-3C; Patzke et al., 2018). Due to the

conformable contact, facies, and limited exposure in the western part of the basin, the 2 km thick

Autridge Formation is interpreted as the finer-grained, deeper water equivalent of the Whyte Inlet

Formation, (Fig. 4-3D; Chandler, 1988). The 40−80 m thick Dybbol diabase sill caps the Autridge

Formation in the southwestern part of the basin. Both the sill and the mafic dykes that crosscut the

Fury and Hecla Group are attributed to the ca. 720 Ma Franklin igneous event, which provides an

upper age constraint on the deposition (Heaman et al., 1992; Steenkamp et al., 2018).

4.4   Methods

Seven sandstone samples, ~ 3.5 kg each, were collected for zircon U-Pb detrital

geochronology from the Fury and Hecla Group (Fig. 4-1C): two from the Nyeboe Formation

(M005 and W003; Fig. 4-3A), one from the Sikosak Bay Formation (W060; Fig. 4-3B), one from

the Agu Bay Formation (M043), two from the Whyte Inlet Formation (W012 and M026; Fig. 4-

3C), and one from the Autridge Formation (M095; Fig. 4-3D; Table 1). Thin section petrography

was conducted on each sample using a standard petrographic microscope (Table 4-1). Zircon U-Pb

geochronological analyses were conducted at the SHRIMP Geochronology Laboratory of the

Geological Survey of Canada (GSC; Ottawa, Ontario, Canada), following the methods and

calibrations described by Stern (1997) and Stern and Amelin (2003). The samples were prepared

using standard zircon separation procedures (e.g., Gehrels et al., 2006), including crushing,

milling, and mineral separation on a Wilfley table. Heavy minerals were further separated using

methylene iodine (MEI) and a Frantz isodynamic magnetic separator, set at 1.8 A and a 10º slope

to isolate the non-magnetic fraction. A random selection of ca. 100 zircons from each sample was

then mounted in epoxy on pucks and polished. The pucks were polished using 9, 6, and 1 µm

diamond compounds, and then evaporatively coated with 10 nm of high purity Au. Backscatter

electron (BSE) and cathodoluminescence (CL) imaging was conducted on the grains utilizing a

Zeiss Evo 50 scanning electron microscope, to identify internal textures and imperfections (e.g.,

cracks and inclusions).

Analyses were conducted on 58 to 65 grains for each sample following the statistical

methods described by Dodson et al. (1988) (Table 4-2). Laser analyses were conducted using an ^{16}

O- primary beam, projected onto the zircon at 10 kV. The sputtered area used for analysis was ca.

35 µm in diameter with a beam current of ca. 15 nA. The count rates at 11 masses including

background were sequentially measured over five scans with a single electron multiplier and a

pulse counting system with deadtime of 23 ns. Off-line data processing was accomplished using

customized in-house software. Reference zircon material included the GSC laboratory standard z1242 with an accepted age of 2675.4 ± 1.1 Ma (Davis et al., 2019). Z1242 yielded a ^{207}Pb/^{206}Pb age of 2678.4 ± 1.8 Ma for samples M005, W003, M043 and M095, and ^{207}Pb/^{206}Pb age of 2677.4 ± 1.7 Ma for samples W060, W012, and M026. The 1σ external errors of ^{206}Pb/^{238}U ratios reported herein incorporate a ±1.0% error for zircon standard calibration (see Stern and Amelin, 2003). No fractionation correction was applied to the Pb-isotope data; common Pb correction utilized the Pb composition of the surface blank (Stern, 1997). Isoplot v. 3.00 (Ludwig, 2003) was used to generate concordia plots and probability density diagrams. Error ellipses on the concordia diagrams, and the weighted mean errors are reported at 2σ. Probability density diagrams were used to display data. Duplicate analyses were omitted according to the measurement with the highest concordance.

4.5   Results

Paleocurrents used for this study are compiled from measurements taken on trough cross-beds, including data from previous publications (Chandler, 1988; Patzke et al., 2021) and data collected in this thesis from the Whyte Inlet Formation located on the northeast cape of Melville Peninsula (Ch. 2; Fig 4).

Lithologic descriptions and interpreted depositional environments for the seven samples, based on previous studies (Greenman et al., 2018, Patzke et al., 2018, and Patzke et al., 2021) are displayed in Table 1. Six samples are fine- to coarse-grained quartzarenite, whereas the Agu Bay sample (M043) is a subarkosic wacke. Most zircon grains are well-rounded with a small sub-angular population, range from non-spherical to spherical, and are pitted, with some even fragmented (Fig. 4-5A). These characteristics are consistent with prolonged reworking in coastal

to nearshore-marine settings (cf. Gärtner et al., 2013; Patzke et al., 2021). Grains range in size from 75−300 µm (measured along the longest axis). Inclusions are present within most of the zircons. Most zircons are clear, but some are tan, orange, pale yellow, light pink or purple (Fig. 4-5A).

Th/U ratios range from 0.04 to 3.30 and show no correlation with stratigraphic level or age (see supplementary data). Five grains fall below 0.1, which is used as a threshold for identifying metamorphic crystallization (Hoskin and Ireland, 2000). Based on internal textures, two of the five spots with Th/U <0.1 were analyzed on what were interpreted to be metamorphic rims; the rest were considered ambiguous. Internal textures of analyzed zircons range from oscillatory zoned to homogenous (Fig. 4-5B). Ninety-seven percent of grains plotted within 10% concordance, which was applied as a filter for the data (Fig. 4-5C). Individual samples display no temporal pattern in discordant ages.

4.5.1 Detrital geochronology

Age and concordance data for each sample are listed in Table 2 and summarized below. Sample M005 is from the lower Nyeboe Formation in an eastern outlier of the basin ca. 100 km from the main exposure (Fig. 4-1). 56 out of 61 grains are within 5% concordance (92% of all grains; Table 4-2) and no grains are outside the 10% concordance threshold. The probability density distribution (PDD) shows a dominant population from 2720 to 2680 Ma, with 26 grains falling concordantly in this age bracket, and a modal peak at ca. 2695 Ma (Fig. 4-6A). 13 concordant grains are >2720 Ma, with minor peaks at ca. 3192, 2905, 2855, and 2760 Ma. Sixteen zircon grains are <2680 Ma, displaying peaks at ca. 2620, 1882, and 1834 Ma.

Sample W003, from the upper Nyeboe Formation in the central part of the basin (Fig. 4-1), yielded 60 of 63 grains within 10% concordance, and 55 within 5% concordance (95% and 87% of all grains, respectively; Table 2). The PDD displays the most prominent population (28 grains) between 2730‒2650 Ma (Fig. 4-6B), with a mode at ca. 2700 Ma. Six grains are >2730 Ma, which are represented by small peaks between ca. 3243‒2810. There are 25 grains <2650 Ma, concentrated at peaks ca. 2188, 1924, and 1868 Ma.

Sample W060 is from the middle to upper Sikosak Bay Formation in the central part of the basin (Fig. 4-1). 63 out of 64 grains are within 10% concordance, and 58 are within 5% concordance (98% and 91% all of grains, respectively; Table 2). 14 grains are between 2750‒2650 Ma, with a mode at ca. 2700 (Fig. 4-6C). 12 grains are >2750 Ma and form peaks at ca. 2800 and ca. 3329 Ma. 36 grains are <2650 Ma and form minor peaks at ca. 2533, 1975, 1905, and 1695 Ma.

Sample M043 is from the upper Agu Bay Formation in the central part of the basin (Fig. 4-1). 66 out of 67 grains are within 10% concordance, and 58 within 5% concordance (99% and 87% of all grains, respectively; Table 2). The Agu Bay Formation age spectrum is more diffuse than older samples, with broader modes. 27 grains are between 2625‒2430 Ma, with a mode at ca. 2593 Ma (Fig. 4-6D). 11 grains are >2625 Ma, with minor peaks at ca. 2846 and 2739 Ma. 28 grains are <2430 Ma, with a broad peak centred at ca. 1900 Ma.

Sample W012 represents the lower Whyte Inlet Formation in the central area of the basin (Fig. 4-1). 62 out of 63 grains are within 10% concordance, and 56 are within 5% concordance (98% and 89% of all grains, respectively; Table 2). The PDD is broadly bimodal, with peaks at 2600‒2480 Ma and 1910‒1880 Ma represented by 21 and 8 grains, respectively (Fig. 4-6E). 5 grains are >2600 Ma, with minor peaks at ca. 2719 and 2670 Ma. 21 grains fall between 2480 and 1910 Ma, with minor peaks at ca. 2314 and 1988 Ma. 7 grains are <1880 Ma, with a minor peak at

ca. 828 Ma.

Sample M026 is from the upper Whyte Inlet Formation in the central part of the basin (Fig. 4-1). 62 out of 63 grains are within 10% concordance, and 59 are within 5% concordance (98% and 94% of all grains, respectively; Table 2). The PDD is broadly bimodal, with concentrations of ages at 2875‒2700 Ma, represented by 26 grains (Fig. 4-6F). Two peaks occur within this mode at ca. 2850 and 2720 Ma. The oldest population within this sample is represented as a small peak at ca. 3010 Ma. 14 concordant grains fall between 2700 and 1925 Ma (23%) and form a peak at ca.1990 Ma. The younger main mode occurs within 1925‒1840 Ma; 23 grains fall into this age bracket (37%). The apex of the younger main mode occurs at ca. 1892 Ma. The youngest population for the upper Whyte Inlet Formation is represented by 4 grains which form a small peak at ca. 1851 Ma.

Sample M095 is from the lower Autridge Formation in the western part of the basin (Fig. 4-1). 54 out of 58 grains are within 5% concordance (93% of all grains), and no grains are outside 10% concordance (Table 4-2). Ages are concentrated in the 1930‒1790 Ma window, with 42 grains (Fig. 4-6G), and a modal peak at ca. 1894 Ma. 13 grains are >1930 Ma, with a minor peak at ca. 2711 Ma. 3 grains are <1790 Ma, with a subpopulation centered at ca. 1730 Ma.

4.6   Discussion

4.6.1   Provenance and the importance of recycling

In the Fury and Hecla Group, Archean zircon grains have a relatively higher proportion in the lower strata and Paleoproterozoic zircon grains more prominent in the upper strata. At first glance, the Fury and Hecla Group detrital zircon ages are representative of derivation from source

terranes generated during the craton-scale tectonic events that affected Laurentia from the late Archean to the early Paleoproterozoic (Fig. 4-7). Fury and Hecla Group zircon ages could represent erosion and transport of detritus directly from source to sink, with unroofing of Paleoproterozoic crust becoming progressively more important up-section. However, considering the known depositional ages of the Bylot basins, and particularly the ca. 1087 Ma age of the middle Fury and Hecla Group (Greenman et al., 2021), the 500 Myr time gap between the youngest detrital population and the depositional age of the Fury and Hecla Group diminishes the likelihood of its sediment being directly transported from its original zircon-forming source (e.g., orogen; Fig. 4-7). For example, zircon grains formed during orogenic events, such as the Snowbird orogeny at ca. 1.9 Ga, might have resided in at least one other sedimentary basin before being transported to the Fury and Hecla Basin ca. 800 Myr later. This possibility is supported by the mature nature of the sedimentary rocks (i.e., quartzarenite; Table 1) and the record of Proterozoic orogenic unroofing elsewhere in the Laurentia (e.g., Rainbird et al., 2017). Provenance studies suggest that orogenic topography was largely eroded by the Neoproterozoic, owing to the occurrence of Grenvillian-aged zircons in northwestern Canada, meaning that if they were sourced from the Grenville Orogen, they must have bypassed the Trans-Hudson, Snowbird, and Thelon-Taltson zones (Rainbird et al., 2017; Ielpi et al., 2017; Rainbird and Davis, 2022).

We propose that the Fury and Hecla Group clastic sediments contain both products of more proximal, first-cycle erosion and far-travelled, multi-cycle fractions. More specifically, detritus eroded from Archean sources was derived from both first-cycle erosion of bedrock surrounding the Fury and Hecla Basin and from recycling of older sedimentary successions containing zircon grains of this age. Local detritus could have been derived from 2.6 to 3.0 Ga granitoid rocks of the

northern Rae craton that presently underlie the Fury and Hecla basin (Hoffman, 1988; Jackson and Berman, 2000; Pehrsson et al., 2013; Corrigan et al., 2013; Fig. 4-7). Local provenance for some sediments in the lower Fury and Hecla Group is corroborated by the record of basin initiation in a half-graben setting (Patzke et al., 2021). Initial subsidence would likely have been accompanied by sediment input from the rift shoulder, providing a relatively high proportion of local zircon grains with 3.0−2.6 Ga ages (Fig. 4-7). The Nyeboe Formation contains volcanic mafic units that are linked to the Mackenzie igneous event at 1.27 Ga, therefore they are likely ca. 200 Myr older than the Agu Bay Formation dated at 1.09 Ga (Greenman et al., 2021). We speculate that the shift in provenance to a relatively higher proportion of post-cratonization ages between the Sikosak Bay Formation and the Agu Bay Formation may record a change in mechanisms of basin subsidence (Fig. 4-6; Greenman et al., 2022). Paleoproterozoic detritus was most plausibly derived mainly via recycling of Paleoproterozoic supracrustal rocks, which host zircon grains derived from unroofing of earlier orogens, and whose relative contributions increased up-section as the catchment area broadened. The area likely broadened with basin expansion as topographic relief decreased at the basin margins. We postulate that the catchment area of the Fury and Hecla Group broadened up-section based on facies mapping and an overall fining-upward trend, especially in the Whyte Inlet and Autridge formations (Chandler, 1988; Patzke et al., 2018; Greenman et al., 2018). To resolve the source regions that most likely contributed to the recycling of Paleoproterozoic detritus, we consider the possible sediment pathways based on both the structural setting of the Bylot basins, and statistical comparison of detrital-age spectra to propose two non-unique scenarios.

The orientation of the Fury and Hecla Basin matches the trend of deep-seated E-W faults in Melville Peninsula (Spratt et al., 2013; Fig. 4-10). In the Fury and Hecla Basin, drainage was

parallel to the basin axis and topographic-high horsts, as is typical in mature horst-graben basins (

Gawthorpe and Leeder, 2000). We posit that sedimentary recycling more likely occurred through

sourcing of older sedimentary basins broadly aligned with the Fury and Hecla Basin's main axis.

Comparing the Fury and Hecla Group detrital-age record to older basins sheds light on the role of

sedimentary recycling. Viable sources from the region distributed throughout the arctic are shown

on Figure 10 and include: the early Paleoproterozoic Piling Group (Partin et al., 2014; Wodicka et

al., 2014), Penrhyn Group (Partin et al., 2014), Amer Group (Rainbird et al., 2010), and Ketyet

River Group (Rainbird et al., 2010) and the late Paleoproterozoic to early Mesoproterozoic Elu

Basin (Ellice Formation; Rainbird and Davis, 2022). Figure 8A shows a comparison of the detrital

zircon signatures of these successions to the Fury and Hecla Group. The Ellice Formation of the

Elu Basin is correlated with the late Paleozoic to early Mesoproterozoic strata of the Thelon,

Athabasca, and Hornby Bay basins, which may have been part of the same system that drained the

Trans-Hudson Orogen mainly to the WNW (Rainbird and Young, 2009; Rainbird and Davis,

2022). The Paleoproterozoic Kilohigok basin located in western Nunavut is too poorly

characterized to test its potential role as a source of sediments to the Fury and Hecla basins (Michel

et al., 2018; Berman et al., 2016; McCormick et al., 2016).

The Amer Group, located 600 km to the southwest of the Fury and Hecla Group, displays a

cumulative distribution of detrital ages that overlaps the Fury and Hecla Group (Fig. 4-8). The

Fury and Hecla Group detrital zircon age spectra are therefore best explained in terms of mixing of

both local, possibly first-cycle Archean sources from the surrounding basement rocks eroding

from the rift shoulder and recycled early Paleoproterozoic Amer Group or equivalent rocks. Here,

two alternative scenarios emerge. In the first scenario, sediment travelled directly from the Amer

Group eastward to the Fury and Hecla Basin (second-cycle sedimentation). Basin-axial paleoflows recorded broadly to the east in the Whyte Inlet Formation support this interpretation. However, no other large sediment delivery system is recorded to have flowed to the east at the time. Except for the Whyte Inlet Formation, most of the Fury and Hecla Group record paleoflow to the west (Fig. 4-4). The second scenario is that the depositional system that deposited the Amer Group could have had outcrops of sediment, or recycled versions of that sediment, further to the east that have not been geochronologically constrained or have since eroded away (n-cycle sedimentation). This scenario is supported by an outcrop of quartzite located in the northwest of the Fury and Hecla Group whose stratigraphic affinity is unknown (Steenkamp et al., 2018). Also, no geochronological information is known from this metamorphosed supracrustal package. At this stage, we cannot exclude that sediment recycling from other basins also took place, at least in part. Forthcoming geochronological work will help refine the hypothesis of recycling presented here.

4.6.2 Comparison with the Borden Basin

We compare our dataset to available detrital zircon data from the other Bylot basins. Thus far, a detrital zircon study has only been conducted on the Borden Basin (Turner, et al., 2016). The Fury and Hecla and Borden basins have been proposed to be correlative as part of the Bylot basin system since early studies (Blackadar and Fraser, 1960) and subsequently revised as new data from individual basins were obtained (Ch. 3; Borden: Jackson and Iannelli, 1981; Fury and Hecla Group: Chandler et al., 1988). Detrital zircon data from the Borden Basin are available from the Nauyat, Angmaat, Strathcona Sound, and Sinasiuvik formations (Fig. 4-2; Turner et al., 2016). We compare the two basins on a formation scale following the most recent correlation available (Greenman et al., 2021; Fig. 4-9). The lower Nyeboe Formation is compared to the basal Nauyat

Formation (Fig. 4-9A). They show peaks at the same time intervals but in different proportions: the Nauyat contains a higher peak centered at ca. 1.9 Ga, while the lower Nyeboe Formation has a higher peak centered at ca. 2.7 Ga. Detrital zircon from the Agu Bay Formation in the Fury and Hecla Group and the Angmaat Formation in the Borden Basin have the highest degree of similarity between the two basins (Fig. 4-9B), suggesting that they had connected sedimentary pathways or similar source regions. The lower Whyte Inlet Formation and basal Strathcona Sound Formation also appear similar as both their prominent age-peaks are similar in magnitude (Fig. 4-9C). However, the peaks in the Strathcona Sound Formation are centered at ages about ca. 100 Myr younger than the peaks in the Whyte Inlet Formation., the Strathcona Sound Formation also has a ca. 500 Myr younger signature that is absent in the Whyte Inlet Formation (Fig. 4-9C). The Autridge Formation and the Sinasiuvik Formation have peaks at similar age ranges. However, the Sinasiuvik Formation is more diffuse, having more peaks in the 2.0 to 2.4 Ga range and containing a younger signature with the youngest peak at ca. 1.1 Ga (Fig. 4-9D).

The lower and upper stratigraphy of the Fury and Hecla and Borden basins show overall mismatching detrital zircon spectra, suggesting different sediment-source pathways through time. A direct connection between the basins – or similar sediment-source pathways – is a likely scenario in the middle strata of the Fury and Hecla Group (Agu Bay Formation) and Borden Basin (Arctic Bay Formation), which both contain penecontemporaneous black shale (Gibson et al., 2018; Greenman et al., 2021). However, differences in provenance need to be explained in the lower and upper strata. First, the differences in the detrital-age records of the older strata can be related to different mechanisms of basin opening. These strata are thought to be deposited around 1.27 Ga and are represented by the Nyeboe and Sikosak Bay formations in the Fury and Hecla

Group and the Nauyat and Adams Sound formations in the Borden Basin. The Fury and Hecla and Borden basins are inferred to initially record, respectively, a graben (Patzke et al., 2021) and a distal sag basin (Long and Turner, 2012). Different provenance signatures are expected for these two basin types; the rift basin setting should record more proximal sources related to uplift and weathering along basin bounding faults, whereas a sag basin would have a broader catchment with better-mixed detrital populations (Andersen et al., 2011). An alternative explanation could be variations in the ages of underlying basement rocks on which the respective basins were deposited (Berman, 2010). We note, again, that this early stratigraphy in both basins record basin forming mechanisms disconnected from those of the ca. 200 Myr younger black shales of the Agu Bay and Arctic Bay formations.

A second approach to justify differences in the detrital-age spectra come from comparisons with cumulative age distributions from nearby basins – an approach that is useful to highlight differences in patterns of sedimentary recycling (Thomas, 2011; Andersen et al., 2019; Fig. 4-8). Specifically, cumulative age distributions from the Bylot Supergroup overlap with those from the Piling Group and the Elu Basin (which are currently located, respectively, ca. 500 km to southeast and ca. 900 km to the southwest: Figs. 4-8 and 4-10). Therefore, we posit that substantial sedimentary recycling from Piling and Elu supracrustal rocks may have contributed to the detrital age spectrum of the Borden Basin (Fig. 4-8). Again, we note the caveat that the Piling and Elu groups may have directly recycled into the Borden Basin (second-cycle sedimentation), or that correlative strata from these sources could have been exposed further to the east but since eroded (n-cycle sedimentation). The caveat especially applies to the Elu Basin given its location 900 km to the west. The proposed recycling sources for the Borden Basin contrasts with the more likely

Amer Group source for the Fury and Hecla Group (Fig. 4-7). This difference could be explained by the east-west axis for the Fury and Hecla and Borden basins, which likely controlled sediment pathways and would have prevented sediment exchange between the basins in the north-south direction. Paleotopographic highs such as the Boothia Arch and Steensby High could also have acted as barricades for detrital input into these basins (Fig. 4-10; Jackson and Iannelli, 1981). In any case, it seems sediment pathways and recycling of previous sedimentary successions are important factors that controlled detrital signatures in the Bylot basins.

The most striking difference between the detrital age spectra of the Borden and Fury and Hecla basins is the lack of the younger Grenvillian signature in the latter. Two viable explanations for this discrepancy are explored. First, topography could have blocked Grenvillian-aged (hereafter used to refer to zircons aged ca. 1.1 Ga) sediment input into the Fury and Hecla Group. In that case, the sinks for the Grenvillian detritus were not a function of distance but of different sediment pathways. An alternative explanation is that the absence of Grenvillian detritus is due to the lack of a stratigraphic record in the Fury and Hecla basin coeval with the Grenvillian unroofing episode. That is, Grenvillian-sourced sediment would have either bypassed the Fury and Hecla Basin due to lack of accommodation space, topographic barriers, or been subsequently eroded. The best time constraint for Grenvillian unroofing is the max depositional age of 1.01 Ga from the Nelson Head Formation (Rainbird et al., 2017). The Nelson Head Formation records abundant Grenvillian orogen-attributed grains deposited in a fluvial setting in the Amundsen Basin west of the Fury and Hecla Group (Rainbird et al., 2017; Fig. 4-10). There are several key differences from the Nelson Head Formation and the Fury and Hecla Group. First, the Nelson Head Formation is a primarily fluvial unit, whereas the Fury and Hecla Group primarily records marine deposition.

Second, the ages of deposition have at least a 100 Myr gap between them. The Borden Basin contains a few probable Grenvillian-aged zircon, but overall, the signature is muted. Further age constraints and basin analysis of the upper strata of both the Fury and Hecla Group and Borden Basin will be required to further test these alternate hypotheses.

4.7   Conclusions

This study presents the first detrital geochronology and provenance study of the Fury and Hecla Basin. Seven representative samples from the Fury and Hecla Basin were collected to conduct a detrital zircon provenance study. Overall, the samples record large Archean to Paleoproterozoic tectonic events that affected the Rae Craton. Archean aged grains centered at ca. 2.7 Ga are more prominent in the lower strata while Paleoproterozoic grains centered at ca. 1.9 Ga are more prominent in the upper strata. The large gap between the depositional age of ca. 1.09 Ga for the basin and the detrital ages point to sourcing from older supracrustal successions. While the lower strata likely record local input from the surrounding Rae Craton basement rocks, the upper strata show the increasing importance of recycling. The Fury and Hecla Group shows overlap to the Amer Group or equivalent strata. Sourcing from the Amer Group correlative strata further east is corroborated by lack of eastward paleocurrents. Compiled paleocurrent data show a dominant westward paleoflow; only the Whyte Inlet Formation shows paleocurrents to the east. When comparing the Fury and Hecla Group to the correlative Borden Basin, the middle strata show similar age spectra, while the upper and lower strata are notably distinct. These differences in the lower and upper strata may be due to variable mechanisms of basin opening and/or recycling of different supracrustal rocks. The Borden Basin also contains scarce amounts of ca. 1.1 Ga zircons that are absent in the Fury and Hecla Group. This distinction could be due to differences in

sediment pathways or a lack of accommodation space in the Fury and Hecla Basin.
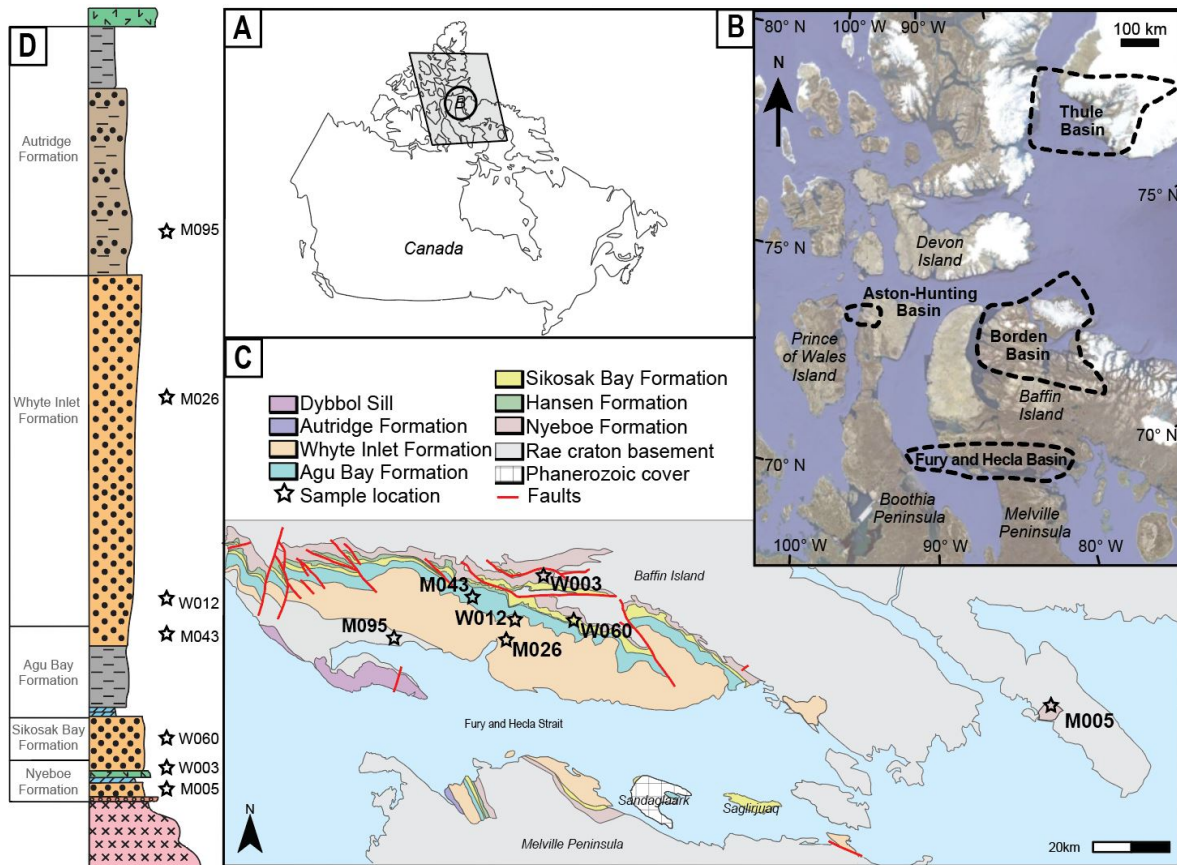
Future work analyzing the ages of supracrustal exposures atop the Rae and neighboring cratons could help constrain potential recycling sources for the Bylot basins. Further geochronological constraints and detrital zircon provenance studies from the other Bylot basins, especially the Thule and Aston-Hunting basins, which lack detrital age data, could further test the proposed interpretations. Forthcoming data with a particular emphasis on sedimentary recycling could refine sediment pathways and the overall understanding of the evolution of these basins and the paleogeographic context at the time of deposition. Together the data would help unravel the evolution of the Bylot basins and potentially highlight the significance of sedimentary recycling in intracratonic basins developed during the amalgamation of the Rodinia supercontinent.

4.8   Acknowledgements

4.9   Figures

Figure 4-1: Regional setting

The Fury and Hecla Group, Nunavut, Canada. (B) Distribution of the Thule, Aston-Hunting, Borden and Fury and Hecla basins in northeastern Canada and Northwestern Greenland. (C) Geology of the Fury and Hecla Group highlighting sample locations (after Chandler 1988). (D) Generalized stratigraphic section of the Fury and Hecla Group (after Chandler, 1988).
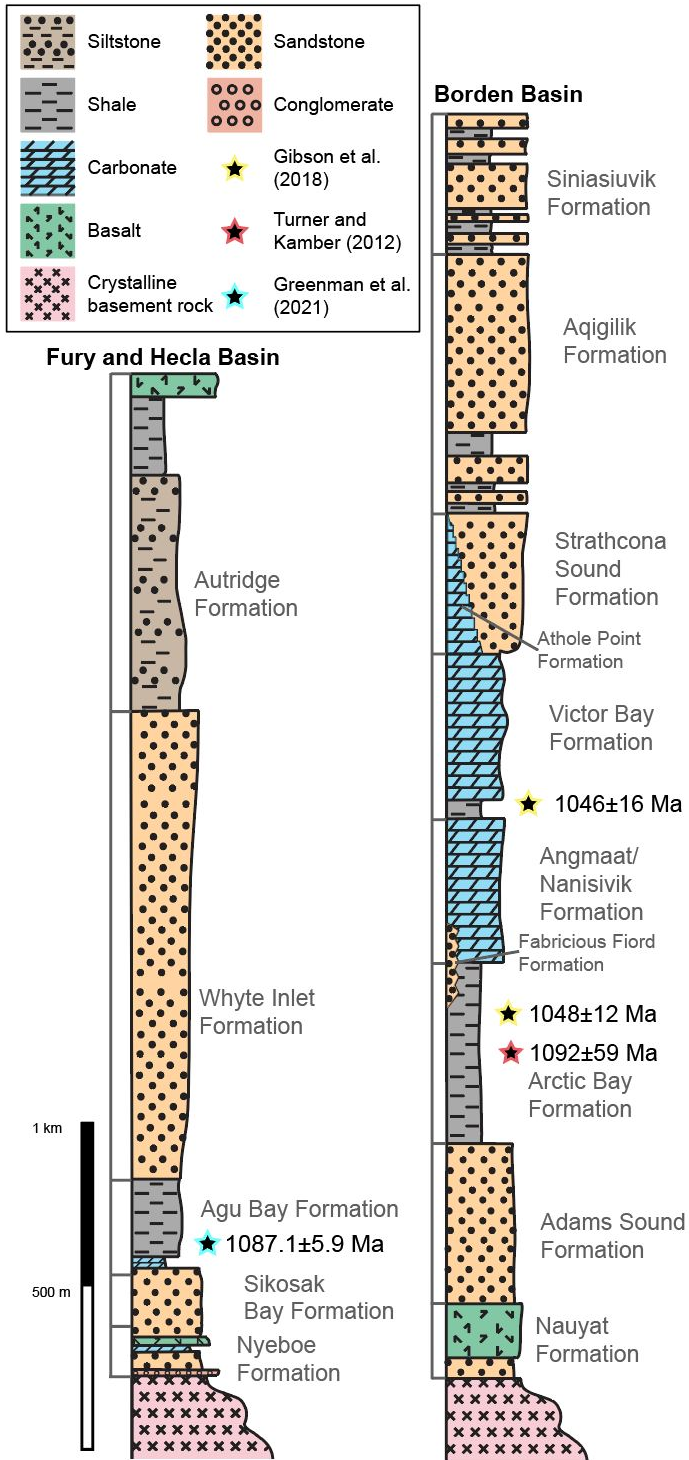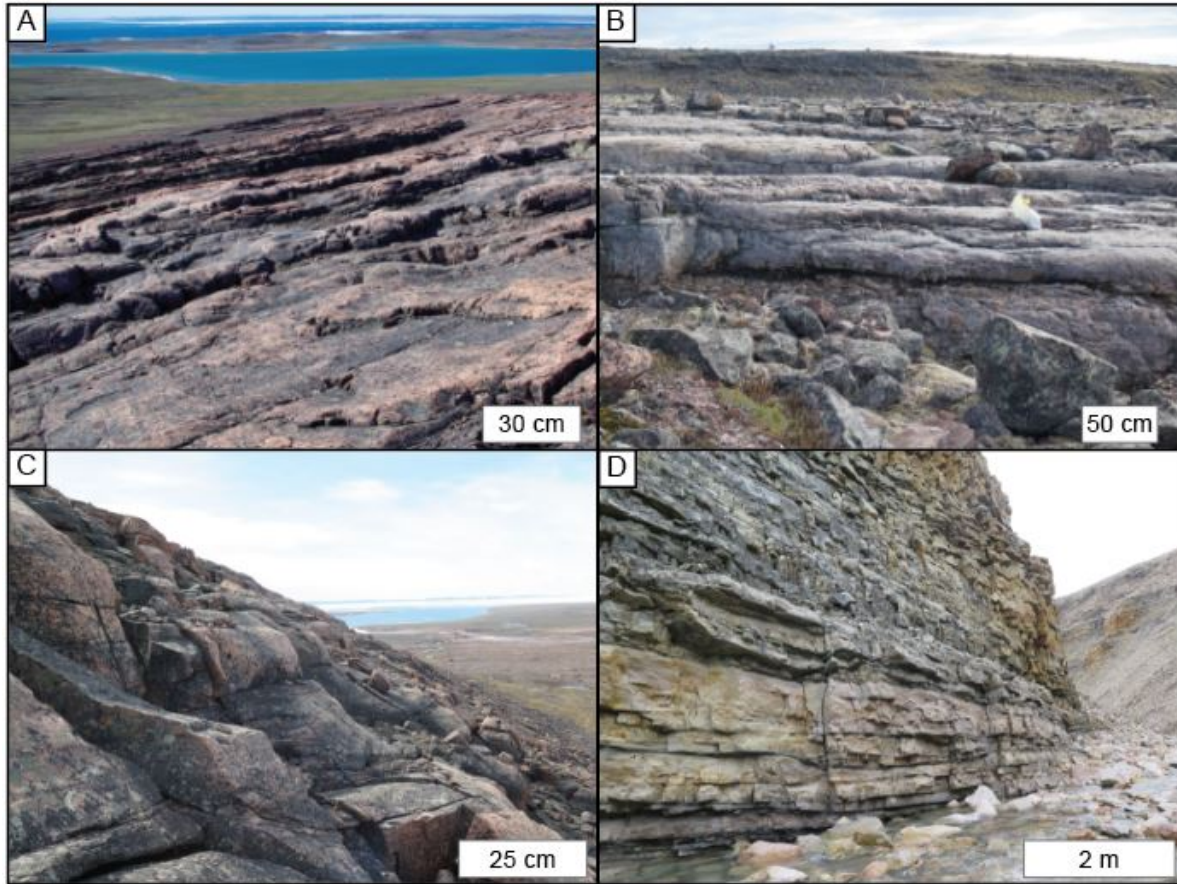
Figure 4-2: Stratigraphic sections of the Fury and Hecla and Borden basins

Stratigraphy of the Fury and Hecla and Borden basins. Depositional ages obtained from black

shale from both basins are indicated with stars.

Figure 4-3: Outcrop photo table

Photo table showing some of the Fury and Hecla Group formations from which samples were taken.

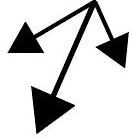| Formation	Paleocurrent vector Trough cross-beds
Autridge	n= 6 (Chandler, 1988)
Whyte Inlet	n= 223 (this publication) n= 13 (Chandler, 1988)
Agu Bay	n= 16 (Chandler, 1988)
Sikosak Bay	n= 13 (Chandler, 1988)
Nyeboe	n= 81 (Patzke et al., 2021) n= 4 (Chandler, 1988)

Figure 4-4: Compilation of Fury and Hecla Group paleocurrents

Compilation of paleocurrent indicators from trough cross-beds recorded in previous literature

(Chandler, 1988; Patzke et al., 2021; Ch. 2).
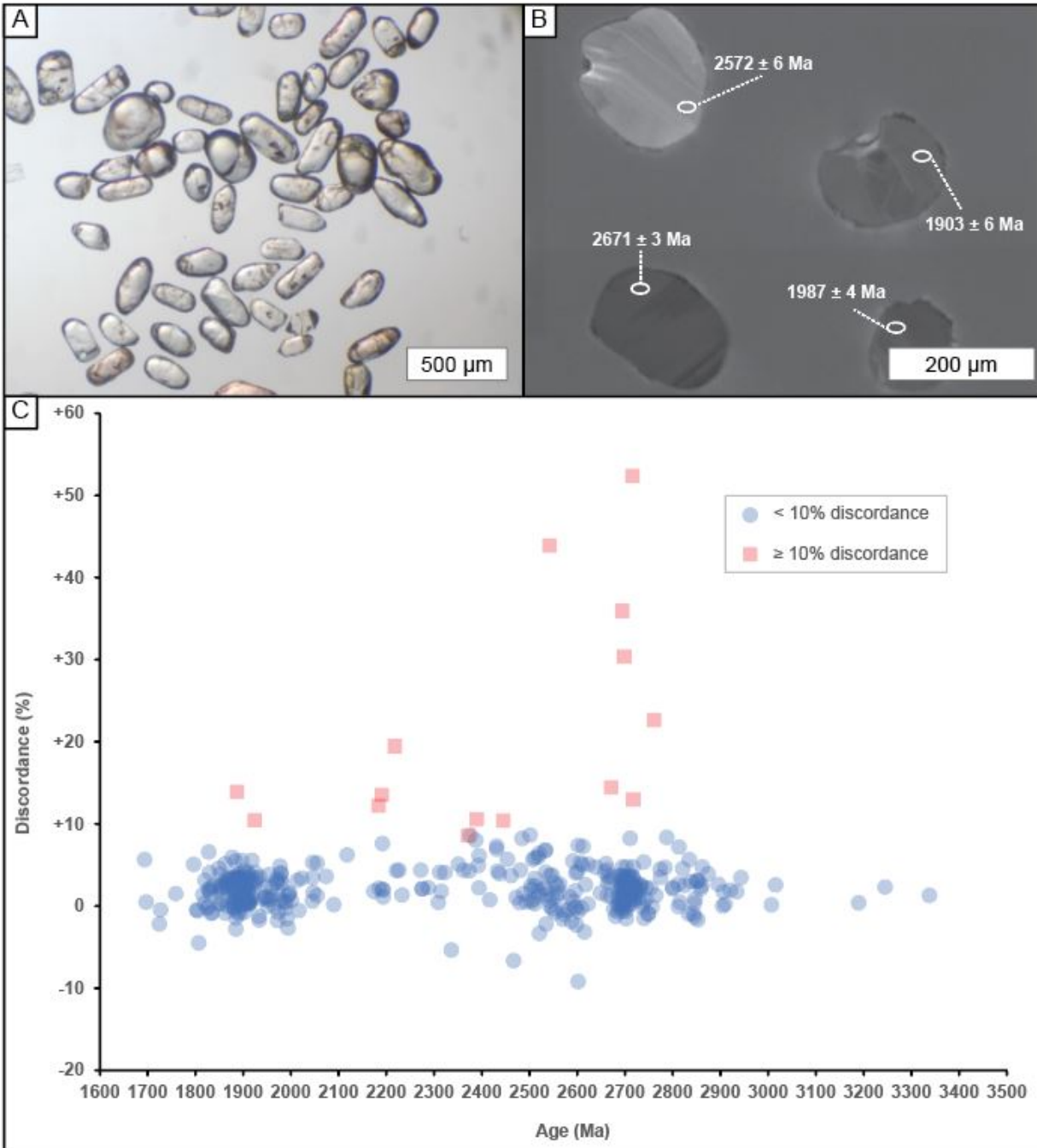
Figure 4-5: Zircon textures and concordance

Photos of grains showing external textures with transmitted light imaging (A), and internal textures with cathodoluminescence imaging (B). Plot of percent discordance vs. age (C). Red squares show analyses not included in the dataset due to 10% discordance filter.
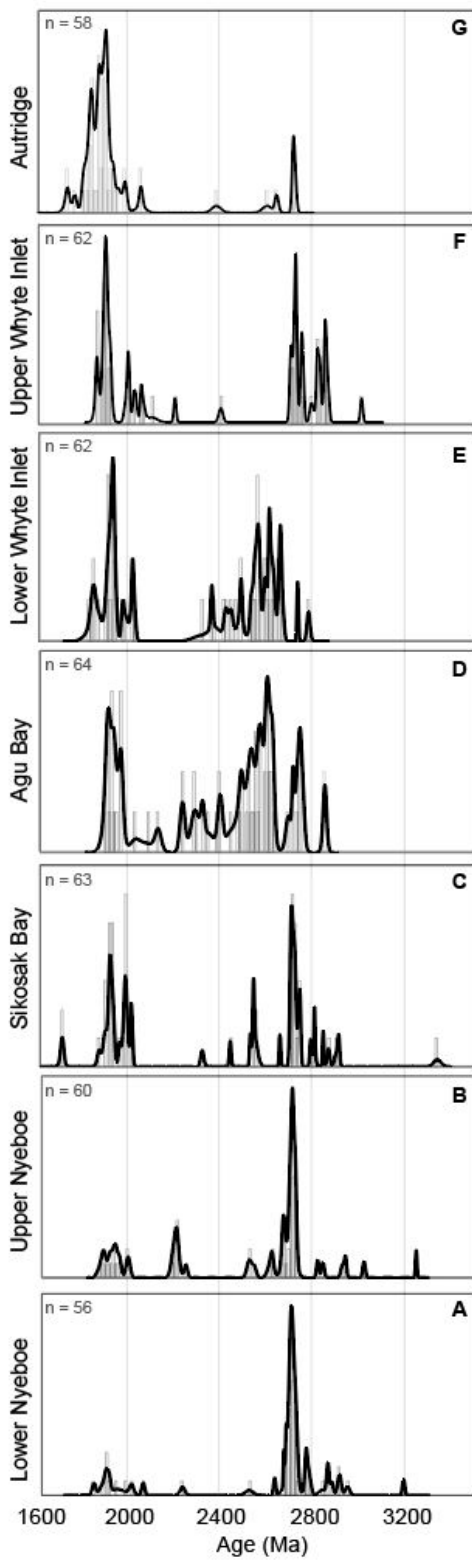
Figure 4-6: Probability density diagrams for the Fury and Hecla Group

Zircon U-Pb geochronology probability density diagrams including histograms and curves for the

Fury and Hecla Basin dataset in stratigraphic order (A-G).
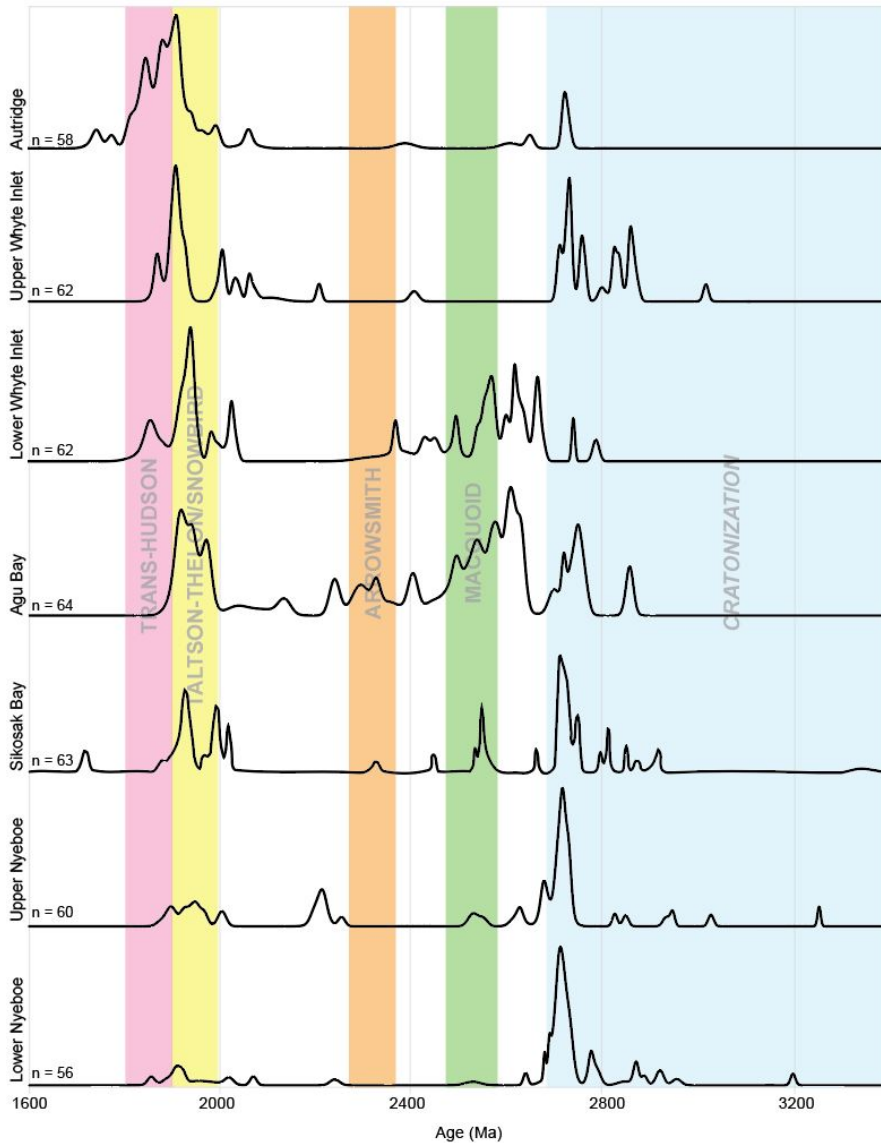
Figure 4-7: Fury and Hecla Group and Rae Craton ages

Probability density curves of the zircon U-Pb data from the seven samples of the Fury and Hecla

Group shaded to show temporal overlap with large zircon-forming events that affected the Rae

craton
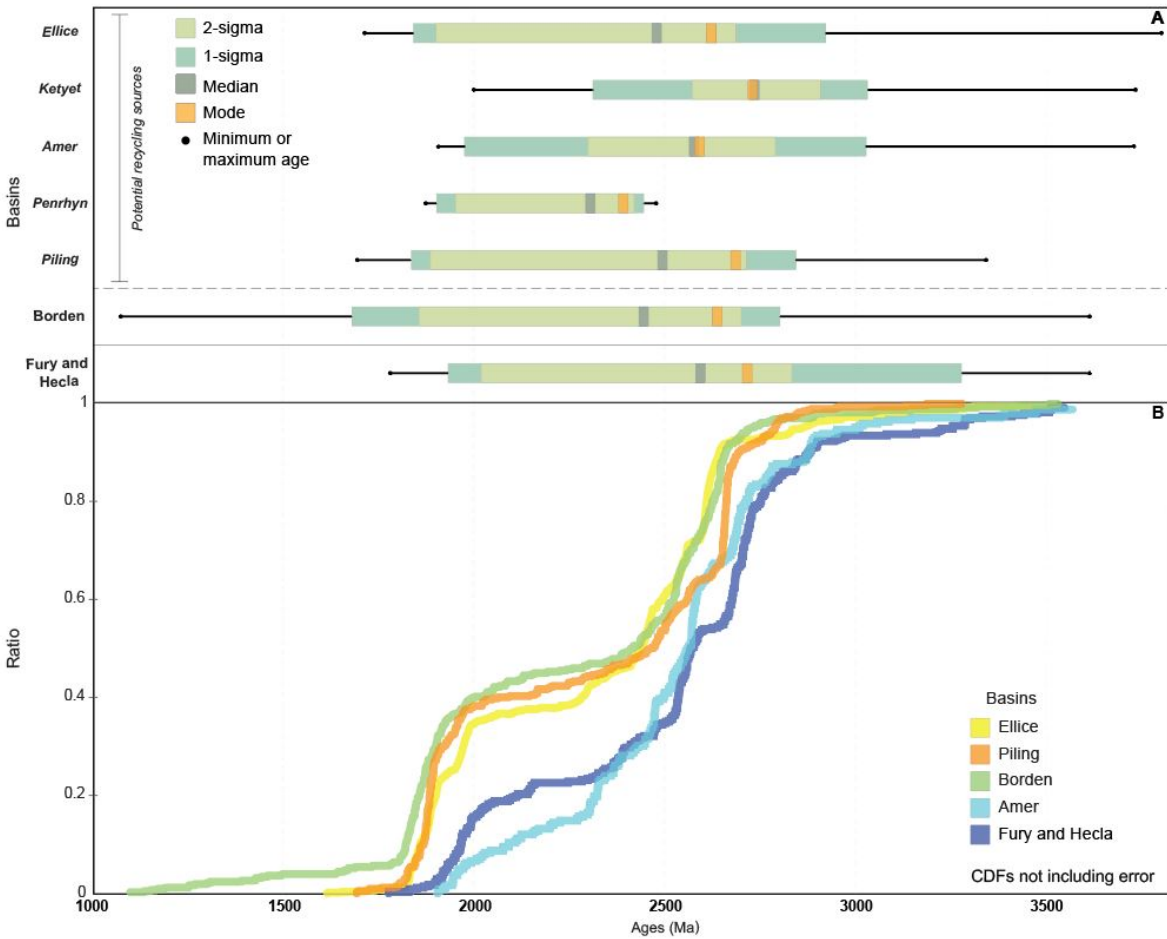
Figure 4-8: Cumulative distribution function of potential recycling sources

Comparison of statistical distributions (A), and cumulative distribution functions (B) of the Fury

and Hecla Group to the Borden basin and other Paleoproterozoic Rae craton supracrustal

assemblages which may have contributed as recycling sources for the Bylot basins.
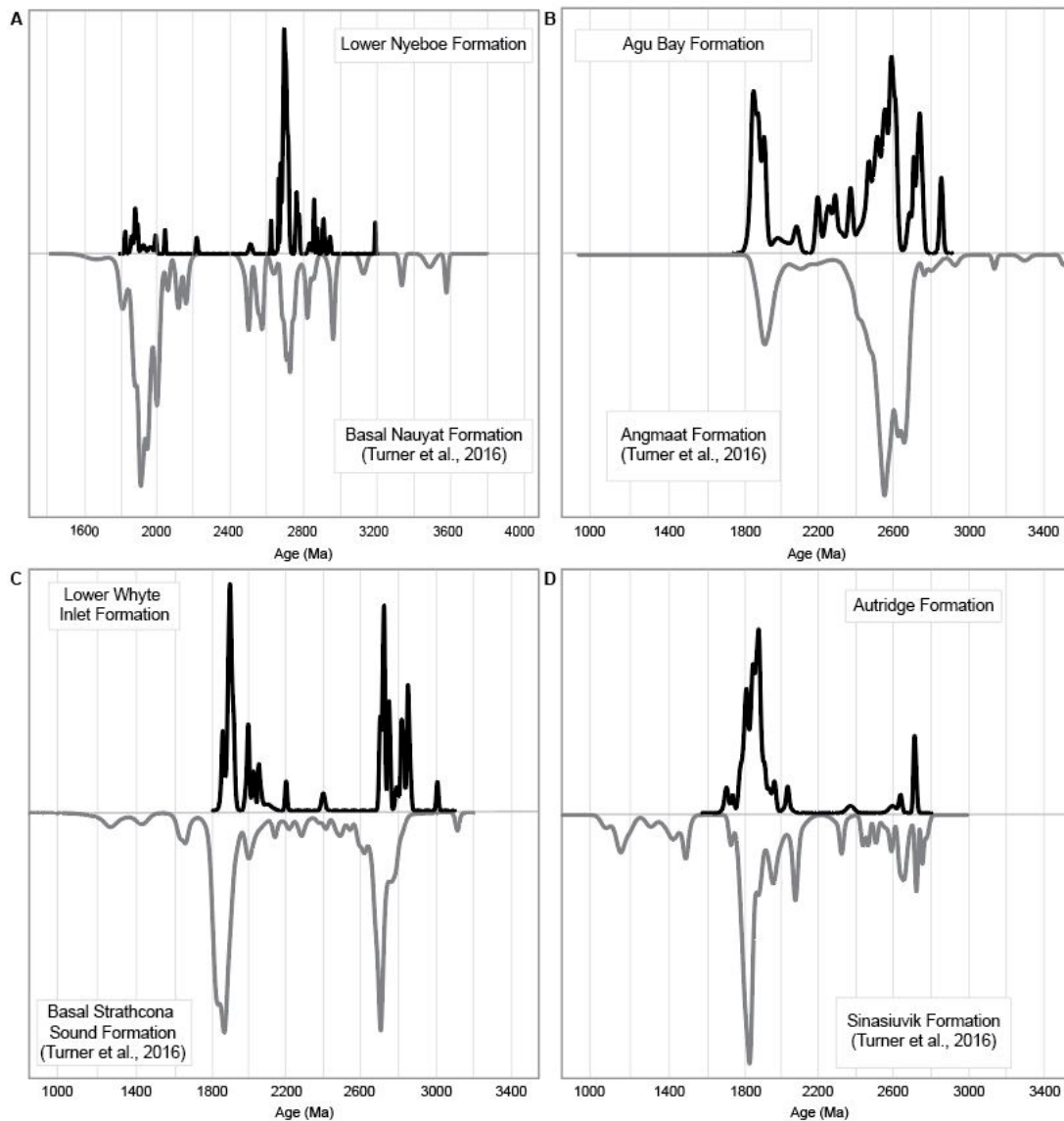
Figure 4-9: Drip plot comparisons of Fury and Hecla and Borden basins' detrital ages

Comparison of the Fury and Hecla Group and Bylot Supergroup discriminating by formation.

Correlative pairings follow Greenman et al. (2021): A) lower Nyeboe Formation to basal Nauyat

Formation; B) Agu Bay Formation to Angmaat Formation; C) Upper Whyte Inlet Formation to

basal Strathcona Sound Formation; D) Autridge Formation to Sinasiuvik Formation. Borden basin

detrital zircon geochronological data from Turner et al. (2016). Note that the scale of U-Pb ages of

grains varies for panel A.
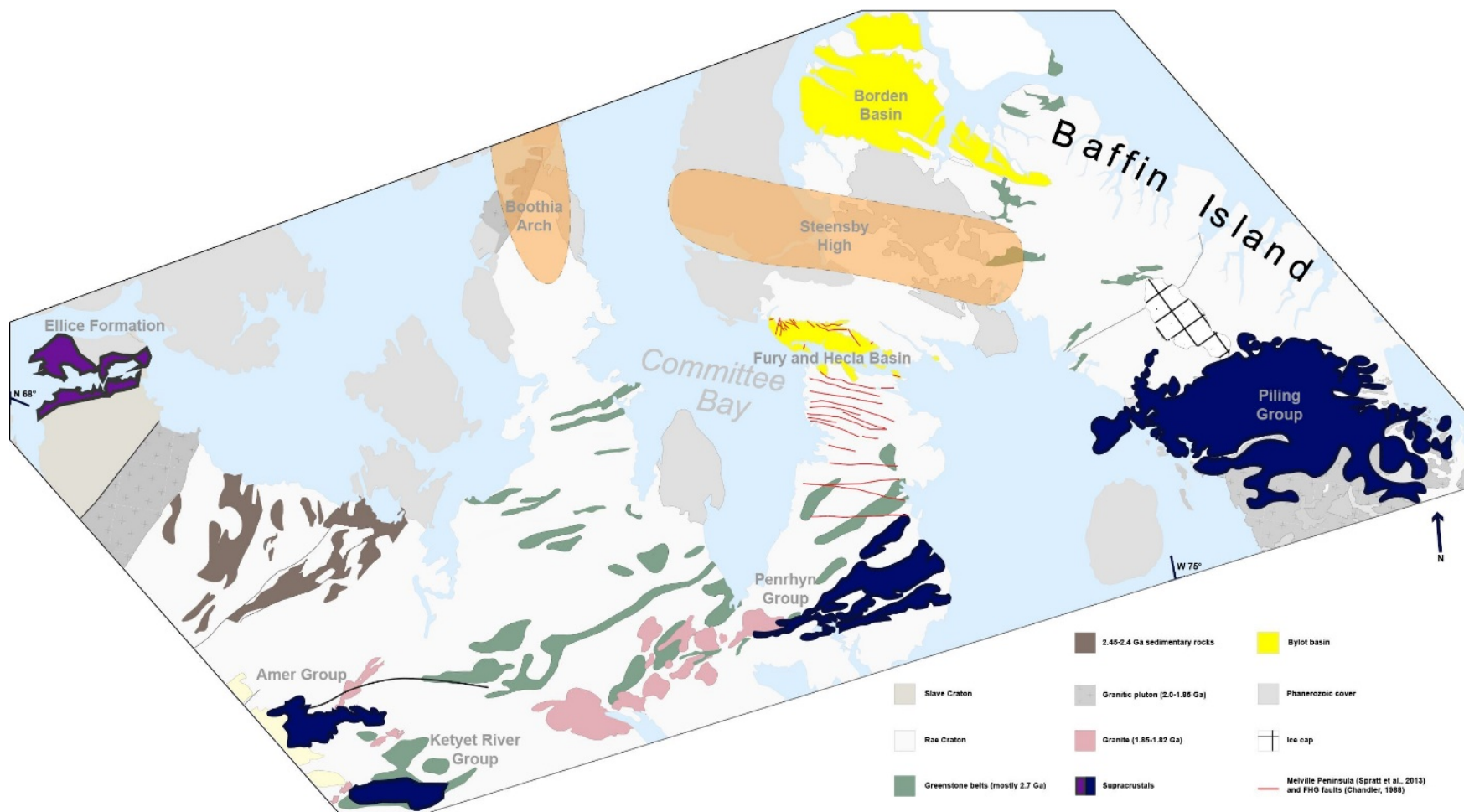
Figure 4-10: Paleogeographic setting

Map of the Rae craton modified from Berman (2010) to highlight suggested paleogeographic topography and input of recycling sources

into the Fury and Hecla Group and Borden basins.

4.10 Tables

Sample name	Location	Formation	Lithology/ texture	Interpreted depositional environment
M095	69°54'22.76"N, 81°22'9.94"W	Autridge	Quartzarenite	Wave-dominated, nearshore marine shelf
M026	70°13'58.73"N, 84°36'5.88"W	Upper Whyte Inlet	Quartzarenite	Wave-dominated, nearshore marine shelf
W012	70° 8'13.59"N, 84° 8'53.46"W	Lower Whyte Inlet	Quartzarenite	Wave-dominated, nearshore marine shelf
M043	70°14'27.67"N, 85°10'4.77"W	Agu Bay	Subarkosic graywacke	Shallow marine
W060	70° 9'49.40"N, 84°36'5.28"W	Sikosak Bay	Quartzarenite	Wave-dominated, nearshore marine shelf
W003	70° 8'40.56"N, 84°43'39.25"W	Upper Nyeboe	Quartzarenite	Wave-dominated, nearshore marine shelf
M005	70° 9'11.23"N, 85°27'20.74"W	Lower Nyeboe	Quart arenite	Terrestrial fluvial

Table 4-1: Sample descriptions

Location, petrography, and sedimentary facies of the Fury and Hecla Group detrital zircon geochronology samples. Depositional

environments from Greenman et al. (2018), Patzke et al. (2018), and Patzke et al. (2021).

Sample; *Formation*	Total grains analyzed	Grains within 5% concordance	Grains within 10% concordance	Youngest population (Ma)	Dominant population(s) (Ma)	Oldest population (Ma)
M095; *Autridge*	58	54	58	ca. 1730	1900−1865	ca. 2710
M026; *upperWhyte Inlet*	63	59	62	ca. 1850	2745−2700; 1915−1855	ca. 3010
W012; *lowerWhyte Inlet*	63	56	62	ca. 1830	2565−2550; 1920−1875	ca. 2720
M043; *Agu Bay*	65	57	64	ca. 1890	2615−2585; 1960−1890	ca. 2845
W060; *Sikosak Bay*	64	58	63	ca. 1695	2735−2695; 1925−1885	ca. 3350
W003; *upper Nyeboe*	63	55	60	ca. 1875	2725−2650	ca. 3245
M005; *lower Nyeboe*	61	56	56	ca. 1835	2735−2650	ca. 3190

Table 4-2: SHRIMP results

Summary of SHRIMP analyzed U-Pb detrital zircon data from the seven samples of the Fury and Hecla Group.

4.11 References

Andersen, T., 2011. Tracing crustal evolution in Fennoscandia using hafnium isotopes(abstract). NGF Abstracts and Proceedings of the Geological Society of Norway1, 2‒3.

Andersen, T., Elburg, M.A. and Van Niekerk, H.S., 2019. Detrital zircon in sandstones from the Palaeoproterozoic Waterberg and Nylstroom basins, South Africa: Provenance and recycling. South African Journal of Geology 2019, 122(1), pp.79-96.

Berman, R.G., Davis, W.J., Pehrsson, S.; 2007, Collisional Snowbird tectonic zone resurrected: Growth of Laurentia during the 1.9 Ga accretionary phase of the Hudsonian orogeny. Geology; 35 (10): 911‒914.

Berman, R.G., 2010. Metamorphic map of the western Churchill Province. Geological Survey of Canada Open File 5279 (3 sheets, 49 pp. report)

Berman, R.G., Pehrsson, S. Davis, W.J., Ryan, J.J., Qui, H., Ashton, K.E., 2013, The Arrowsmith orogeny: Geochronological and thermobarometric constraints on its extent and tectonic setting in the Rae craton, with implications for pre-Nuna supercontinent reconstruction, Precambrian Research, Volume 232, Pages 44-69,

Berman, R.G., Sanborn-Barrie, M., Nadeau, L., Brouillette, P., Camacho, A., Davis, W.J., McCurdy, M.W., McMartin, I., Weller, O.M., Chadwick, T. and Liikane, D.A., 2016. Report of activities for the geology and mineral potential of the Chantrey-Thelon area: GEM-2 Rae project. Geological Survey of Canada.

Blackadar, R.G. and Fraser, J.A., 1960. Precambrian geology of Arctic Canada: a summary account (No. 60). Department of Mines and Technical Surveys.

Bleeker, W., 2003. The late Archean record: a puzzle in ca. 35 pieces. Lithos, 71(2-4), pp.99-134.

Bradley D.C., 2011, Secular trends in the geologic record and the supercontinent cycle: Earth-Science Reviews , v. 108, p. 16−33,

Cawood, P.A., Hawkesworth, C.J., Dhuime, B., 2012. Detrital zircon record and tec-tonic setting. Geology40, 875−878.

Cawood, P.A., Hawkesworth, C.J., Dhuime, B., 2013. The continental record and the generation of continental crust. GSA Bull.125, 14−32.

Cawood, P.A., Strachan, R.A., Pisarevsky, S.A., Gladkochub, D.P. and Murphy, J.B., 2016. Linking collisional and accretionary orogens during Rodinia assembly and breakup: Implications for models of supercontinent cycles. Earth and Planetary Science Letters, 449, pp.118-126.

Cawood, P.A. and Pisarevsky, S.A., 2017. Laurentia-Baltica-Amazonia relations during Rodinia assembly. Precambrian Research, 292, pp.386-397.

Chandler, F.W., 1988, Geology of the Late Precambrian Fury and Hecla Group, Northwest Baffin Island, District of Franklin: Geological Survey of Canada, Bulletin 370, p. 26−32.

Corrigan, D., Nadeau, L., Brouillette, P., Wodicka, N., Houlé, M G., Tremblay, T., Machado, G., Keating, P., 2013. Geological Survey of Canada, Current Research (Online) no. 2013-19, 21 p.

Davis, W.J., Pestaj, T., Rayner, N., McNicoll, V.M., 2019. Long-term reproducibility of 207Pb/206Pb age at the GSC SHRIMP lab based on the GSC Archean reference zircon z1242. Geol. Surv. Canada Sci. Present. 111.

Dickinson, W.R., Klute, M.A., Hayes, M.J., Janecke, S.U., Lundin, E.R., McKittrick, M.A. and Olivares, M.D., 1988. Paleogeographic and paleotectonic setting of Laramide sedimentary basins in the central Rocky Mountain region. Geological Society of America Bulletin, 100(7), pp.1023-1039.

Dodson, M.H., Compston, W., Williams, I.S., Wilson, J.F., 1988. A search for ancient detrital zircons in Zimbabwean sediments. J. Geol. Soc. London 145, 977‒983.

Dufour, F., Stevenson, R. and Skulski, T., 2020. Geochemical comparison of Mackenzie and Franklin igneous mafic rocks in Nunavut, Northwest Territories and northwestern Greenland. Summary of Activities, pp. 33-46.

Evans, D.A., 2009. The palaeomagnetically viable, long-lived and all-inclusive Rodinia supercontinent reconstruction. Geological Society, London, Special Publications, 327(1), pp.371-404.

Evans, D.A. and Mitchell, R.N., 2011. Assembly and breakup of the core of Paleoproterozoic‒Mesoproterozoic supercontinent Nuna. Geology, 39(5), pp.443-446.

Fahrig, W.F., Christie, K.W., and Jones, D.L., 1981, Paleomagnetism of the Bylot basins: evidence for Mackenzie continental tensional tectonics; Proterozoic Basins of Canada:Geological Survey of Canada, Paper, v. 81, p. 303‒312.

Fedo, C.M., Sircombe, K.N. and Rainbird, R.H., 2003. Detrital zircon analysis of the sedimentary record. Reviews in Mineralogy and Geochemistry, 53(1), pp.277-303.

Gärtner, A., Linnemann, U., Sagawe, A., Hoffman, M., Ullrich, B., Kleber, A., 2013. Morphology of zircon crystal grains in sediments ‒ Characteristics, classifications, definitions. Geol.

Saxonica 59, 65‒73.

Gawthorpe, R.L., And Leeder, M.R., 2000, Tectono-sedimentary evolution of active extensional basins: Basin Research, v. 12, p. 195‒218.

Gehrels, G., Valencia, V. and Pullen, A., 2006. Detrital zircon geochronology by laser-ablation multicollector ICPMS at the Arizona LaserChron Center. The Paleontological Society Papers, 12, pp.67-76.

Gibson, T.M., Shih, P.M., Cumming, V.M., Fischer, W.W., Crockford, P.W., Hodgskiss, M.S.W., Wörndle, S., Creaser, R.A., Rainbird, R.H., Skulski, T.M., and Halverson, G.P., 2018, Precise age of Bangiomorpha pubescens dates the origin of eukaryotic photosynthesis: Geology, v. 46, p. 135‒138.

Greenman, J.W., Patzke, M., Halverson, G.P., and Ielpi, A., 2018, Refinement of the stratigraphy of the late Mesoproterozoic Fury and Hecla Basin, Baffin Island, Nunavut, with a specific focus on the Agu Bay and Autridge formations: Canada‒Nunavut Geoscience Office, Summary of Activities 2018, p. 85‒96.

Greenman, J.W., Rooney, A.D., Patzke, M., Ielpi, A., And Halverson, G.P., 2021, Re-Os geochronology highlights widespread latest Mesoproterozoic (ca. 1090‒1050) cratonic basin development on northern Laurentia: Geology, v. 49, p. 779‒783.

Greenman, J.W., dos Santos, A., Patzke, M., Gibson, T.M., Ielpi, A., Halverson, G.P., 2022, A tectonostratigraphic framework for the late Mesoproterozoic Bylot basins of Laurentia. Journal of the Geological Society. *In review.*

Gumsley, A.P., Chamberlain, K.R., Bleeker, W., Söderlund, U., de Kock, M.O., Larsson, E.R. and Bekker, A., 2017. Timing and tempo of the Great Oxidation Event. Proceedings of the National Academy of Sciences, 114(8), pp.1811-1816.

Heaman, L.M., Lecheminant, A.N., And Rainbird, R.H., 1992, Nature and timing of Franklin igneous events, Canada: implications for a Late Proterozoic mantle plume and the breakup of Laurentia: Earth and Planetary Science Letters, v. 109, p. 117‑131.

Hoffman, P.F., 1988. United Plates of America, the birth of a craton-Early Proterozoic assembly and growth of Laurentia. Annual Review of Earth and Planetary Sciences, 16, pp.543-603.

Hoskin, P.W. and Ireland, T.R., 2000. Rare earth element chemistry of zircon and its use as a provenance indicator. Geology, 28(7), pp.627-630.

Hynes, A. and Rivers, T., 2010. Protracted continental collision‑ Evidence from the Grenville orogen. Canadian Journal of Earth Sciences, 47(5), pp.591-620.

Ielpi, A., Rainbird, R.H., Ventra, D., Ghinassi, M., 2017. Morphometric convergence between Proterozoic and post-vegetation rivers. Nat. Commun. 8, 15250. https://doi.org/10.1038/ncomms15250.

Jackson, G.D., and Iannelli, T.R., 1981, Rift-related cyclic sedimentation in the Neohelikian Borden Basin, northern Baffin Island in Campbell, F.H.A., ed., Proterozoic Basins of Canada: Geological Survey of Canada, Paper 81-10, p. 269‑302.

Jackson, G.D. and Berman, R.G., 2000. Precambrian metamorphic and tectonic evolution of northern Baffin Island, Nunavut, Canada. The Canadian Mineralogist, 38(2), pp.399-421.

Knight, R D; Jackson, G D., 1994, Sedimentology and stratigraphy of the Mesoproterozoic Elwin Subgroup (Aqigilik and Sinasiuvik formations), uppermost Bylot Supergroup, Borden Rift Basin, northern Baffin Island; Geological Survey of Canada, Bulletin 455, 48 p.

Lecheminant, A.N., And Heaman, L.M., 1989, Mackenzie igneous events, Canada: Middle Proterozoic hotspot magmatism associated with ocean opening: Earth and Planetary Science Letters, v. 96, p. 38−48.

Li, Z.X., Bogdanova, S., Collins, A.S., Davidson, A., De Waele, B., Ernst, R.E., Fitzsimons, I.C.W., Fuck, R.A., Gladkochub, D.P., Jacobs, J. and Karlstrom, K.E., 2008. Assembly, configuration, and break-up history of Rodinia: a synthesis. Precambrian research, 160(1-2), pp.179-210.

Long, D.G.F., And Turner, E.C., 2012, Tectonic, sedimentary and metallogenic reevaluation of basal strata in the Mesoproterozoic Bylot basins, Nunavut, Canada: Are unconformity-type uranium concentrations a realistic expectation?: Precambrian Research. v. 214−215, p. 192−209.

Ludwig, K.R., 2003. User's manual for Isoplot/Ex rev. 3.00: a Geochronological Toolkit for Microsoft Excel. Special Publication, 4, Berkeley Geochronology Center, Berkeley, 70 p.

McCormick, D.S. 1992. Evolution of an early proterozoic alluvially-dominated foreland basis, Burnside Formation, Kilohigok Basin, N.W.T., Canada. Thesis (Ph. D.)--Massachusetts Institute of Technology, Dept. of Earth, Atmospheric, and Planetary Science

McLelland, J., Selleck, B. and Bickford, M., 2013. Tectonic evolution of the Adirondack Mountains and Grenville orogen inliers within the USA. Geoscience Canada: Journal of

the Geological Association of Canada/Geoscience Canada: journal de l'Association Géologique du Canada, 40(4), pp.318-352.

Michel, S. and Ielpi, A. 2018: Sedimentology and stratigraphy of the Paleoproterozoic Kimerot Group in Bear Creek Hills, Kilohigok Basin, western Nunavut; in Summary of Activities 2018, Canada-Nunavut Geoscience Office, p. 15‑28.

Moecher, D. P., and Samson, S. D., 2006, Differential zircon fertility of source terranes and natural bias in the detrital zircon record: Implications for sedimentary provenance analysis: Earth and Planetary Science Letters, v. 247, no. 3-4, p. 252-266.

Olson, R.A., 1977, Geology and genesis of zinc-lead deposits within a late Proterozoic dolomite, Northern Baffin Island, N.W.T. [Ph.D. Thesis]: University of British Colombia, 387 p.

Partin, C.A., Bekker, A., Corrigan, D., Modeland, S., Francis, D. and Davis, D.W., 2014. Sedimentological and geochemical basin analysis of the Paleoproterozoic Penrhyn and Piling groups of Arctic Canada. Precambrian Research, 251, pp.80-101.

Patzke, M., Greenman, J.W., Ielpi, A., And Halverson, G.P., 2018, Sedimentology of the sandstone-dominated units in the Fury and Hecla Basin, Northern Baffin Island, Nunavut: Canada‑Nunavut Geoscience Office, Summary of Activities 2018, p. 75‑84.

Patzke, M., Greenman, J.W., Halverson, G.P. and Ielpi, A., 2021. The initiation of the Mesoproterozoic Bylot basins (Nunavut, Arctic Canada) as recorded in the Nyeboe Formation, Fury and Hecla Group. Journal of Sedimentary Research, 91(11), pp.1166-1187.

Pehrsson, S.J., Berman, R.G., And Davis, W.J., 2013, Paleoproterozoic orogenesis during Nuna aggregation: a case study of reworking of the Rae craton, Woodburn Lake,Nunavut: Precambrian Research, v. 232, p. 167−188.

Rainbird, R.H., Heaman, L.M. and Young, G., 1992. Sampling Laurentia: Detrital zircon geochronology offers evidence for an extensive Neoproterozoic river system originating from the Grenville orogen. Geology, 20(4), pp.351-354.

Rainbird, R.H., Davis, W.J., Stern, R.A., Peterson, T.D., Smith, S.R., Parrish, R.R. and Hadlari, T., 2006. Ar-Ar and U-Pb geochronology of a late Paleoproterozoic Rift Basin: Support for a genetic link with Hudsonian orogenesis, western Churchill Province, Nunavut, Canada. The Journal of Geology, 114(1), pp.1-17.

Rainbird, R.H. and Davis, W.J., 2007. U-Pb detrital zircon geochronology and provenance of the late Paleoproterozoic Dubawnt Supergroup: Linking sedimentation with tectonic reworking of the western Churchill Province, Canada. Geological Society of America Bulletin, 119(3-4), pp.314-328.

Rainbird, R. H., Stern, R. A., Rayner, N. M., and Jefferson, C. W., 2007, Age, provenance, and regional correlation of the Athabasca Group, Alberta and Saskatchewan, constrained by igneous and detrital zircon geochronology, in Jefferson, C. W., and Delaney, G. D., eds., EXTECH IV: Geology and Uranium EXploration TECHnology of the Proterozoic Athabasca Basin, Saskatchewan and Alberta,Geological Survey of Canada, Bulletin 588, p. (also Saskatchewan Geological Society, Special Publication 18; Geological Association of Canada, Mineral Deposits Division, Special Publication 4). p. 193-209

Rainbird, R.H., And Young, G., 2009, Colossal rivers, massive mountains and supercontinents: Earth Magazine, v. 54, p. 52‒61.

Rainbird, R.H., Davis, W.J., Pehrsson, S.J., Wodicka, N., Rayner, N. and Skulski, T., 2010. Early Paleoproterozoic supracrustal assemblages of the Rae domain, Nunavut, Canada: Intracratonic basin development during supercontinent break-up and assembly. Precambrian Research, 181(1-4), pp.167-186.

Rainbird, R., Cawood, P., Gehrels, G., Busby, C. and Azor, A., 2012. The great Grenvillian sedimentation episode: Record of supercontinent Rodinia's assembly. Tectonics of sedimentary basins: Recent advances, pp.583-601.

Rainbird, R.H., Rayner, N.M., Hadlari, T., Heaman, L.M., Ielpi, A., Turner, E.C. and MacNaughton, R.B., 2017. Zircon provenance data record the lateral extent of pancontinental, early Neoproterozoic rivers and erosional unroofing history of the Grenville orogen. GSA Bulletin, 129(11-12), pp.1408-1423.

Rainbird, R.H., Rooney, A.D., Creaser, R.A. and Skulski, T., 2020. Shale and pyrite Re-Os ages from the Hornby Bay and Amundsen basins provide new chronological markers for Mesoproterozoic stratigraphic successions of northern Canada. Earth and Planetary Science Letters, 548, p.116492.

Rainbird, R.H.; Davis, W.J. 2022. On the Statherian-Calymmian paleogeography of northwestern Laurentia. Journal of the Geological Society. jgs2022-062. 10.1144/jgs2022-062.

Reimink, J.R., Davies, J.H. and Ielpi, A., 2021. Global zircon analysis records a gradual rise of continental crust throughout the Neoarchean. Earth and Planetary Science Letters, 554,

p.116654.

Sengor, A.M.C., 1995. Sedimentation and tectonics of fossil rifts. In: Tectonics of sedimentary basins (C.J. Busby and R.V. Ingersoll, eds), pp. 53‑117. Blackwell, Blackwell Science, Cambridge Mass.

Sherman, A.G., Narbonne, G.M. and James, N.P., 2001. Anatomy of a cyclically packaged Mesoproterozoic carbonate ramp in northern Canada. Sedimentary Geology, 139(3-4), pp.171-203.

Sherman, A.G., James, N.P. and Narbonne, G.M., 2002. Evidence for reversal of basin polarity during carbonate ramp development in the Mesoproterozoic Borden Basin, Baffin Island. Canadian Journal of Earth Sciences, 39(4), pp.519-538.

Spratt, J., Jones, A.G., Corrigan, J.D., And Hogg, C., 2013, Lithospheric geometry revealed by deep-probing magnetotelluric surveying, Melville Peninsula, Nunavut: Geological Survey of Canada Current Research 2013-12, 14 p.

Steenkamp, H.M., Bovingdon, P.J., Dufour, F., Généreux, C., Greenman, J.W., Ielpi, A., Patzke, M., And Tinkham, D., 2018, New regional mapping of Precambrian rocks north of Fury and Hecla Strait, northwestern Baffin Island, Nunavut: Canada‑Nunavut Geoscience Office, Summary of Activities 2018, p. 47‑62.

Stern, R.A., 1997, The GSC Sensitive High Resolution Ion Microprobe (SHRIMP): analytical techniques of zircon U-Th-Pb age determinations and performance evaluation: in Radiogenic Age and Isotopic Studies, Report 10, Geological Survey of Canada, Current Research 1997-F, p. 1-31.

Stern, R.A., Amelin, Y., 2003. Assessment of errors in SIMS zircon U-Pb geochronology using a natural zircon standard and NIST SRM 610 glass. Chem. Geol. 197, 111‒146.

St. Onge, M.R., Searle, M.P. and Wodicka, N., 2006. Trans-Hudson Orogen of North America and Himalaya-Karakoram-Tibetan Orogen of Asia: Structural and thermal characteristics of the lower and upper plates. Tectonics, 25(4).

Surpless, K.D., Gulliver, K.D., Ingersoll, R.V., Graham, S.A. and Lawton, T.F., 2018. Provenance analysis of the Ochoco basin, central Oregon: A window into the Late Cretaceous paleogeography of the northern US Cordillera. In Tectonics, Sedimentary Basins, and Provenance: A Celebration of the Career of William R. Dickinson (pp. 235-266). Geological Society of America.

Swanson-Hysell, N.L., Ramezani, J., Fairchild, L.M. and Rose, I.R., 2019. Failed rifting and fast drifting: Midcontinent Rift development, Laurentia's rapid motion and the driver of Grenvillian orogenesis. GSA Bulletin, 131(5-6), pp.913-940.

Thomas, W.A., 2011. Detrital-zircon geochronology and sedimentary provenance. Lithosphere, 3(4), pp. 304-308.

Turner, E.C., 2009. Mesoproterozoic carbonate systems in the Borden Basin, Nunavut. Canadian Journal of Earth Sciences, 46(12), pp.915-938.

Turner, E.C., 2011. Structural and stratigraphic controls on carbonate-hosted base metal mineralization in the Mesoproterozoic Borden Basin (Nanisivik District), Nunavut. Economic Geology, 106(7), pp.1197-1223.

Turner, E.C. and Kamber, B.S., 2012. Arctic Bay Formation, Borden Basin, Nunavut (Canada): Basin evolution, black shale, and dissolved metal systematics in the Mesoproterozoic ocean. Precambrian Research, 208, pp.1-18.

Turner, E.C., Long, D.G.F., Rainbird, R.H., Petrus, J.A., And Rayner, N.M., 2016, Late Mesoproterozoic rifting in Arctic Canada during Rodinia assembly: impactogens, transcontinental far-field stress and zinc mineralisation: Terra Nova, v. 28, p. 188‒194.

Wang, C., Liang, X., Foster, D.A., Tong, C., Liu, P., Liang, X. and Zhang, L., 2019. Linking source and sink: Detrital zircon provenance record of drainage systems in Vietnam and the Yinggehai‒Song Hong Basin, South China Sea. Bulletin, 131(1-2), pp.191-204.

Wodicka, N., St-Onge, M.R., Corrigan, D., Scott, D.J. and Whalen, J.B., 2014. Did a proto-ocean basin form along the southeastern Rae cratonic margin? Evidence from U-Pb geochronology, geochemistry (Sm-Nd and whole-rock), and stratigraphy of the Paleoproterozoic Piling Group, northern Canada. Bulletin, 126(11-12), pp.1625-1653.

Zhao, G., Cawood, P.A., Wilde, S.A. and Sun, M., 2002. Review of global 2.1‒1.8 Ga orogens: implications for a pre-Rodinia supercontinent. Earth-Science Reviews, 59(1-4), pp.125-162.

Chapter 5

5 Concluding statements

5.1 Conclusions

This thesis entailed the analysis of the depositional settings, evolution, and provenance of the Fury and Hecla Basin (Nunavut, Canada). The integration of these approaches was aimed at providing a clearer picture on the geodynamic setting of the broader Bylot basins. Specifically, this thesis presented the first detailed and basin-wide facies-analysis for the sandstone-dominated units in the Fury and Hecla Basin and provided its first detrital zircon geochronological dataset. Results indicate that the Fury and Hecla Group records a range of depositional environments (from terrestrial to offshore marine), which owing to their spectacular exposure in tundra terrain, may serve as template for forthcoming studies on Precambrian-aged, clastic-depositional environments elsewhere. First, a multidisciplinary study that integrated techniques such as facies analysis and stratigraphic logging with photogrammetry revealed, for the first time in the Precambrian marine record, the architecture of shelf-scale sandwave depositional elements (e.g., stacked clinoforms). Then, a tectono-depositional model for basin initiation was presented based on detailed facies analysis of the lowermost unit, the Nyeboe Formation. Finally, a geochronological investigation of detrital zircon grains from seven samples collected throughout the Fury and Hecla Group formed the basis of a provenance study that illustrated the competing inputs of detritus from local sources and recycling of older Proterozoic sedimentary basins in northeastern Nunavut. The salient conclusions from the three core science chapters of the thesis are summarized as follows.

5.1.1 Sedimentology and architectural analyses

Facies analysis and mapping confirmed that three units of the Fury and Hecla Group are sandstone-dominated, from the stratigraphically lowest: the Nyeboe Formation, Sikosak Bay Formation and Whyte Inlet Formation. The Nyeboe Formation records three main depositional settings: terrestrial to coastal (including alluvial-fan, fluvial, and backshore eolian), carbonate-clastic nearshore marine, and marine shelf. The Nyeboe Formation also contains several thin subaqueous mafic flows. The Sikosak Bay formation record nearshore marine shelf deposition, and the Whyte Inlet mostly records marine shelf deposition with local fluvial deposition exposed in eastern part of the basin.

High-resolution architectural analysis of a prominent exposure in the northernmost part of Melville Peninsula informed aspects of the marine shelf deposition recorded in the Whyte Inlet Formation. Architectural line drawings and photogrammetric analyses on high-resolution satellite imagery was corroborated by ground-checking and accompanied by measurement of a stratigraphic section and paleoflow data. Results indicate the presence of large clinoforms created by shelf progradation and aggradation through successive migration and stacking of marine sandwave complexes. Individual clinoforms are largely composed of stacks of trough cross beds bounded by wave-rippled surface, and occasionally contain floating clasts. The direction of shelf progradation was likely sub-normal to the paleo-coastline and resulted from longshore drift combined with both fair- and storm-weather wave action. Modern-day examples akin to the one preserved in the Whyte Inlet Formation have been described offshore South Africa and Belgium (Flemming, 1980; Berne et al., 1994) but have to date not been recognized in this level of detail in the Precambrian record. The repeated buildup of sandwave complexes supports the

paleogeographic inference that deposition occurred in an open-ocean setting characterized by large fetch rather than in a restricted embayment. Driven by this observation, it can be speculated that sandwave complexes of this size may be indicative of hurricane- and typhoon type storms that are typical of low-latitude marine basins. This latter inference is in principle consistent with the proposed paleogeography of Laurentian at the time of Whyte Inlet deposition (ca. 1.1 Ga; Greenman et al., 2021; Li et al., 2008).

5.1.2   Basin initiation

The Nyeboe Formation represents the lowest stratigraphic unit of the Fury and Hecla Group, and as such constitutes an important target to understand the mechanisms of basin inception. Field observations led to the recognition of five facies associations, which are interpreted to record: alluvial-fan to fluvial, eolian-backshore marine, marine intertidal, wave-dominated marine shelf, and marine-offshore transition depositional environments. Structural observation driven by field relationships suggest that the basin accommodated brittle deformation through displacement along faults that can be separated into different groups based on their strike. Faults striking sub-parallel to the main axis of the basin are recognized on the Melville Peninsula and possibly associated with deep-seated, long-lived deformation (Spratt et al., 2013). Owing to location and geometry of these faults, and the distribution of facies associations, we propose that the Nyeboe Formation opened in a half-graben setting with the master fault striking ca.115° on the north side of the basin. Paleoflow indicators suggest that most of distribution of sediment followed a basin-axial pattern, with a prevalent westward component. Based on its stratigraphic position, occurrence of mafic flows within, and facies associations, the Nyeboe Formation is inferred to correlate with the Nauyat and Adams Sound formations of the Borden Basin (Jackson and Iannelli,

1981; Long and Turner, 2012).

5.1.3 Detrital geochronology

We present the first provenance study for the Fury and Hecla Basin through a geochronological study of detrital zircon from seven sandstone samples that span the basin geographically and stratigraphically. Detrital zircon ages from the Fury and Hecla Group span from ca. 3350 to ca. 1695 Ma and represent large zircon-forming events that affected the Rae Craton throughout the Archean and Paleoproterozoic. Detrital ages are mostly bimodal, with a peak at ca. 2.7 Ga prominent in the lower stratigraphy, and a peak at ca. 1.9 Ga that becomes more important up-section. If the basin initiation took place in a half-graben setting, the detrital zircon age signature of the lower stratigraphy reflects local basement rocks derivation. Considering the >600 Myr gap between the depositional age of the basin (ca. 1.1 Ga; Greenman et al., 2021) and the bulk of the detrital ages, we suggest that sedimentary recycling from nearby basins likely played a key role, and that it became progressively more important in the upper stratigraphy. This consideration is driven by the notion that detritus with broadly Trans-Hudsonian signatures (ca. 1.9 Ga) could not have been first cycle, since independent provenance studies suggest that the Trans-Hudson topography would have been largely peneplaned by the late Mesoproterozoic (Ielpi et al., 2017; Rainbird et al., 2017). Comparison of cumulative density distributions of detrital ages shows that the Fury and Hecla Group overlaps with the older (1.9 Ga) Amer Group located to the southwest (Rainbird et al., 2010). However, as most palaeoflows in the region (and the Proterozoic of Laurentian more broadly) record westward sediment transport (Rainbird et al., 1997; Rainbird et al., 2017; Rainbird and Davis, 2022), we speculate that since eroded or undiscovered Amer Group equivalent rocks might have contributed sediment to the Fury and Hecla Group.

The Borden Basin is the only other Bylot basin for which detrital geochronological data is available. Strata of the Eqalulik Group from the Borden Basin show overlap with middle strata of the Fury and Hecla Group, whereas lower and upper strata in the two basins show mismatching provenance (Turner et al., 2016). This observation can indicate different mechanisms of basin initiation and evolution, or different sources of sedimentary recycling.

5.2   Future work

Future directions of work in the region should be broadly aimed at refining the relationships between facies distribution and provenance in the Fury and Hecla and other Bylot basins, to arrive at more accurate tectono-stratigraphic models and supra-regional correlations for the Proterozoic of Laurentia. For example, Chapter 2 concluded that the Whyte Inlet Formation contains a relatively large exposure on monotonous quartzarenite. However, chapter 3 concluded that significant changes in provenance occur within this unit. A more detailed sedimentological and detrital zircon study of the Whyte Inlet Formation could possibly identify a cryptic surface of stratigraphic discontinuity within the quartzarenite of the Whyte Inlet Formation. Changes in provenance and stratigraphic analysis of discontinuities in Proterozoic sediments of Laurentia has proven in the past to be powerful tool to inform craton-scale basin analysis (Rainbird et al., 1996).

Chapter 3 concluded, using sedimentological evidence and observations of large-scale faults based on field relationships alone, that the basin opened as a half graben. An in-depth structural analysis could test this hypothesis by identifying faults north and south of basin to investigate establish patterns of accommodation production and uplift. Additional studies of this nature from the other Bylot and correlative basins could delineate if similar tectonic mechanisms

were responsible for basin opening during the amalgamation and tenure of the supercontinent Rodinia.

Finally, Chapter 4 concluded that sedimentary recycling played a significant role for the sediment input into the Fury and Hecla Group. This inference is perhaps not surprising considering the intracratonic setting for the Fury and Hecla Basin, but this possibility has not been explored for the coeval Borden basin or many other Precambrian intracratonic basins on Laurentia. The detrital record of penecontemporaneous basins of Laurentia could be reanalyzed in higher detail and integrated petrographic and paleocurrent analysis to test similar models of poly-cyclic sandstone sedimentation. Additional methods such as zircon hafnium isotopes could further resolve detritus to their sources. Furthermore, sedimentary recycling sources identified in chapter 4 remain somewhat speculative considering the paleoflow data at hand ‒ an aspect that requires further attention for the region and beyond. Our results may be used in forthcoming mapping efforts aimed at identifying hitherto unmapped or poorly constrained metasedimentary panels found nearby the present-day Fury and Hecla Basin. All in all, the comparison of cumulative density distributions of detrital ages proved a powerful tool to test hypothetical pathways of poly-cyclical sedimentation. If applied widely, this tool may soon disclose further complexities in the paleogeography of the sedimentary basins of Laurentia that witnessed supercontinent amalgamation and crustal unroofing of large orogens.

5.3 References

Berne, S., Trentesaux, A., Stolk, A., Missiaen, T., and De Batist, M., 1994, Architecture and long-term evolution of a tidal sand bank: The Middelkerke Bank (southern North Sea); Marine

Geology, v. 121, p. 57−72.

Flemming, B.W., 1980: Sand transport and bedform patterns on the continental shelf between Durban and Port Elizabeth (southeast African continental margin); Sedimentary Geology, v. 26, p. 170−205.

Greenman, J. W., Rooney, A. D., Patzke, M., Ielpi, A., & Halverson, G. P. 2021. Re-Os geochronology highlights widespread latest Mesoproterozoic (ca. 1090−1050 Ma) cratonic basin development on northern Laurentia. Geology, 49(7), 779-783.

Ielpi, A., Rainbird, R. H., Ventra, D., & Ghinassi, M. 2017. Morphometric convergence between Proterozoic and post-vegetation rivers. Nature Communications, 8(1), 1-8.

Jackson, G.D. and Iannelli, T.R. 1981: Rift-related cyclic sedimentation in the Neohelikian Borden Basin, Northern Baffin Island; in Proterozoic Basins of Canada, F.H.A. Campbell (ed.), Geological Survey of Canada, Paper 81-10, p. 269−302.

Li, Z. X., Bogdanova, S. V., Collins, A. S., Davidson, A., De Waele, B., Ernst, R. E., Fitzsimons, I.C.W., Fuck, R.A., Gladkochub, D.P., Jacobs, J. Karlstrom, K.E., Lu, S., Natapov, L.M., Pease, V., Pisarevsky, S.A., Thrane, K., Vernikovsky, V., 2008: Assembly, configuration, and break-up history of Rodinia: A synthesis; Precambrian Research, 160(1-2), 179−210.

Long, D. G., & Turner, E. C. 2012. Tectonic, sedimentary and metallogenic re-evaluation of basal strata in the Mesoproterozoic Bylot basins, Nunavut, Canada: Are unconformity-type uranium concentrations a realistic expectation?. Precambrian Research, 214, 192-209.

Rainbird, R. H., Jefferson, C. W., & Young, G. M. 1996. The early Neoproterozoic sedimentary Succession B of northwestern Laurentia: Correlations and paleogeographic significance.

Geological Society of America Bulletin, 108(4), 454-470.

Rainbird, R. H., McNicoll, V. J., Theriault, R. J., Heaman, L. M., Abbott, J. G., Long, D. G. F., & Thorkelson, D. J. 1997. Pan-continental river system draining Grenville Orogen recorded by U-Pb and Sm-Nd geochronology of Neoproterozoic quartzarenites and mudrocks, northwestern Canada. The Journal of Geology, 105(1), 1-17.

Rainbird, R. H., Davis, W. J., Pehrsson, S. J., Wodicka, N., Rayner, N., & Skulski, T. 2010. Early Paleoproterozoic supracrustal assemblages of the Rae domain, Nunavut, Canada: Intracratonic basin development during supercontinent break-up and assembly. Precambrian Research, 181(1-4), 167-186.

Rainbird, R. H., Rayner, N. M., Hadlari, T., Heaman, L. M., Ielpi, A., Turner, E. C., & MacNaughton, R. B. 2017. Zircon provenance data record the lateral extent of pancontinental, early Neoproterozoic rivers and erosional unroofing history of the Grenville orogen. GSA Bulletin, 129(11-12), 1408-1423.

Rainbird, R.H.; Davis, W.J. 2022. On the Statherian-Calymmian paleogeography of northwestern Laurentia. Journal of the Geological Society. jgs2022-062. 10.1144/jgs2022-062.

Spratt, J., Jones, A.G., Corrigan, J.D., And Hogg, C., 2013, Lithospheric geometry revealed by deep-probing magnetotelluric surveying, Melville Peninsula, Nunavut: Geological Survey of Canada Current Research 2013-12, 14 p.

Turner, E. C., Long, D. G., Rainbird, R. H., Petrus, J. A., & Rayner, N. M. 2016. Late Mesoproterozoic rifting in Arctic Canada during Rodinia assembly: impactogens, trans-continental far-field stress and zinc mineralisation. Terra Nova, 28(3), 188-194.

Appendix

See separate file.